Matching Attribute Resolution to Scale:

The Effects of Filtering on DEM Resolution

by

ANDREW J. STAUFFER

B. S., Penn State University, 2011

A thesis submitted to the

Faculty of the Graduate School of the

University of Colorado in partial fulfillment

of the requirement for the degree of

Masters of Arts

Department of Geography

2013

This thesis entitled:
Matching Attribute Resolution to Scale: The Effects of Filtering on DEM Resolution
Written by Andrew J. Stauffer
has been approved for the Department of Geography

_____
Barbara Buttenfield

_____
Stefan Leyk

_____
Elisabeth Root

Date_____

The final copy of this thesis has been examined by the signatories, and we find that both the content and the form meet acceptable presentation standards of scholarly work in the above mentioned discipline.

Stauffer, Andrew J. (MA, Geography)

Matching Attribute Resolution to Scale: The Effects of Filtering on DEM Resolution

Thesis directed by Professor Barbara Buttenfield

Abstract:

Raster datasets are important for spatial analysis and modeling as well as for cartographic display. As raster data becomes more readily available at finer spatial resolutions, generalization is required to meet project needs. The modification of detail in Digital Terrain Models through the generalization process of smoothing using a Gaussian Filter will be examined. While it can be assumed that the smoothing process will simplify the terrain through reduction of attribute complexity, the rate of generalization, variations for rough and smooth terrain, and differences in specific landscape conditions, as well as any intermediate spatial resolutions are unknown after iterative filtering.

The theoretical contribution of this thesis is to systematically explore the concept of "implicit" resolution (attribute resolution) change, defined in the thesis as a modification to resolution which is the consequence of data processing or modeling without knowing in advance of the operation what is the precise resolution of the output. Several concerns arise after smoothing regarding data resolution and vertical integration with other datasets.

This thesis will compare filtered Digital Elevation Models (DEM) to other National Elevation Datasets and National Hydrography Datasets of various spatial resolutions. A standard deviation and semivariogram analysis will relate the attribute resolution of a filtered DEM to a known spatial resolution, which can then be linked to a target mapping scale. A conflation

analysis will determine the success rate of vertical data integration between a filtered DEM and an external, vector dataset.

Results of this analysis have identified that aggressive smoothing can have a large, global impact on the spatial dependencies within the DEM. This suggests that smoothing is only useful for small changes in scale or resolution. Additionally, smoothing can have strong impacts on the rate of vertical integration on flat landscapes, where features (i.e. valleys) are only defined by a low relief.

Table of Contents

List of Figures

List of Tables

Chapter 1. Problem Statement

1.1 Introduction

Raster datasets are important for spatial analysis and modeling as well as for cartographic display. As raster data becomes more readily available at finer spatial resolutions, generalization is required to meet project needs pertaining to small scale mapping or GIS analysis over large geographic extents. This thesis will focus on terrain generalization through attribute modification (specifically filtering) for a cartographic purpose. However, several concerns arise regarding data resolution and vertical integration and topological alignment with other datasets. In creation of cartographic products, these concerns are at the heart of cartographic best-practices.

The purpose of this thesis is not to define generalization rules for cartographic representation of terrain, but rather to provide insight into how the filtering process may alter resolution and the ability for a dataset to integrate with others. Specifically, this thesis will allow the cartographer answer specific questions regarding the requirements for generalization of a DEM. These questions may include 1) is a filtered DEM appropriate for my map's display; 2) is it more appropriate to filter or resample my DEM based on my map's scale or requirements or how aggressively should I filter my DEM; and 3) will a filtered DEM "fit" or integrate with other datasets that have been compiled at a different spatial resolution than my DEM?

This chapter will first define generalization and resolution. A key driver of generalization is the target mapping scale. Commonly, cartographers relate spatial resolution to a mapping scale. However, this relationship can become ambiguous, especially after smoothing. This chapter will pose several main research questions that will be answered in the remainder of this thesis. These questions will fill the knowledge gap of how generalization changes attribute

resolution of a DEM and how this affects the data's fitness for use for a specific mapping purpose.

1.2 Clarifying key definitions

1.2.1 Defining Generalization

Generalization can imply many meanings and is needed for all maps. From a cartographic standpoint, generalization commonly refers to a process of modification and symbolization of data that results in a reduction of the amount of specific detail carried on a map, yet preserves enough information to maintain a conceptual meaning (Dent et al., 2009). Imhof (2007) uses the term more to discuss the interplay of elements on a map that requires manipulation to create a cohesive and pleasurable cartographic display. Others similarly discuss the manipulation processes with a focus on map clarity at a given scale and for a given purpose (Tyner, 2010; McMaster, 1989; ICA, 1973; British National Committee for Geography, 1966). While many of the processes listed here focus on the concept of detail reduction in a map, generalization can also introduce detail when interpolating or exaggerating data to improve a map's message (Buttenfield and Mark, 1991). All of these definitions here highlight the process of data manipulation in accordance with a subjective user to improve a map's message.

Although every map can be considered as an example of this proverbial "generalization of reality", many things can catalyze further generalization. Some common catalysts include map purpose, scale reduction, and data complexity (Weibel, 1987; Robinson and Sale, 1969). The first catalyst, map purpose, is always a driving cause of generalization. As it is impossible to map everything, the cartographer must choose what to represent. This form of generalization, through selection and omission, clarifies the purpose of a map and falls within the scope of many definitions of cartographic generalization. The second catalyst, scale reduction, is heavily

dependent upon the amount of page space which is available after a scale change. Data must be simplified, aggregated, or displaced in order maintain the same amount of information. The final catalyst, data complexity, refers to the level of geographic detail in the data. It is frequently broken up into either spatial complexity or attribute complexity, which is either reduced or enhanced to improve the fitness of use per the map's scale and purpose (Goodchild and Proctor, 1997; McMaster and Shea, 1992).

Spatial data complexity is the amount of geographic detail in a dataset. Datasets with high levels of spatial data complexity will require more generalization when scale is reduced. Spatial data complexity is often, but not always, related to a data's collection scale which will permit varying amounts of detail. Exemplified by this concept is the National Hydrography Dataset (NHD) which is delivered nationwide in multiple forms of varying spatial data complexity (Simley and Carswell, 2009) (Figure 1.1). The left panel of Figure 1.1 is the high resolution data, collected at a scale of 1:24,000, and contains many more stream features and has more detail in the features (number of vertices). Conversely, the medium resolution data (right panel of Figure 1.1), compiled at a scale of 1:100,000, has fewer streams and relatively straighter or less complex line features. Through scale reduction, the high resolution NHD will either have to be generalized more aggressively or replaced with a dataset of lesser detail.

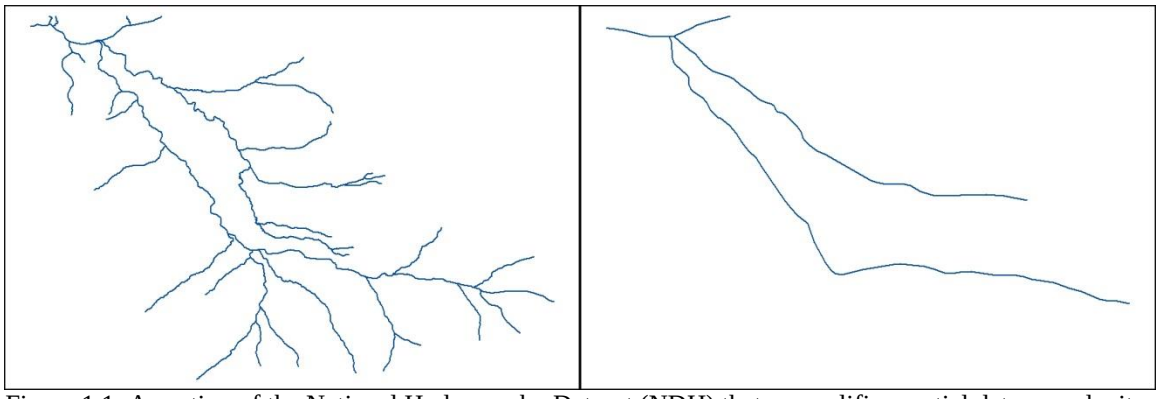

Figure 1.1: A portion of the National Hydrography Dataset (NDH) that exemplifies spatial data complexity.

Attribute complexity can refer to either quantity of attribute information or the attribute precision. Attribute complexity and spatial complexity can be related. Aggregating attribute data will often change the spatial complexity and symbology of the representation of the data. The National Land Cover Database (NLCD) is an example that demonstrates levels of attribute complexity (Homer et al., 2012) using a hierarchical land cover classification system (Anderson et al., 1976). Figure 1.2 illustrates a portion of the NLCD and its legend. The data's attributes are coded based on eight different classes. The attribute detail is then enhanced as each of these eight classes then has further subcategories, forming a total of twenty classes. Figure 1.2 shows four classes of developed area which demonstrate a relatively high degree of attribute detail. As scale is reduced, these four levels of development may be aggregated to the single "Developed" category. This reduction in attribute detail will immediately impact the spatial complexity.

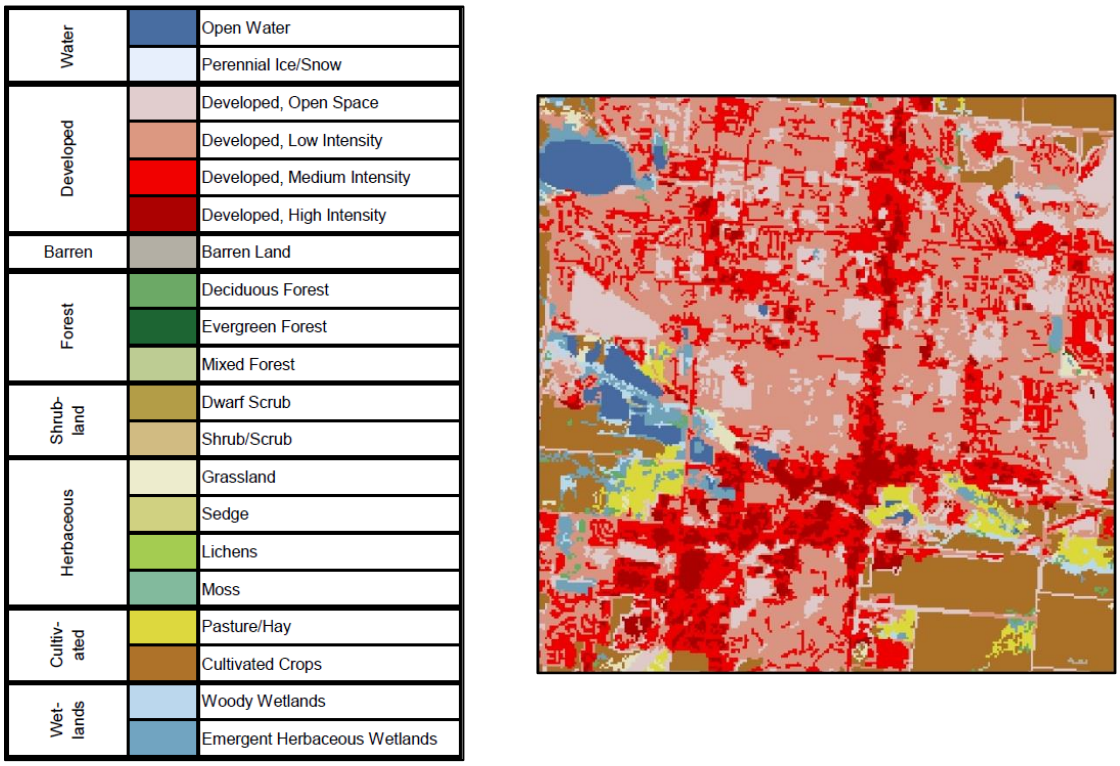

Figure 1.2: An example of raster attribute complexity shown as nested attributes in the National Land Cover Database (sample taken from Longmont, CO).

It is important to note the potential problems that can arise by altering attribute data, especially when generalizing raster data. Raster based datasets can be generalized through modification of spatial detail (cell size) or by modifying the attributes (or cell values) of the grid. The direct results of these generalization methods can be more easily measured and observed when dealing with categorical data such as the NLCD. However, the direct effects become ambiguous when dealing with continuous datasets such as elevation, temperature, or population density. It is important for the cartographer to understand how this attribute generalization affects a dataset.

Though many reasons have been defined for generalization, little has been studied about creating a standardized process to generalize geospatial data. This is understandable given the vast array of purposes for geospatial data. Imhof (2007) reflects on how terrain should be generalized, but does not explicitly mention how or when to manipulate the terrain data. The generalization processes and the order in which processes occur will vary over space to reflect the local landscapes (Stanislawski and Buttenfield, 2011). Common generalization processes are frequently exemplified in the definitions of generalization including selection and simplification (Tyner, 2010). Others add to this list by including combination, displacement (Weibel, 1987), classification, and even symbolization (Dent et al., 2009). In this thesis, the purposes of generalization include the modification to reduce or systematically introduce (enhance) spatial or attribute detail (Buttenfield and Mark, 1991).

1.2.2 Defining Resolution

Resolution can be divided into three categories which include temporal, spectral, and spatial (Longley et al., 2005). Temporal resolution is the frequency with which data is collected

and references the data's currency. Spectral resolution refers to the part of the electromagnetic spectrum in which the data is collected and is related to the number of bands in a raster image. Spatial resolution references the pixel dimensions for gridded data, or alternatively refers to the shortest distance between two items in a data set.

Resolution will be examined in this thesis and can be broken into two categories including attribute and spatial resolutions. Attribute resolution refers to the precision or level of detail in the variables contained in the data set. For terrain data, attribute resolution refers to the details in the z-values, essentially the vertical resolution; and for other types of raster data, it refers to the thematic characteristics stored in each grid cell. Considering Figure 1.2, the NLCD data has 22 unique land cover values. These values are further categorized into 8 classes, simplifying the attribute resolution. The attribute resolution is linked to the level of detail that can be extracted from a dataset (Slocum et al., 2009; Wade and Sommer, 2006; Tomlinson, 2003). Spatial resolution is often defined as the ground measurements of cell size or pixel of a remotely sensed image or the distance between two objects within a dataset (Bolstad, 2008; Wade and Sommer, 2006; Tomlinson, 2003; Lee, 1991). The spatial resolution can also be exemplified in Figure 1.1 by evaluating the number of feature vertices in the main river stems. Spatial resolution is also identified as the minimum mapping unit (MMU), which is the smallest detectable feature in the dataset.

The spatial resolution can manifest itself differently between vector and raster datasets. In a vector dataset, spatial resolution manifests as the minimum mapping unit, which is dependent upon the dataset and the scale at which the data is being used. An example of this would be changing an aggregation unit from states to counties in order to represent some data. In a raster dataset, the attribute and spatial resolutions are much more interrelated because

attributes are imbedded into the pixels. Spatial resolution manifests itself into the size of the pixels and the granularity of the dataset (i.e. are ridges and valleys readily detectable within the data?). DeMers (2002) suggests that the minimum mapping unit or granularity, should be used to define the pixel size, where the pixel size is 25% the size of the MMU. While the cell size is frequently determined by the collection sensor, cell sizes can also be defined using interpolation methods to conform to model needs, or to integrate with other vector data (DeMers, 2002). Figure 1.3 represents spatial resolution. The left panel shows a DEM and hillshade with fine spatial resolution. The pixel size is 3 meters. The middle panel shows a coarse spatial resolution with a pixel size of 100 meters. The fine spatial resolution shows too much detail and appears noisy. Conversely, when the spatial resolution is too coarse, the result appears blurry or aliased.

Figure 1.3: Examples of spatial resolution in a DEM. The right panel combines the two spatial resolutions to make a more appropriate display (discussed in section 1.3.1).

The second is the attribute resolution, or the apparent feature granularity (Figure 1.4). Both panels in Figure 1.4 have a spatial resolution of 3 meters. The left panel has a fine attribute resolution. The right panel is the same DEM as represented in the left panel, but has been filtered. This has reduced the attribute detail and coarsened the attribute resolution. Minor stream tributaries and braids can be seen in the fine attribute resolution image. Much of this detail is lost, or blurred, in the image with coarse attribute resolution, but the major features still

remain. Filtering has not changed the physical spatial resolution (the pixel size) but has modified the level of detail that can be extracted from a dataset, which is one definition of attribute resolution (Slocum et al., 2009). The filtered terrain is suitable for some smaller target scale, but at present, empirically derived guidelines do not exist for how much to filter data to approximate a specific target scale (or range of target scales).

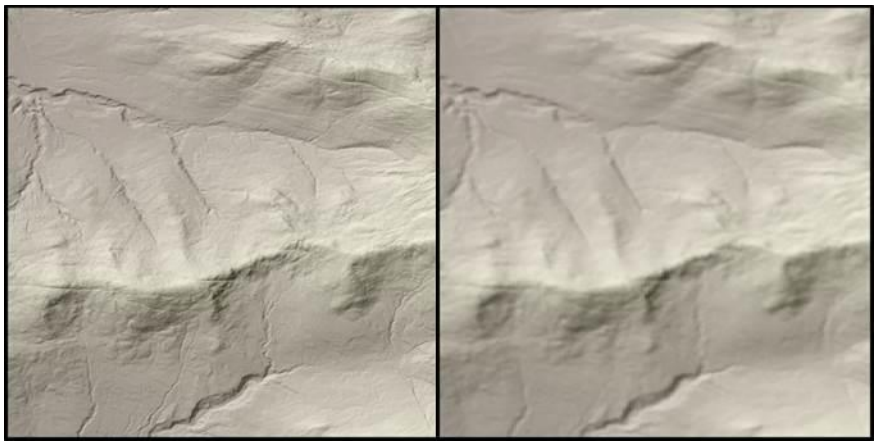

Figure 1.4: Attribute resolution is the amount of detail that can be extracted from an image (granularity).

The main goal of this thesis will be to relate the attribute resolution of a filtered dataset to a specific spatial resolution in order to guide cartographic data processing for terrain mapping at reduced scales. The USGS hosts DEMs in three spatial resolutions. Because terrain data is sensitive to scale change, it is likely that a target mapping scale will be out of the useable range for these spatial resolutions. If the DEM resolution is too fine for the mapping scale, it will appear too detailed and distract from the map's purpose. In order to accommodate some intermediate or small mapping scale, cartographers frequently filter DEMs to remove excess detail. However, no systematic exploration has been done to identify how filtering can alter the data or how much filtering is needed to create a terrain representation for a specific scale. This leads the cartographer to filter by trial and error, causing an inefficient and inconsistent methodology for terrain generalization.

1.3 The central problem – matching spatial resolution and mapping scale

Terrain generalization is a common practice in GIS data processing and is becoming more important as raster data collection improves to finer spatial resolutions. Digital Elevation Models (DEMs) are increasingly available with spatial resolutions of roughly 3, 10 and 30 meters (1/9, 1/3, and 1 arc-second respectively), for the conterminous United States. However, terrain is acknowledged to be a data layer which is extremely sensitive to scale (Mark, 1991). A question arises, specifically, which spatial resolution is appropriate for integrating DEMs with existing vector data sets at a given mapping scale?

1.3.1 The effects of resolution on DEM representation

For cartographic displays, using a dataset at too fine a resolution for a given mapping scale yields a busy appearance, while using a dataset at too coarse a resolution can appear aliased or blurry (Figure 1.3). Cartographers must generalize data to an appropriate resolution for proper display based on the controls of generalization (Robinson and Sale, 1969). In manual shaded relief, the cartographer determines which landscape features to show. Imhof (2007) offers some general guidelines about removing the smallest landscape features first (gullies, alluvial deposits, etc.), then removing larger features such as ridges, and finally combining mountain chains and exaggerating height. However, these decisions are both subjective and manual and difficult to implement in a fully automated system. At present, cartographers implement these processes digitally by heuristic methods and generalization of structure lines. Other methods have also been created such as “resolution bumping” (Patterson, 2001), which combines coarse spatial resolution data with fine spatial resolution data to represent the largest landscape features and enrich them with minor detail. The rightmost panel in Figure 1.3 demonstrates how resolution

bumping is accomplished. By overlaying the fine and coarse spatial resolutions, a more appropriate representation of the terrain can be achieved for cartographic display. However, this method of terrain representation is subjective and requires trial and error to develop an appropriate display.

Other methods filter the attribute resolution, or resample to a coarser spatial resolution, to reach a target mapping scale. Generally, these methods are applied uniformly, which can homogenize detail and remove some important but smaller terrain features preserved in manual strategies. Filtering the data will smooth out and gradually "erase" minor landscape features. Iterative filtering or filtering with increasingly large focal windows will gradually smooth out much of the landscape detail to be clearly represented at smaller scales (Leonowicz et al., 2010a). Vertical exaggeration can emphasize high-relief areas, creating clear boundaries between landscape types at small scales (Patterson, 2000; Patterson, 2001) but this method does not work as well in less rugged terrain.

Cartographers need to understand the filtering process, and how it may affect the granularity of a raster dataset. Appropriate DEM representation requires that terrain integrates vertically with other data layers (especially hydrography and transportation networks). Depending on landscape characteristics (aridity, terrain roughness, etc.), different amounts of filtering may be required. Using coarse resolution data for rugged terrain may not be adequate to integrate with other data; using fine resolution data may appear too detailed in low-relief areas.

1.3.2 Relating resolution to scale

Relating data resolution to an appropriate mapping scale is an ongoing research question. The question is commonly answered in the Remote Sensing literature by using the term of

minimum mapping unit (MMU). The MMU is the smallest areal object to be mapped at a given scale (Lillesand et al., 2007; Goodchild and Proctor, 1997). However, this relates to either vector-based data or discrete raster data where a specific minimum size can be established (the smallest size feature encountered or expected to be encountered in a dataset). The National Wetlands Inventory defines the MMU of any [feature] to be displayed on a 1:24,000 scale map to be at least 1 to 3 acres in size (U.S. Fish and Wildlife Service, 2004). Of course, this MMU specification must be altered when displayed at different scales. For raster-based data, DeMers (2002) suggests that the intended MMU should be four times the spatial resolution to provide enough detail for modeling purposes.

The use of the minimum mapping unit becomes difficult, if not impossible, to apply to continuous raster data because finite boundaries become ambiguous in gridded data. Cartographers have sought other ways to relate the spatial resolution of data to a mapping scale. Similar to the principles of a minimum mapping unit, Tobler (1988) first identifies the detectable size of a dataset, which is the smallest feature to appear on the map or in a dataset. Alternatively, Kimerling (2011) uses an output media resolution (on-screen display, hardcopy print, etc.) to establish a spatial resolution for a raster dataset. This strategy optimizes the amount of detail in the raster dataset for the best display quality but it constrains the use to a particular media type.

MMU and scale-to-resolution conversions do not completely solve the problem. First, these methods rely on a known spatial resolution of the dataset, which becomes ambiguous after filtering. Second, the scale-to-resolution relationships characterize data as a homogeneous granularity and ignore local characteristics such as terrain roughness.

1.3.3 Generalization

Since much of the readily available data is produced for large scale purposes, raster data must be generalized to accommodate smaller scales to improve processing times or create appropriate visual displays. Many projects, especially those dealing with global models, require smaller mapping scales and generalized data.

Large scale maps are considered to range between 1:5,000 or larger scales and are used for local mapping or project-specific needs (Steward, 1974). At that time, the U.S. Geological Survey (USGS) made large scale maps at a scale of 1:24,000. Larger scale maps and project specific data were often created elsewhere. Since then, data used for USGS maps and datasets have increasingly fine spatial resolution. For example, the U. S. Geological Survey's National Elevation Dataset is continuing to improve availability of 3-meter DEMs nationwide and in Alaska (Gesch et al., 2009).

1.4 Problem Statement

Few generalization guidelines have been proposed that offer insight into how aggressively a dataset must be smoothed to conform to a given mapping scale. A better understanding of how the generalization process, specifically filtering, affects the attribute resolution of a dataset will help to lay a framework in which guidelines can be formed. However, these guidelines will differ from project to project based on the controls of generalization. Therefore, a set of comprehensive guidelines is beyond the scope of this thesis. Nonetheless, the information produced by this work will help to define specific filtering thresholds based on a desired target scale or map purpose.

To gain the knowledge to formulate the framework for these guidelines, this thesis will explore the relationship between terrain filtering and attribute resolution for a range of landscape types. The result of this work will address the question of how DEM attribute resolution changes through iterative spatial filtering. This thesis will explore two specific facets of terrain data including 1) the rate of attribute resolution change, and 2) the problems of integration of generalized data with other datasets.

The theoretical contribution of this thesis is to systematically explore the concept of "implicit" resolution change, defined in the thesis as a modification to attribute resolution. Filtering provides an example of implicit resolution change, as do vector forms of cartographic generalization by enhancement (Buttenfield and Mark, 1991), such as refinement or exaggeration. These generalization processes often alter attribute resolution in order to manipulate the geometric representation of a dataset. In contrast, resampling is a generalization operator that has a pre-determined output spatial resolution, which is an explicitly stated parameter.

1.5 Research questions

Since the filtering process alters attribute resolution but does not alter the spatial resolution, the output resolution is unknown. Without knowing this information, the appropriate spatial resolution for a given mapping scale is also unknown. This thesis will iteratively filter DEMs to explore the relationship between filtering, detail homogenization, and attribute resolution for a range of landscape types. The result of this work will address two key questions:

1. What is the rate of attribute resolution change during filtering and how does it differ between various landscape characteristics? Is the rate of change constant for

all filtering iterations, or do certain iterations exist where dramatic changes occur? This will aid in determining appropriate mapping scales for a filtered dataset, and the appropriate number of filtering iterations to apply to reach a given level of attribute granularity.

2. How well does the filtered dataset integrate with other vector layers at a given target scale? A filtered dataset must still integrate with other existing vector data. If it cannot, the filtering process that leads to the new attribute resolution is not adequate for the target scale.

In respect to the first research question, this thesis will iteratively filter fine spatial resolution DEMs for a selection of landscape types (rugged and smooth, in dry or humid conditions). The resulting filtered output will be compared to known coarser spatial resolution benchmark datasets using the standard deviation of elevation, and semivariogram analysis. By comparing many filtering iterations to coarser spatial resolution benchmarks, the rate of attribute resolution change can be studied in the context of landscape characteristics (ruggedness, aridity, etc.). The vertical integration of the filtered DEMs will be examined by using a Coefficient of Line Correspondence metric (Stanislawski, 2009) which will measure how well an existing vector dataset integrates with the DEM. Through these questions, this thesis will explore the relationships between spatial and attribute resolution in the context of filtering raster terrain and clarify the impact of filtering on creation of cartographic products.

1.6 Significance of research

Terrain is one of the most frequently included data layers used in GIS spatial analysis. It is frequently used as a foundation for base mapping to represent relative elevations and macro-

scale landforms. Terrain is also an important data layer for analytic purposes, across a range of geographic footprints that span several hundred square meters to the entire globe, requiring a wide range of spatial and attribute resolutions. Most applications require a coarser resolution than is readily available. To accommodate the need for coarser resolution, digital terrain is generalized to improve vertical data integration and sometimes improve processing times. To date, a numeric relationship between source spatial resolution, number of filtering iterations, and attribute resolution has not appeared in the literature. A lack of understanding about the rate at which filtering modifies rough or smooth terrain has led to poor cartographic and analytic practice, where inappropriately filtered terrain layers do not integrate with other data and thus distort mapping and modeling results.

The answer to the rate of attribute resolution change in iteratively filtered DEMs through various physiographic regions can support analytical and graphical guidelines to setting generalization thresholds. The rate at which attribute resolution changes may be directly applied to modify such resolution-to-scale relationships as Kimerling's (2011) formula, and in so doing, to assist users in deciding how much filtering is required. For many modelers who work with larger geographic footprints (for example global climate modelers), knowing how attribute resolution is changed through iterative filtering can assist in vertical data integration, setting target resolutions, and better interpretation of results to examine a given scale-specific geographic process (e.g., erosion, migration, or urbanization).

Maintaining the spatial relationships among various GIS data layers and data integration between vector and raster datasets is critical for GIS analysis and proper cartographic displays (Piwowar et al., 1990). Data that is mismatched will yield poor model results or produce misleading map displays. The USGS's The National Map portal provides nationwide datasets

for eight themes (Sugarbaker and Carswell, 2011). While the USGS is not responsible for creation of all eight, integration problems are commonplace among themes. With users expecting quality data, problems with data integration can cause errors in planning, management, and safety decisions. To improve data integration, The National Map program is actively interested in and researching integration between multiple geospatial data layers (Usery et al., 2009). An assessment of raster – vector data integration after generalization will improve understanding of how these layers interact with one another through generalization and how data can be mapped across multiple scales.

1.7 Summary

The remainder of this thesis is organized as follows. Chapter 2 situates this work in the context of existing literature. This expands upon topics including why cartographers generalize raster and terrain data, and what methods exist to generalize terrain. Chapter 2 will overview specific cases of raster generalization and what the known effects of generalization are on terrain data. Chapter 3 will introduce the data to be used during the analysis of the thesis. It will describe the research framework and methodology for the analysis including how the DEMs will be filtered, how the rate of attribute resolution change will be measured, and how the vertical integration will be assessed. Chapter 4 presents the results of the analysis. Finally, Chapter 5 presents implications for the research, limitations of the study, and directions for future work.

Chapter 2. Literature Review

2.1 Introduction

The purpose of this thesis is to gain an understanding of how the process of generalization affects terrain data to be displayed at a given mapping scale. Smoothing data to reduce detail is useful in its own respect, but can become problematic because the process alters the attribute resolution without altering spatial resolution of the data. Linking spatial resolution to a mapping scale ensures the data is displayed appropriately. The disconnect between spatial and attribute resolution here makes the resolution-to-mapping scale relationship ambiguous.

To understand the complexity of relationships between spatial and attribute resolutions, it is first important to understand the history of digital cartographic generalization, which evolved from hundreds of years of manual generalization. This chapter provides a brief chronology of terrain representation followed by a detailed explanation of digital generalization practices that are applied to terrain. Because terrain is frequently represented in grid format, a relatively new technology to the field of cartography, it is important to first understand the generalization practices and frameworks that have been developed for raster based generalization. Next, a short discussion is provided on easily accessible terrain data and an explanation of why U.S. Geological Survey (USGS) data is used in this thesis. Appropriate mapping scales of available data are explored with an in depth discussion of the resolution-to-scale relationships. Finally, documented impacts of the generalization process on raster data are provided.

2.2 Terrain representation – a brief chronology

Terrain representation has been a part of cartographic design for centuries and has gone through many methods of depiction. Some of the earliest representations of terrain were simple

molehills that portrayed an oblique view of a ridgeline on a planimetric map that often was incomplete or filled empty map space rather than depicting terrain structure accurately. Over time, these became more detailed and complete. The pictoral molehill symbols transitioned into more accurate depictions using slope lines and shadow hachures. Increases in accuracy evolved into slope hachuring, shaded relief, and contours (Imhof, 2007) as well as inclined plane contours (Robinson and Thrower, 1957) and physiographic symbols (Raisz, 1931). Currently, automated shaded relief is the predominant form of representation showcasing the intensity of light cast by a point light source to produce a three-dimensional effect (Brassel, 1974).

In order to create a map at an economic and pragmatic size, some generalization or removal of detail must occur. In the past, generalization was manual and required specialized expertise that incorporated a degree of subjectivity to support scale change and map purpose. Patterson and Jenny (2012) exemplify the subjectivity in terrain generalization through shaded relief examples of similar regions by different cartographers (Figure 2.1). While all of these maps were compiled at small scales, he main landscape features are all present and easily detectable (i.e. Appalachian Mountain Chain versus Great Plains versus Rocky Mountain Chain), yet they all have subtle differences and are intrinsically unique despite having identical subject matter.

It is the objective of the cartographer to generalize map data to harmonize the amount of detail within the map without causing the data to become unrecognizable. To this, Erwin Raisz (1962) stated that no rules can be given for generalization, implying that it is a wholly subjective matter. Steward (1974) claimed that many would disagree with Raisz's proclamation, urging cartographers to establish defined rules for the generalization process.

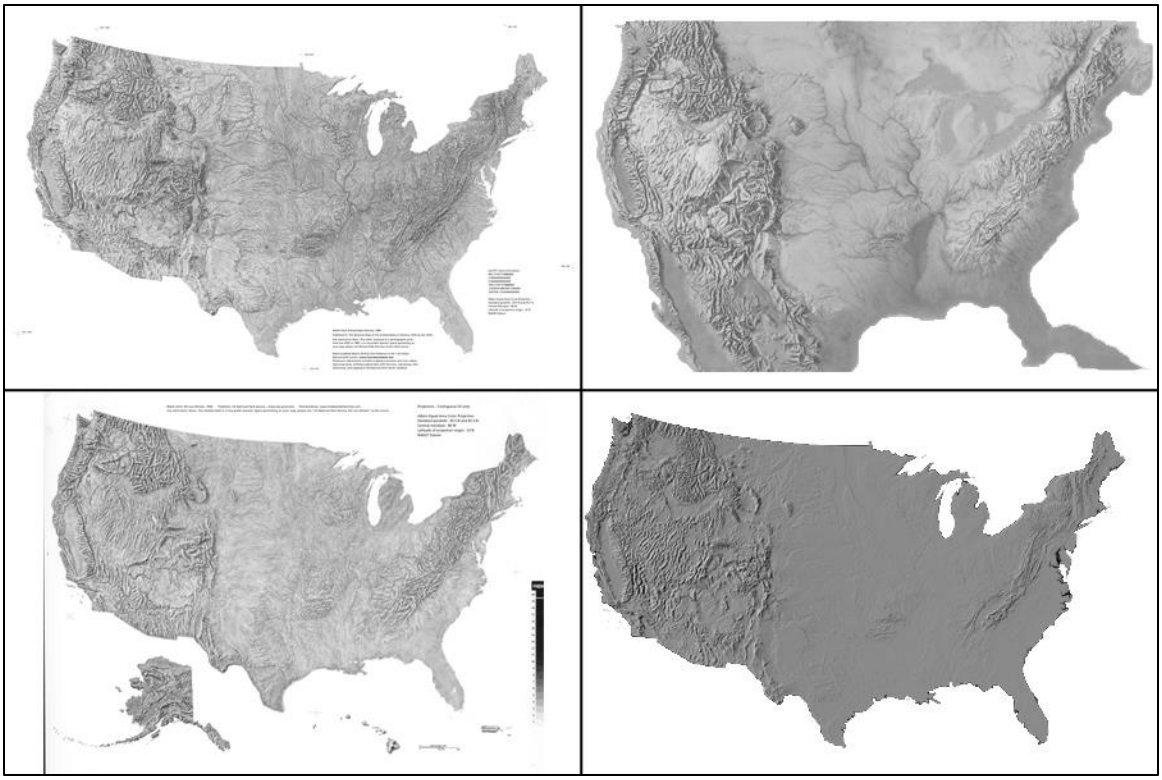

Figure 2.1: Manual shaded relief renderings by three North American Cartographers: Richard Edes Harrison (upper left) originally published at a scale of 1:7,500,000; Herwig G. Schutzler (upper right) unknown published scale; Bill von Allmen (lower left) unknown published scale; and a digital shaded relief by Gail Thelin and Richard Pike (lower right) originally published at a scale of 1:3,500,000.

2.3 Analytical Cartography

As GIS and graphical software developed, cartographers have continued to experiment with replication and automation of manual cartographic practices, especially after the automation of shaded relief for very small scales, shown in Figure 2.1 (Pike and Thelin, 1990). As cartographers begin to simulate manual terrain representation using digital techniques (for example, Leonowicz et al., 2010a; Jenny and Hurni, 2006; Patterson and Kelso, 2004), and DEMs become widely available, the need to automate and formalize the generalization process also increases.

Analytical cartography evolved out of this need to automate generalization (Tobler, 1976). Analytical cartography applies a theoretical structure to the specific implementation of

some digital cartographic process and today is influenced by many external fields including mathematics, computer science, and image analysis (Moellering, 2000; Clarke and Cloud, 2000). Rooted in this subfield is a need to understand the underlying data structures and properties to apply mathematical solutions to a spatial problem (Franklin, 2000). While analytical cartography will help to induce best standard practices for automated generalization and allow results to be replicable, the main purpose is to help cartographers automate processes involved in data and map production at intermediate and smaller scales. By understanding the effects of a generalization process on a dataset, cartographers can defend design choices and select appropriate generalization thresholds for a map's purpose. As Eckert (1908, p.347) once defended the use of scientific judgment applied to map production, his statement can also be related to the need for a deep understanding of the automated generalization processes used today: "[This] will prevent any erratic flight of the imagination and will impart to the map a fundamentally objective character where generalized maps should be products of art, clarified by science."

Similarly, as Tóth (2010, p. 26) reminisces on his career as a relief artist, he declares that "… there is no definite work routine to … digital relief production. Each project presents a different set of challenges and will require its own unique solutions." The benefits of manual terrain representation and generalization allow great flexibility in localized generalization decisions. The downside is the results may not replicate and geographic accuracy is often an "inconvenient afterthought" (Patterson, 2001). However, complete automation coupled with a lack of knowledge of the generalization process could result in inappropriate solutions to terrain generalization. The uses of generalization guidelines are useful in determining a starting point for generalization with a cartographer's intuition to guide the final product's design from there.

A solid foundation of knowledge, derived by mathematical transformations of the data will improve replicability and minimize the effects of accuracy being an afterthought while allowing unique solutions to be applied for a given map's purpose or scale.

2.4 What is generalization: when and how do we use it?

2.4.1 Defining generalization

As discussed in the previous chapter, generalization is the process of systematically reducing or introducing (enhancing) spatial or attribute detail (Buttenfield and Mark, 1991) of a dataset for the purpose of a scale change to a cartographic product. One critical element within many of the formalized definitions of generalization mention the use of multiple generalization operators (e.g. generalization algorithms) that combine to form a process of generalization. By treating generalization as a process, a flow of tasks can be implemented, often iteratively, to ensure the generalized product matches the requirements for its use.

The process of generalization can be organized several ways. Some categorize the process into two steps that include simplification, the removal of excessive data, and amplification, the enhancement of sparse data (Wright, 1942). Others include more categories that deal with how the data will be modified and include selection, classification, simplification, and symbolization (Dent et al., 2009). Alternatively, the generalization process can be categorized based on whether attributes or geometry is altered (McMaster and Shea, 1992). While the generalization operators are critical components to modifying detail to clarify a map's purpose, the order in which these operators are applied is just as important and is frequently an iterative process (Beard and Mackaness, 1991). The sequencing or repetition of tasks is often strongly dependent upon the cartographer to ensure the generalization process has been

completed successfully or adequately (Bard, 2004). Morrison (1974) even designates some generalization operators as a pre-processing step.

Controls of generalization determine why and how generalization operations must be applied. These include map objective, map scale, data quality, graphic limits (Robinson and Sale, 1969; Steward, 1974; Brassel and Weibel, 1988), and more recently, expected audience (Slocum et al., 2009). Target map scale is the single most influential control as it directly relates to the amount of generalization that must occur to allow all map content to fit in the allotted space. The map's objective reflects what purpose the map serves, and thus what types of detail must be displayed most prominently. The objective is closely related to the map's expected audience. A map must be designed differently for children compared to adults or general users compared to specialized users. Data quality can reference spatial or attribute precision (Weibel, 1987). Finally, the graphic limits refer to the output medium, which controls how much detail can be displayed on the map. The graphic limits of different types of data vary. For instance, terrain and hydrography must be generalized more intensely than transportation due to the detail inherent within the datasets and inability to be pushed through a large change in scale (Mark, 1991; Buttenfield, 1995).

2.4.2 Operators of raster generalization

Raster generalization focuses on the modification of attribute values of the gird cells (McMaster, 1989). Raster datasets can be organized into two data structures including continuous and discrete data. Continuous raster datasets are grids in which each cell has a floating point value, that represent volumetric data (elevation, temperature, or population density). Discrete raster datasets represent categorical data with integer values, classed

attributes, and abrupt boundaries (e.g., land use, soil type, or rural/urban zones) (MacEachren, 1995). Because a DEM is commonly distributed as a continuous raster dataset, this type of raster will be discussed in more detail. McMaster and Monmonier (1989) identify four ways in which raster data can be generalized. Structural generalization is appropriate for either continuous or discrete data and involves changing the size (structure) of the grid cells. Numerical generalization involves altering the attribute detail through spatial filtering. The other two raster methods are less relevant to this thesis, and include numerical-categorization generalization which is used for converting a continuous data type to a categorical (discrete) data type and categorical generalization, which is only appropriate for discrete datasets.

Structural generalization alters the cell size and/or shape systematically, while not changing the size of the grid as a whole. This spatial resolution change aggressively generalizes data to be suitable for a new scale, but can corrupt an underlying structure. When changing spatial resolution directly, care must be taken in determining how new cell values are assigned. A commonly applied method of structural generalization is resampling, which modifies pixel sizes. Resampling involves combining values in original cells into the new cell sizes, and is usually accomplished by interpolation. Nearest neighbor and majority resampling are most appropriate for discrete data because it maintains the original cell values of the source raster. Bilinear and cubic-convolution are appropriate resampling methods for continuous data and take a weighted average over four or eight neighboring cells respectively to approximate new values (Wade and Sommer, 2006). Additionally, structural generalization can involve either vector-to-raster or raster-to-vector data conversions.

Numerical generalization, frequently referred to as spatial filtering, generalizes raster data locally by focusing on a defined neighborhood (commonly 3x3 cells), called a kernel, to smooth

the data which concurrently reduces the variance within the dataset. Larger neighborhood sizes filter more aggressively by removing local characteristics. Several types of filtering can generalize raster details in varying ways. This is commonly done through frequency filters that suppress specific parts of a raster's frequency and focuses on modifying the variance within the kernel. High-pass filtering attenuates low frequency changes, and emphasizes differences between neighboring cells, thus highlighting boundaries between features. It is also known as edge enhancement because it highlights areas of rapid change, essentially increasing the variance within the kernel. Low-pass filtering conversely attenuates high frequencies, which removes noise in the data via two kinds of averaging. Arithmetic averaging blurs the image systematically while weighted averaging reduces the variance of data values, yet retains local characteristics. Filtering can improve visual quality for reduced scales, but should only be used for small scale changes (Weibel, 1992).

Other methods of raster based generalization have also been derived which are analogous to vector-based enhancement; these include interpolation and heuristic generalization. Interpolation is used to recreate a surface from structure points (spot heights and benchmarks) by assuming some relationship between the structure points and estimating the values between each point (Burrough and McDonnell, 1998). Interpolation can preserve critical features; and converting the raster terrain into a triangulated irregular network (TIN) greatly reduces data size. Data reduction through TINs greatly improves processing time and reduces file size, but can create artifacts which can omit local characteristics if the interpolated structure points have been poorly selected (Wang and Lo, 1999). Heuristic generalization extracts vector structure lines from an existing raster. These features are then generalized using vector-based operators. The generalized structure features are then interpolated to recreate the raster surface. However,

heuristic methods generally are not based on statistical threshold and require significant input from the cartographer (Weibel, 1992). Others have focused on alternative methods of detail enhancement and feature exaggeration (Leonowicz et al., 2010b; Imhof, 2007; Patterson, 2001).

2.4.3 Raster based generalization framework

One of the earliest raster-based frameworks (Weibel, 1992) divides the generalization process into categories of methods that are partially determined by terrain characteristics. Terrain is defined as any type of surface, described by continuous data. The categories include heuristic and filtering methods and are based on the Brassel and Weibel (1988) framework. A critical part of the framework is the inclusion of a feedback loop after the generalization process; if the generalization results do not meet the needs for the map, the generalization process is repeated.

Heuristic generalization methods involve the generalization of extracted structure features in the terrain. The feature extraction and identification is often related to manual methods opposed to decisions based in well-founded theory (Weibel, 1992). Therefore, this type of generalization can emulate manual generalization decisions for terrain data, but can be difficult to replicate. The first step of this method is to identify 'significant' structure features and extract them from a terrain. The set of the structural features forms a vector 'terrain skeleton' which is generalized using vector operators. After the terrain skeleton is generalized, the terrain is interpolated to convert back to a raster format. Due to the dependence of the cartographer to make feature extraction decisions, heuristic methods are difficult to implement in an automated environment (for more detail see Zhou and Chen, 2010; Ai and Li, 2009; Zaksek and Podobnikar, 2005; Weibel, 1992).

The second category of terrain generalization is filtering, which is used for minor scale reductions or for low-relief terrain. The filtering category can be selective or global. Selective filtering is considered a structural process (McMaster and Monmonier, 1989) because it changes the structure and spatial resolution of the data by systematically using selection and elimination to reduce detail. Global filtering is a numerical process because it retains the number of samples points within the data, but changes the attribute values to reduce detail.

Selective filtering is useful for terrain with mixed low-to-high relief and is accomplished via elimination until the terrain is adequately generalized. In selective filtering, critical terrain points (peaks, pits, saddles) are selected. Other elevation points are systematically compared to these critical points and eliminated if similar to the critical point. The raster terrain is then re-created from the remaining points. Alternatively, Heller (1990) proposes a similar approach where sample points are systematically added to the surface in a hierarchical manner until the desired amount of detail is acquired. This method is useful in removing minor details and reducing the files size of the data while preserving the true structure points of the source data.

Global spatial filtering can be effective for minor scale reductions or for flat terrain because it slowly reduced or highlights specific areas within the data by applying an attribute transformation to the sample points within the grid. This is commonly referred to as frequency filtering and is most commonly done by transforming a cell value by averaging its neighbors. Neighbors are commonly defined as a 3x3-, 5x5-, or 7x7-cell matrix around a focal cell (Burrough and McDonnell, 1998; Wade and Sommer, 2006). However, these are not the only dimensions to define a neighborhood and can be much larger, where the larger the focal window, the more intense the generalization (McMaster, 1989). The neighborhood definitions can also take various shapes. Commonly, the neighborhoods are defined using a queen (nearest 8 cells)

or rook (nearest 4) cells contiguity. However, other shapes and configurations can be used including circles, wedges, or concentric rings (donut). Low pass frequency filtering averages values within a defined neighborhood or focal window. This effect squeezes out extreme values and reduces the variance of the dataset by increasing local minima and decreasing local maxima (McMaster and Monmonier, 1989). Other forms of global filtering include other types of statistical transformations including minimum, maximum, quintile, median, or mode statistics and frequency filtering to sharpening or edge detection using high-pass or Laplacian filters (Leonowicz and Jenny, 2011; Jain et al., 1995). This project focuses on the effects of low pass filtering on a DEM's attribute resolution.

2.4.4 Raster generalization in use: examples of terrain representation

Significant work on terrain generalization has been conducted in all three of these categories defined in Weibel's framework (1992), most of which involve an integration of multiple methods. Leonowicz et al. (2010a) attempt to mimic very small scale manual relief shading by using arithmetic mean filtering techniques to smooth the terrain and heuristic techniques to replicate the exaggeration of landforms. Data is also masked to take advantage of local terrains characteristics and to generalize the terrain types differentially. A later study utilizes quartile filters to generalize low relief and high relief landscapes for different effects to produce a smooth hypsometric tinting for very small scale mapping (Leonowicz and Jenny, 2011).

Other generalization methods with an emphasis on local terrain variations (selective filtering and heuristic generalization) have also been studied for large scale mapping purposes. Ai and Li (2009) use structure lines and watershed characteristics to identify insignificant valley

features. These features are then removed by a filling procedure to smooth the terrain. They claim that the process can be done iteratively to accommodate larger scale changes. Others try to examine selective filtering methods on the effects of visual display while trying to minimize database size. Based on critical point extraction, it is possible to maintain legible topographic structures while using a small fraction of the original sample points (Zhou and Chen, 2010).

2.5 Data availability

Terrain data is commonly obtained in a raster grid format and is widely available from many sources. This section will discuss some of the most prevalent data that is available by providing a brief history of the dataset and comment of strengths and weaknesses of each.

Digital elevation data has become far more available and accessible in recent decades. Global data is freely available from many sources and users have seen improvements in accuracy and spatial resolution. Some of the most common global datasets available are derived from remote sensing technology and include SRTM, ASTER, and GTOPO30. The United States' National Elevation Dataset (NED) is available at fine spatial resolutions for the conterminous United States and some of its territories. Several of these datasets are available in multiple spatial resolutions, which vary from about 3-meters to 1000-meters. Alternatively, very fine spatial resolution datasets are available that can have sub-meter spatial resolutions. Project specific initiatives can collect Light Detection and Ranging (LiDAR) data, but LiDAR data availability is extremely limited and not often freely available. Figure 2.2 compares samples of elevation datasets reviewed in this thesis that are freely available for public use.

The Shuttle Radar Topography Mission (SRTM) is a joint collaboration between NASA and the National Geospatial-Intelligence Agency to produce a fine spatial resolution global

elevation model. The data was collected in 2000 by using interferometric synthetic aperture radar (InSAR), which uses two radar images to measure topography (Farr et al., 2007). The data is collected at a 30-meter sampling interval between 60° north and south, known as SRTM-1. The data was then processed to SRTM-3, with a 90-meter spatial resolution. SRTM-3 was created by resampling the SRTM-1 dataset by averaging a 3x3-cell neighborhood. The SRTM-1 dataset is only available for the United States while SRTM-3 is available on a global scale. The error sources in the datasets have been thoroughly studied (Rodríguez et al., 2005) and are frequently introduced by positioning of the space shuttle during the collection process and can easily be accounted for. However, due to the use of radar imaging techniques, dense vegetation can obscure bare-earth measurements, which can cause high degrees of error in vegetated areas.

Since 2000, NASA's Advanced Spaceborne Thermal Emission and Reflection Radiometer (ASTER) satellite has been collecting near infrared stereo images of the Earth between 83° north and south. In 2009, a joint project between the United States (NASA) and Japan (METI), begun to combine the stereo images to create a Global Digital Elevation Model (GDEM). Upon release, GDEM had an effective spatial resolution of about 120-meters and was plagued with artifacts from data gaps in high latitude areas, cloud cover, water masking, and canopy displacement (ASTER GDEM Validation Team, 2011). At the end of 2011, a revised version of GDEM was released, called GDEM2. GDEM2 improved the spatial resolution to about 30-meters and reduced many of the artifacts inherent in GDEM1. The methods used to enhance the spatial resolution of the data have also increased the presence of high-frequency noise, which add improper detail to shaded relief images (compare GDEM to NED in Figure 2.2). The ASTER GDEM Validation Team recommend the use of the ASTER GDEM2 product

as a fine spatial resolution global product, but caution users to be aware of the existing artifacts that have been addressed in the new release, but not completely removed.

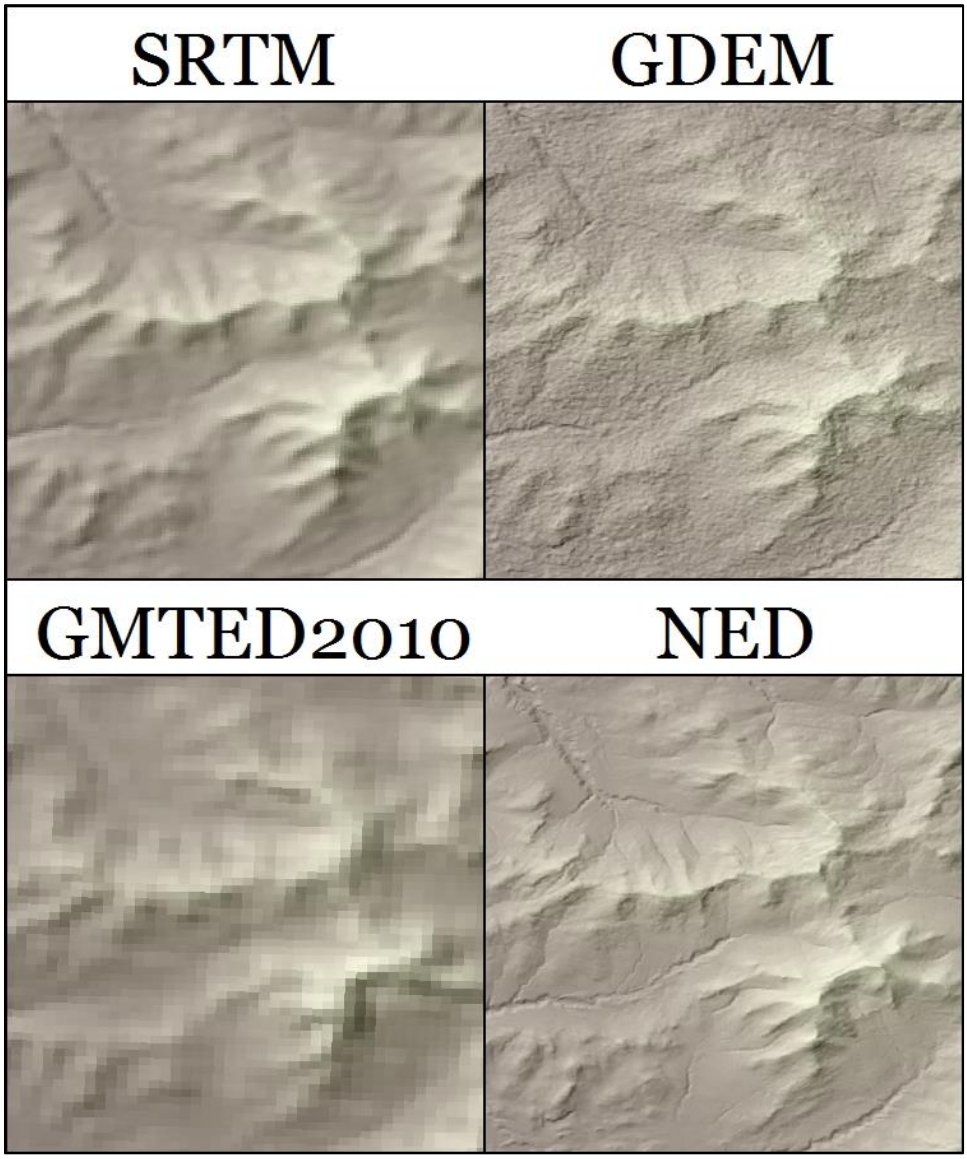

Figure 2.2: Four freely accessible elevation datasets at varying spatial resolutions displayed at a scale of 1:250,000. SRTM spatial resolution shown is 90-meters. GDEM spatial resolution shown is 30-meters. The GMTED2010 spatial resolution shown is 250-meters. NED spatial resolution is 30-meters for the coterminous United States and is the only dataset shown here that does not have global coverage.

Coarser spatial resolution elevation data is available through the Global Multi-resolution Terrain Elevation Data 2010 (GMTED2010) and is available in spatial resolutions of 1000, 500, and 250 meters (Danielson and Gesch, 2011). This product was designed to replace the outdated

U.S. Geologic Survey's (USGS) GTOPO30 elevation model, which had a spatial resolution of 1000 meters. While being a primary source for continental-wide data, the data quality varied greatly and had no metadata associated with it. The GMTED2010 elevation data is a composite of eleven data sources, with the primary being SRTM. Other datasets are used to fill in data outside SRTM collection latitudes and fill in voids.

The final elevation dataset of discussion is the USGS's National Elevation Dataset (NED), a fine spatial resolution, seamless, national coverage product for the conterminous United States (Gesch, 2007; Gesch et al., 2002). The NED project began in the 1970's and was designed to have a 30 meter spatial resolution. As time passed, the NED was refined to 1/3-, 1-, and 2-arc-second spatial resolutions (or about 10, 30, and 60 meter spatial resolutions, respectively). In 1999, full U.S. coverage of 1-arc-second data was completed and in 2002, 1/3-arc-second (about 10m) spatial resolution began construction to conform to vertical and horizontal accuracy standards (USGS, 1999). The datasets were derived from photogrammetric and Digital Line Graphic (DLG) interpolations methods and are now edited for hydrological enforcement rules to improve data integration (Osborn et al., 2001). Due to the DLG interpolation methods of contours, which were produced individually on a 7.5-minute grid, several aliasing artifacts exist in the 1- and 1/3-arc-second datasets along compilation grid boundaries. The NED currently is being updated to 1/9-arc-second (about 3m) spatial resolution but is not yet available for the entire conterminous United States (Gesch et al., 2002). 1/9-arc-second data are derived by LiDAR and IFSAR remote sensing methods which, because of the finer spatial resolution, are not hydrologically enforced.

While all of the DEM data sources discussed above are useful in their own regard, the USGS's NED will be used for the remainder of this thesis. First, the NED contains several

spatial resolutions, each of which was compiled independently. Second, accuracy standards for the NED are standardized between spatial resolutions and enforced and well documented. By using several spatial resolutions of the NED, expectations can already be made about where and how errors may occur. Third, the USGS also supplies other data themes that are of similar spatial resolutions to the NED and follow similar standards requirements. This will be discussed in more detail in the next chapter.

Overall, several trends can be identified when looking at the history of these DEM products. First, spatial resolutions are becoming increasingly fine. Second, the data is becoming better quality. Both of these trends are promising for cartographers because of increased availability in terms of coverage and spatial resolutions. However, a key questions yet remains as to what spatial or attribute resolution is appropriate for a given mapping scale or purpose?

2.6 Relating resolution to scale

As the availability of today's spatial data is always being updated to finer spatial resolutions, the need for generalization is therefore growing in importance more so than ever before. Cartographers frequently alter a dataset's spatial resolution in order to match its appropriateness at a target mapping scale. There are options in which cartographers perform this task. Kimerling (2011) recently posted an equation to help answer the question that relates the spatial resolution of a raster dataset to a map's anticipated output resolution. Kimerling cites a common, smooth rendering for mapping occurs at a display resolution of roughly 40 pixels/cm (or about 100 pixels/in) for a computer display. Using these expectations, the applicable scales for USGS DEMs compiled at 1/9, 1/3 and 1 arc second are 1:12,000, 1:40,000 and 1:120,000.

Due to the changing relationship between arc-seconds and ground distance, smaller map scales are applicable at higher latitudes.

Tobler (1988) posed a similar mathematical formula that converts mapping scale to a corresponding spatial resolution for a dataset. An intermediate step is to calculate the detectable size of a feature within the map. This is the smallest object on the map that is expected to be identifiable. Similar to a minimum mapping unit, he defines this as the detectable size and that the data's spatial resolution should be half of this value. A 1/9-, 1/3-, and 1-arc-second DEM can be displayed at scales of 1:6,000, 1:20,000, and 1:60,000 respectively. The objective in this equation is to match data spatial resolutions, which should support improved data integration within a database.

A third relationship, defined by Patterson (2012), relates the spatial resolution of a raster to mapping scales for a Web Mercator display. This is the only relationship specifically designed for raster data display. Spatial resolution is calculated by determining the number of pixels that are required to circle the equator at a given zoom level. The number of pixels at the equator can be calculated as 2(zoom level). For the USGS DEMs, mapping scales of approximately 1:9,000, 1:36,000, and 1:144,000 are appropriate. The downside to this equation is that the scale isn't a direct input. Instead, it depends on the display resolution, which for a Web Mercator map can be directly related to a mapping scale. Although this isn't likely to be the go-to solution for many cartographers, it provides insight into an alternative method of relating data's spatial resolution to mapping scale.

All three of the suggestions have slightly different mapping scales due to the differences in which the data is expected to be used. While the use of these formulas can be helpful in providing insights, they do not completely solve the problem. Firstly, these methods rely on a

known spatial resolution of the dataset, which becomes ambiguous after altering the attribute resolution. Secondly, the scale-to-resolution relationships characterize data as a homogeneous unit and ignore data-specific characteristics such as terrain roughness or attribute detail. Without acknowledging terrain characteristics, inappropriate or unexpected over-generalization or under-generalization may occur per the map's purpose. In other words, these equations only address one specific control of the generalization process and must be adjusted according to the others.

2.7 Documented effects of generalization and needs of generalization products

Raster datasets that represent natural features are susceptible to changes in scale and resolution. Some note that terrain is only effective for a scale change of 2 times the compilation scale without generalization being applied (Brewer and Buttenfield, 2010; Mark, 1991). Steward (1974) identifies several agencies that define scale ranges where large scale maps are frequently considered to range between 1:5,000 and 1:100,000. The appropriate mapping scales for USGS DEMs calculated above mostly fall within this range. Therefore, the process of generalization is becoming an increasingly important requirement for cartographic products.

In today's era of Google Maps and other map viewers, multiple representations of data layers are used to provide a smooth and effective transition through scale. To meet this goal, multi-resolution databases are used that store duplicate pieces of data with varying detail which call for different Levels of Detail (LoDs) based on the current mapping scale (Brewer and Buttenfield, 2007; Frank and Timpf, 1994; Kilpeläin and Sarjakoski, 1995). It is understood that many types of data (terrain, hydrography, road networks, urban areas) have structural scale dependencies. Some researchers have used these dependencies in a way to create multi-scale databases that hold the critical structure features of these data (Clarke, 1988; Chaudhry and

Mackaness, 2010) to easily create LODs for multiple scales. The multiple representations of data require a seamless transition between layers of the same theme (i.e. terrain to terrain or hydrography to hydrography) and support of vertical integration between themes (i.e. terrain to hydrography).

With the use of generalization well established in creating multiple representations of data, it is just as important to understand what types of uncertainties or error are introduced to the data through the generalization process. While cartographic generalization results should never be used for model purposes, a brief examination can provide insight into expectations of vertical data integration. Barber and Shortridge (2005) resample very fine spatial resolution DEMs to coarser spatial resolutions and make comparisons to USGS derived DEMs. When hydrologic modeling was conducted on the resampled DEMs, comparisons were equivalent to that derived from USGS DEM data, implying that such fine spatial resolution data can be effectively generalized when comparing to third party datasets of similar spatial resolutions. However, as discussed earlier, USGS DEMs still have a relatively fine spatial resolution. An initial generalization of a fine spatial resolution data tends to improve feature delineation (Clarke and Lee, 2007) however, the results tend to become worse if the generalization is too aggressive or the spatial resolution change is too great (Wu et al., 2005; Usery et al., 2004).

Few works have studied this effect directly on hillshades, but some work has examined the effects of spatial resolution on output terrain derivatives (Chang and Tsai, 1991; Carter, 1992; Kienzel, 2004). It is common practice to generalize a DEM before generating a cartographic derivative (i.e. hillshade). By studying the resulting terrain derivatives, insights into how a hillshade may react after constructed from a generalized surface can be derived. One of the critical aspects identified in these studies were the sensitivity of landscape type. Slope

calculations were frequently more deranged in areas of steep slope while aspect was deranged in areas of low slope. Like a shaded relief, both of these terrain derivatives are continuous datasets however, aspect is often represented as discrete data. Identifying some assumptions here may provide insight into expected effects on generalized hillshades.

While extensive literature exists on exploring the effects of generalization on data, until recently, little has been done to on generalization evaluation to ensure the generalization process was successful and meets the cartographer's needs. In response, Bard (2004) implements a sort of quality assessment using three steps including characterization, evaluation, and aggregation functions. The characterization defines how features should appear at multiple scales in terms of individual characteristics and geometries. Evaluation assesses if the generalization process has met the criteria set forth by the characterization definitions. The final function, aggregation, compiles the feature-by-feature evaluations into a report of the effectiveness of the generalizations. If the results are unsatisfactory, the process must be redone or refined to produce an adequately generalized map, formalizing a sense of an iterative process via a feedback loop. Mackaness and Ruas (2007) also suggest that in addition to evaluation of the generalization process, the efficacy of the symbolization in the map's design is just as important.

2.8 Summary

This chapter has provided an overview of the generalization process for terrain data. To accommodate the generalization for scale change, it has been shown that many cartographers focus on the resolution-to-scale relationship. However, this relationship becomes ambiguous when the generalization process involves numerical generalization operators that alter the attribute resolution opposed to spatial resolution. The following chapter will identify a

methodology that will alleviate some of this ambiguity of the resolution-to-scale relationships when numerical generalization such as smoothing is applied.

Chapter 3. Methodology

3.1 Introduction

As cartography has shifted from manual to digital practice, cartographers have created and refined digital software to perform generalization. From this, a vast literature pool has been developed on raster based generalization including many "best-practice" guidelines. Included in these guidelines are the mathematical relationships developed that relate spatial resolution with scale. Yet, little attention has been paid beyond this, such as how the operators of generalization specifically alter attribute resolution.

The modification of attribute detail in Digital Terrain Models through the generalization process of smoothing will be examined. While it can be assumed that the smoothing process will simplify the terrain through reduction of attribute complexity, the rate of generalization, variations for different landscape conditions, and any intermediate attribute resolutions are unknown after iterative filtering.

This chapter will lay out the framework used in this thesis to examine how attribute resolution is changed after filtering a DEM. Data used in this project will consist of the U. S. Geological Survey's National Elevation Dataset and will be taken from various parts of the United States to understand how the effects of generalization vary in different landscapes. Data will be iteratively filtered using a Gaussian filter and will be compared to coarser spatial resolution data using statistical and geostatistical methods. When a generalized DEM can be declared as structurally similar to a coarser spatial resolution, the attribute resolution can be considered to have changed. A final step to analyze data integration will be conducted. Here, an un-generalized vector line dataset will be overlaid with the generalized DEM and checked for

percentage of line correspondence, or how well the vectors align with the DEM, effectively measuring vertical integration.

3.2 Data and Study Sites

As discussed in the previous chapter, there are many elevation datasets that are readily available, varying in terms of data quality and spatial resolution. Data used in this thesis are part of the National Elevation Dataset (NED), a multi-resolution, seamless, national coverage product developed by the U. S. Geologic Survey (USGS) (Gesch, 2007; Gesch et al., 2002). Currently, USGS's *The National Map* portal hosts three layers in the NED, including 1-, 1/3-, and 1/9-arc-second data, referred to as 30-, 10-, and 3- meter through the remainder of this thesis (Gesch et al., 2009). These three NED layers are an optimal choice for analyzing the effects of generalization because of the large range of spatial resolutions available and their conformity to existing accuracy standards.

3.2.1 The NED and Study Site Selection

One goal of this project is to identify how the generalization process differs among landscapes. The need to tailor generalization processing to specific landscape characteristics has been demonstrated for hydrography (Buttenfield et al., 2011; Stanislawski and Buttenfield, 2011), for transportation networks (Stanislawski et al., 2012 a; c), and for elevation-derived streams (Stanislawski et al., 2012b). In order to understand how the generalization differs among landscape characteristics, a total of eight study areas are used (Figure 3.1).

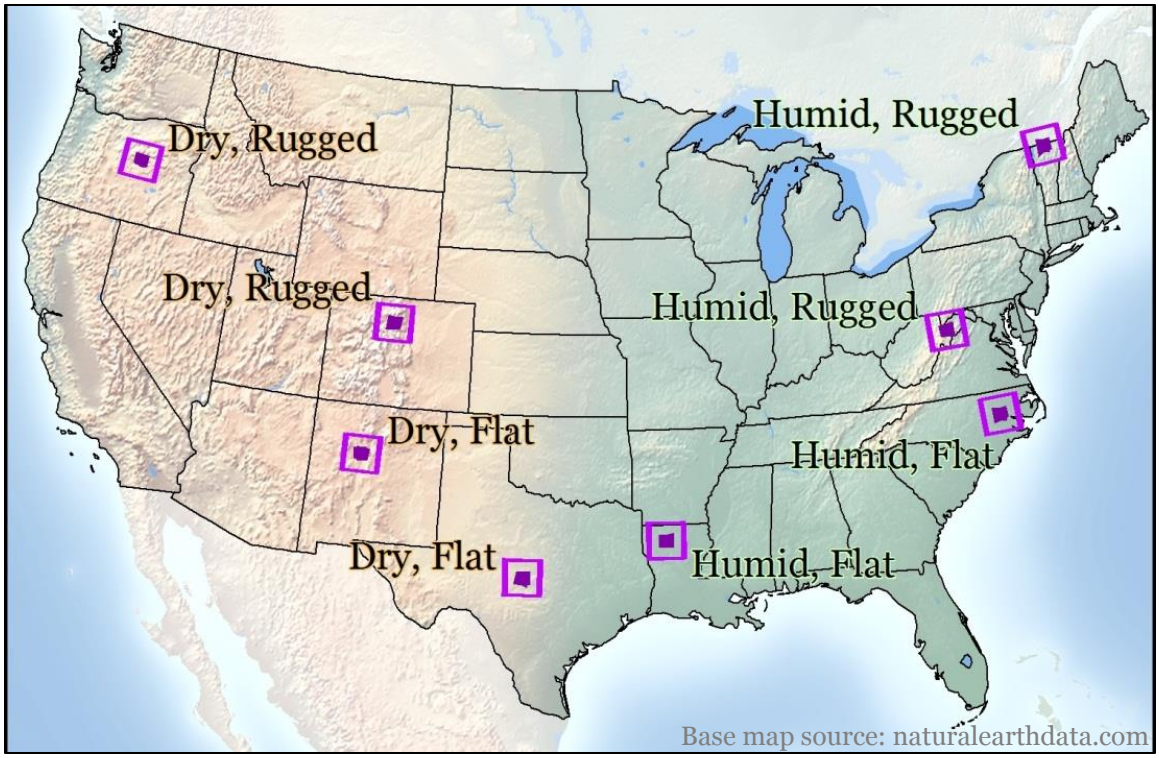

Figure 3.1: The distribution of the eight study areas to be used.

The study areas were chosen based on aridity and terrain ruggedness and guided by the landscape characteristics and partitions defined by Buttenfield et al. (2011) and Stanislawski et al. (in press). "Runoff estimates in millimeters per year (mm/year) for the 5-km cells were obtained from James Falcone and Dave Wolock of the USGS. Estimates were developed using the water balance model (Wolock and McCabe, 1999) that estimates watershed annual runoff mean from 1951 to 2000. The model only considers the effects of precipitation and temperature, but not other factors, such as land use, water use, or regulation" (Stanislawski et al., in press).

Because the 3-meter spatial resolution of the NED is available only for specific portions of the conterminous United States, the selection of study areas are somewhat restricted. The study areas are categorized into four landscape partitions including humid-rugged (Vermont, West Virginia), humid-flat (Louisiana, North Carolina), dry-rugged (Colorado, Oregon), and dry-flat (New Mexico, Texas).

Each landscape partition consists of two study areas and each study area consists of two neighboring USGS 7.5 minute quadrangles (Figure 3.2). The duplication in each study area and landscape partition will allow for comparison and quality checking, ensuring consistency of results.

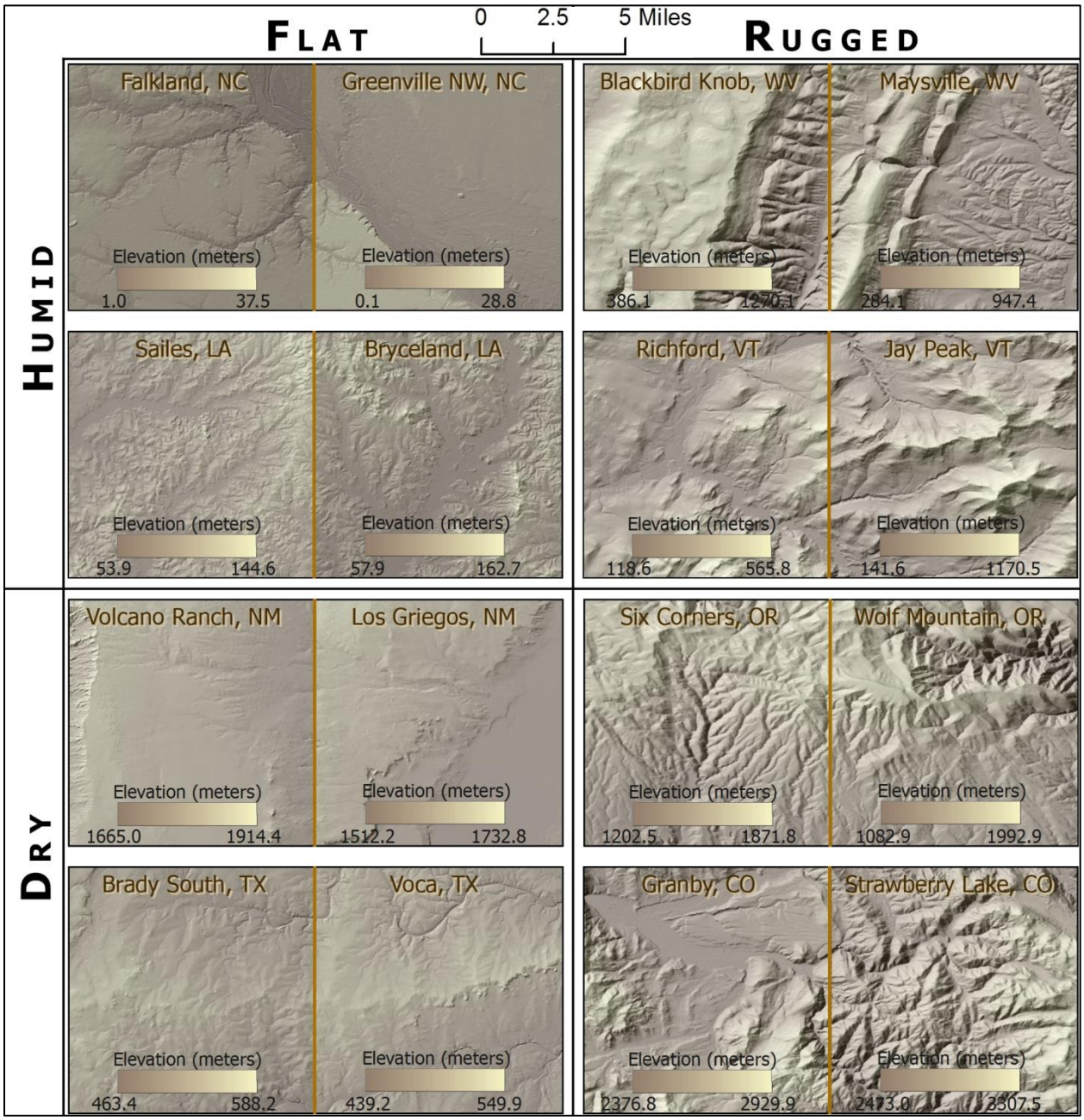

Figure 3.2: Sample shaded relief of each study site categorized by landscape characteristics. Maps shown here are at a scale of 1:365,000.

3.2.2 Benchmark Data

The thesis will accomplish the task of identifying new attribute resolutions by comparing filtered data with other datasets, referred to as "benchmarks". A vector and raster benchmark will be used during the analysis.

The analysis will use the 10-meter and 30-meter DEMs that exist in the NED as raster benchmark. The benefits of using the NED as the benchmark dataset is that it provides a large range (3x to10x change) in cell size. These benchmark DEMs will be useful because they were generated independently from DLGs, yet all conform to similar national mapping accuracy standards.

The vector benchmark will be provided by the National Hydrography Dataset (NHD), which consists of streams for the conterminous United States at two compilation scales (1:24,000 or high resolution, and 1:100,000 or medium resolution), along with densification of selected 1:24,000 streams to 1:5,000 scale (local resolution). These represent spatial resolutions of 12- and 50-meters respectively (2.5-meters for the 1:5,000 densification), and feature detection resolutions of 24- and 100-meters respectively (Tobler, 1987); and are therefore similar to that of the DEMs provided in the NED. The NHD benchmarks will be used during the vertical integration analysis.

3.3 Processing

The 3-meter DEM will be used as the test dataset and will be iteratively filtered 100 times. Common filters used for image processing include frequency filtering and spatial filtering. Spatial filtering passes a moving window to calculate a new value for the central cell using a kernel, or set of weights. This type of function is commonly referred to as convolution

(Burrough and McDonnell, 1998). Examples of commonly applied filters are band-pass filters that either preserve low frequencies (smoothing) or high frequencies (edge enhancement). This thesis will focus on low-pass frequency filters.

3.3.1 Focal Smoothing – The Gaussian Filter

Gaussian filters use a weighted average kernel that represents a two-dimensional normal distribution. Because it is a radial kernel, the smoothing is performed in all directions equally, removing directional biases. The Gaussian filter is effective for preserving local features (Jain et al., 1995). When considering small terrain features, it is especially important that local maxima and minima are not completely removed after multiple filtering iterations.

The Gaussian filter that will be used in this thesis will be a 3x3 weighted average using $\sigma = 0.8$. The sigma value determines the shape, or spread, of the normal distribution to be used. Values greater than 1.0 yield a distribution with a larger spread (i.e. the weights are spread over a larger focal window); values less than 1.0 yield a distribution with weights are spread over a smaller focal window. A sigma value of 0.8 produces a weights matrix of:

0.062	0.124	0.062
0.124	0.249	0.124
0.062	0.124	0.062

This weights matrix is useful with using a 3x3 kernel because the sum of weights is 0.995. Maintaining a sum of weights close to 1.0 will minimize distortion of original data values. Gaussian filters traditionally take into account all data values in a dataset with the kernel becoming less and less influential with distance. Using a sigma of 0.8 allows the weights to

taper off to about 0.0 after about one annulus, allowing excess values to be truncated without greatly impacting the result of the weighted average. The 3-meter spatial resolution DEM will be filtered through 100 iterations (Figure 3.3a).

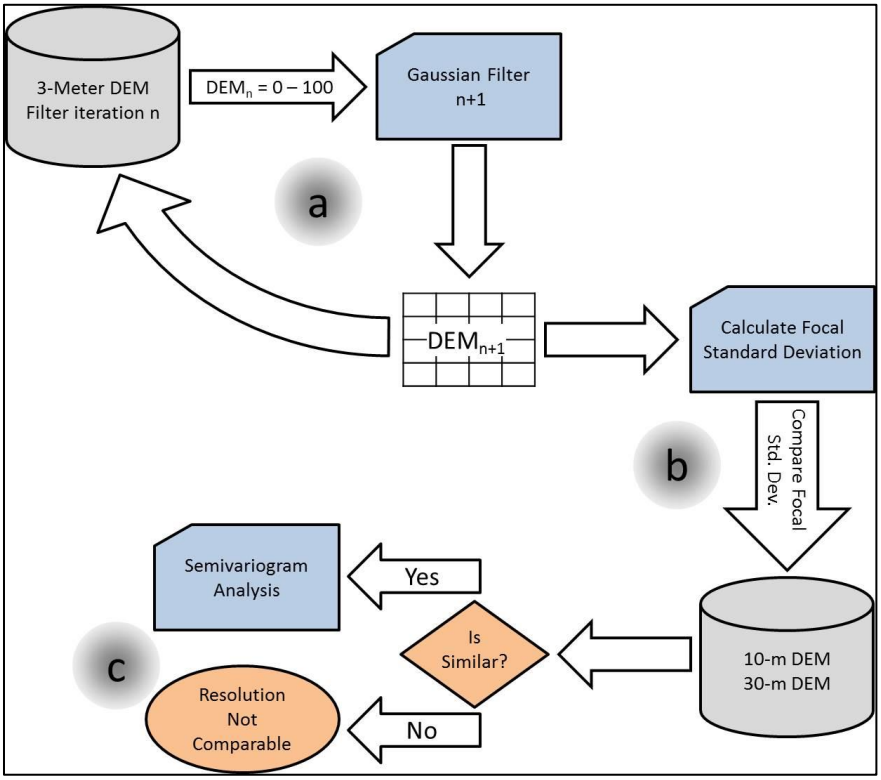

Figure 3.3: Workflow for DEM filtering and attribute resolution detection.

The filtered outputs will be used as inputs for the subsequent filtering iterations to create a cascading Gaussian filter. Computing many filter iterations can be computationally expensive, so many cartographers and image processors filter with a large filtering window. This problem can be addressed using the Gaussian filter's ability to cascade (Jain et al., 1995). Cascading describes how a filter window scales, or how multiple filter iterations of a given window size relate to a single filter of a larger window. Jain et al. (1995) define this relationship as the square root of the sum of squares of the filtering spread. Because this thesis is using the same filter window each time, the equation can be simplified as:

$$R = \sqrt{n \cdot r^2}$$

Where:

R is the radius of the single, larger filter window;
n is the number of times the smaller filter is applied;
and *r* is the radius of the smaller filter window that is iteratively applied

The radius of the Gaussian Filter is equivalent to half of the filtering window. In the case of using a 3x3 cell neighborhood definition, the radius would be 1.5 cells. The cascading property will permit iterative filtering using smaller focal windows to achieve the same effect as a single, larger focal window. Data will be filtered iteratively using a 3x3 cell focal window (r = 1.5). After 100 iterations (n = 100), the output result will be comparable to a single filter iteration using a 550x550 cell focal window (R = 225).

3.3.2 Potential Problems of Processing

A negative impact from filtering spatial data iteratively is the edge effect. Edge effects become problematic when performing a spatial analysis on a study area with an arbitrary border where neighbors outside of the study boundary may influence a process within the study boundary (Fotheringham and Rogerson, 1993; Griffith 1980). This is most common in point pattern analysis, but can also impact a non-stationary process encoded as a continuous surface.

The boundary problem arises from arbitrarily created boundaries which do not take into account the patterns of the underlying data, which is particularly important for this project which uses a gridded 7.5 minute quadrangle boundary that ignores terrain features. A more proper designation of study areas would use watershed boundaries that follow ridge lines and encompass an entire drainage unit. While this would have been a better mapping unit to identify study areas, the shapes and sizes of the watersheds would be inconsistent and possibly ignore opposing sides of the defining ridgelines. Quadrangles remain the best choice for bounding

areas due to manageable processing sizes and built in NED edge effects. Since the NED is compiled on a quadrangle-by-quadrangle basis, the data does not synchronize exactly, causing a slight aliasing-appearance (stair step) along quadrangle boundaries (Gesch, 2007).

The boundary problem is part of the Modifiable Areal Unit Problem (MAUP) (Openshaw, 1983). MAUP is derived from data collected at arbitrary spatial units and can be considered in terms of scale and shape. At various scales and levels of aggregation, descriptive statistics will systematically vary. At larger aggregation units, much of the variance within the underlying data is lost. The shape of the aggregation unit re-addresses the boundary problem in terms of appropriately capturing directional trends within the aggregation area. The focal question of determining the shape of an aggregation unit is, 'how well is the variance retained within the aggregation shape?' Openshaw (1983) states that MAUP is often thought of as an "insolvable problem" or can be effectively ignored by "assuming it away" but goes on to argue that it is "endemic to spatial studies" and methodology should be developed to handle MAUP in a purposeful way. Some techniques have been developed to mitigate effects of MAUP such as image buffering and the use of decay functions for image processing and filtering (Ge and Cheng, 2007).

The problems of edge effects will be addressed in several ways. To reduce the impact of edge effects in the filtering process, a one-cell border will be removed from the DEM each time it is filtered. This will prevent errors caused by the border edges and inappropriate filtering weights from creeping into the center of the DEM through the iterative filtering process. Since each study area is approximately 4000x4000 cells, removing 100 cells from all sides (~0.1% of total cells) should not impact any global calculations.

3.4 Detecting Attribute Resolution Changes

Each filter iteration will be compared to the benchmark DEMs provided in the NED (Figure 3.3b, c). Comparing filtered data to DEMs with known coarser spatial resolution will determine the rate of attribute resolution change and how many filtering iterations (which Gaussian window size) are required to produce these coarser spatial resolutions. This methodology will involve a two-step sequential process by comparing local variance within the data using descriptive statistical (standard deviation) and geostatistical (semivariogram) methods.

3.4.1 Standard Deviation Analysis

Standard deviation is frequently used in measuring surface roughness because it is a stable metric for assessing vertical ruggedness of terrain compared to the range or inter-quartile range of the data (Evans, 1972). Mark (1975) overviews several vertical and horizontal measures of surface ruggedness including relief, slope, slope and aspect dispersion, and hypsometry. He identifies several measures within each category and which of these can often be skewed by local extremes that hide major relief characteristics. Standardizing data by examining standard deviation of these metrics is a common practice in analyzing surface roughness and is still done today (for example, see Frankel and Dolan, 2007; Grohmann et al., 2010).

Standard deviation is defined as the square root of the average of the squared deviations about their mean (Burt et al., 2009). Just like the mean, the standard deviation is sensitive to skewed data and can be highly influenced by outliers. As data is filtered using a mean function, the standard deviation of data will continue to become smaller. Thus, the standard deviation is a useful measure for assessing homogenizing attribute complexity. As elevation values are

incrementally homogenized within a focal window, a new attribute resolution can be considered to have been created. The question is, how many iterations introduce sufficient change in standard deviation to incur a meaningful change in spatial resolution?

Due to the ecological fallacy problem, calculating the global standard deviation for an entire DEM will be inappropriate. As the aggregation unit increases in size, the summary statistics will become biased (Robinson, 1950; Diez-Roux, 2003). The 3-meter grids used for each study site are about 4000x4000 cells in size. A global metric from a grid this large will essentially be grouping 16 million individual observations. To overcome this, a local (focal) standard deviation will be examined. This will aggregate individual pixels into larger units and will likely be more "true" to the micro-scale heterogeneity created by the filtering window. In order to compensate for edge effects, the focal standard deviation will only be calculated for cells whose focal window will be fully contained within the data. In a similar manner to the cell removal in the filtering process, if a focal window of 3x3 is used, the focal cell must be 1 cell away from the DEM boundary; if the focal window is 10x10, the focal cell must be 4 cells away from the DEM boundary.

The rate of change in attribute resolution after each filtering iteration is dependent upon the filtering algorithm used and the landscape type, and is unknown before the application of the filter. Calculating standard deviation within the focal window will help to describe the rate of change by measuring the variation of attribute values, or the rate of homogenization of the data. The assumption in using 100 iterations is that changes to attribute resolution will be insignificant beyond 100 filtering steps. To associate filtered data with a specific attribute resolution, focal standard deviations of the filtered datasets will be compared to focal standard deviations of the benchmark DEMs. By relating the attribute resolution of a generalized dataset to the attribute

resolution of a known spatial resolution, one can identify when the appropriate scale of use has changed and identify the rate of spatial resolution change.

A 3x3 cell focal standard deviation will be calculated for the 10- and 30-meter benchmark DEMs. In order to make comparisons more interpretable, the mean of these values will be used to generate a single, aggregate focal standard deviation statistic that can be used as a benchmark value. When comparable focal standard deviation values are observed between the filtered DEM and benchmark DEM, the attribute resolution will be considered to have changed enough that the filtered DEM is appropriate for representation at the benchmark DEM spatial resolution(s).

If the focal standard deviation of the 3-meter DEMs are calculated using a 3x3 cell window, accurate comparisons to coarser spatial resolutions will not be possible. In this case, the ground distance of a 3x3 cell window will cover an area of 9x9 meters, while a 3x3 cell window will cover areas of 30x30 meters and 90x90 meters for the 10- and 30-meter DEMs. To nest DEM pixels among filtered and benchmark DEMs, two focal standard deviation statistics will be calculated for each filtered DEM. The first focal window will be 10x10 cells in size, which will cover an area of 30x30 meters, equivalent to the 10-meter benchmark DEM. The second window will be 30x30 cells in size, which will cover an area of 90x90 meters, equivalent to the 30-meter benchmark DEM. This conformity will help in overcoming varying areal sizes when calculating an aggregated statistic based on individual samples.

Although using standard deviation can be useful for approximating attribute resolution change, it will be unable to precisely predict change due to edge effects and the nature of "implicit" resolution change. Spatial autocorrelation will help to refine the prediction by measuring the similarities between the filtered DEM and benchmark DEMs at a range of scales

(local to global). Once the focal standard deviation statistic identifies the change in attribute resolution, that filter iteration will be examined more closely. Since spatial autocorrelation is scale dependent, the use of a semivariogram will describe the autocorrelation at varying lag distances.

3.4.2 Semivariogram Analysis

A semivariogram plots the semivariance against distance (Cressie, 1993; Isaaks and Srivanstava, 1989). The semivariance at a given lag distance is defined as:

$$\gamma = \frac{\sum_{i=1}^{n}(x_i - y_i)^2}{2n}$$

Where:

γ is the semivariance;
n is the number of sample points; and
x and y are a pair of sample points

When plotted, the semivariogram describes the variation of all data points from one another. However this can be extremely computationally expensive, generating a total of (n)*(n-1)/2 data points (Burt et al., 2009). Experimental, or empirical, semivariograms do not take into account all the points of a dataset, but only a subset or sample. These can be useful because they are frequently a good estimator of the theoretical semivariogram's characteristics. A model is fitted to the empirical semivariogram to describe the rate at which semivariance changes with distance.

The semivariogram model is made up of three "parts" including the nugget, sill, and range. The nugget represents micro-scale heterogeneity within the data and is frequently used as an error term for the variogram model. The sill is the largest semivariance reported in the semivariogram, and is often noted by a "leveling-off" of the variogram model under a stationary

process. The range is the lagged distance in which the sill occurs. This is an important value when considering the sphere of influence in autocorrelation. The range represents the maximum distance in which the value at one point will influence the value of another. This can be interpreted as the "characteristic length of the geographic distribution of a variable" (Goodchild and Proctor, 1997). Because it is unlikely to observe a sill empirically, the range will be the maximum lagged distance (Burt et al., 2009).

Semivariograms carry the assumption of stationarity, or the assumption that a process does not change over space (O'Sullivan and Unwin, 2010). Stationarity is often broken into two categories including 1st-order and 2nd-order. First order stationarity indicates that there is no variation in intensity of a process over space while second order stationarity indicates that there is no interaction between samples over space (O'Sullivan and Unwin, 2010; Cressie, 1993). Conversely, a non-stationary process indicates that the process is changing over space and results in a semivariogram with the semivariance increasing indefinitely with lag distance.

Non-stationarity indicates an underlying process that influences the sample values which has not been accounted for and is often referred to as spatial drift. (Chilès and Delfiner, 1999). The effects of spatial drift can often be handled by recalculating the semivariogram based on the residuals of a trend surface. Alternatively, non-stationarity may be avoided by accounting for an underlying anisotropic trend in the data.

Two sets of semivariograms will be created. The first will be within the focal window of the standard deviation analysis. This will allow for a focused examination of how the iterative filtering will alter the DEM at a local scale. The second will be across the entire study site which will allow for examining how the filtering affects the DEM at a global scale.

Comparing empirical semivariograms between filtered DEMs and benchmark DEMs will provide insight into how the attribute resolution matches at various scales, from within the focal standard deviation window to the entire study site. The degree to which the variograms interact will confirm the appropriateness of attribute resolution change defined by the standard deviation. Because creating semivariograms can be computationally intense, only the filtered DEMs that are defined as being most similar to the benchmark DEMs will be used in this stage of the analysis. By examining the filtered DEM semivariance to the benchmark DEM semivariance, the autocorrelation can be assessed across the DEM as a whole.

The empirical semivariograms will be calculated by randomly selecting 10,000 points and finding a paired neighbor at a randomly generated angle. The semivariance will be calculated among the 10,000 point pairs and will be recorded. This process will provide the semivariance value at a given lag distance and will be repeated for each lag. The process will be repeated 500 times to create a distribution of semivariances for each lagged distance.

In order to calculate the lag distance or the number lags required to build an appropriate semivariogram, the following rule of thumb (Burrough and McDonnell, 1998) will be used:

$$\#\ lags = \frac{{}^{1}/_{2} \cdot max\ distance\ between\ points}{lag\ distance}$$

The maximum distance between any point pair will be along the diagonal of the DEM, and is 16,970 meters for all study sites. Burrough and McDonnell (1998) suggest that the number of lags necessary to achieve a stable semivariogram is at least 50 to 100. This implies that the lag sizes will appropriately range between 85 meters and 170 meters.

Due to the amount of time required to build a semivariogram, 50 lags will be used when calculating the semivariogram of the entire study site. This means that the lag distances will be

170 meters. This should provide enough lags to represent the spatial dependencies within the data. When calculating the semivariograms within the focal standard deviation window, a lag distance of 1 cell will be used. This will relate to a distance of 3-meters, 10-meters, or 30-meters depending on the source DEM's spatial resolution. Therefore, the number of lags will vary. The 10- and 30- meter benchmark DEMs will each have 3 lags. The 3-meter DEM will either have 10 or 30 lags depending on what benchmark the semivariogram will be compared against. The number of lags and lag distances for the semivariograms within the focal standard deviation window don't conform to traditional ways of constructing a semivariogram. However, the purposes of constructing these are to closely examine the micro-scale fluctuations of semivariance and better understand the spatial structure for each filtered DEM and how it compares to the benchmark DEMs.

By plotting the maximum and minimum observed semivariance values for each lag distance, a semivariance envelope (similar to a confidence interval) of the "true" semivariance can be approximated for every DEM. This will be done for the filtered DEM and its benchmark counterpart. By comparing the semivariogram of a filtered DEM to the semivariogram of a benchmark DEM, the attribute resolution can be compared at many lag distances, or scales. When the semivariogram envelope of the filtered DEM nests completely within the envelope of the benchmark DEM, one can accept that the attribute resolution is appropriate at all lags. When the filtered DEM semivariance is greater than the benchmark, the data can be considered to be under-generalized leaving too much detail; when the filtered DEM semivariance is less than the benchmark, the data can be considered to be over-generalized and too much detail has been smoothed away (Figure 3.4).

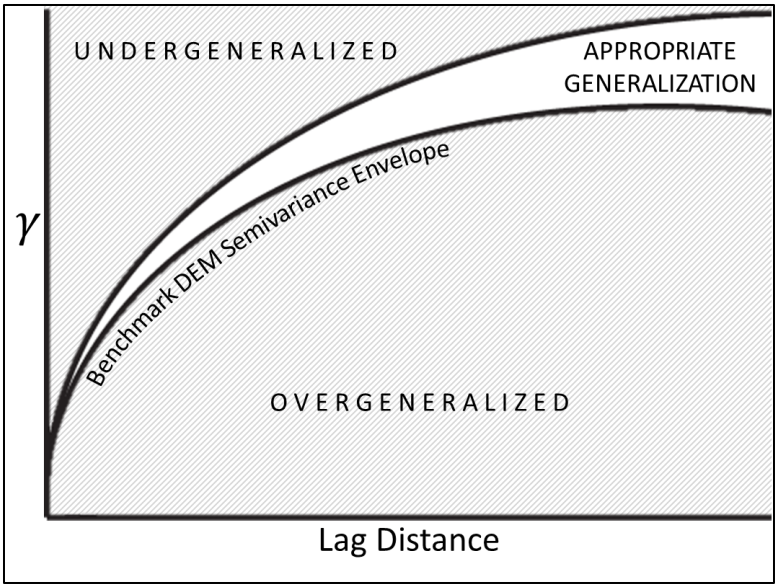

Figure 3.4: A semivariogram envelope of a benchmark DEM will be used to approximate generalization appropriateness of a filtered DEM.

It is expected that the semivariograms calculated for the DEMs will show similar characteristics as represented in Figure 3.4, where there is a small range between minimum and maximum semivariance for small lags and a large range for large lags will exist. In this case, it may be difficult to interpret the best match at all scales. While the level of match for the entire semivariogram will represent overall similarity, the degree of match at small lags is much more important because it will represent the micro-scale homogeneity that is being created by the filtering window.

The semivariograms will be compared in two ways. The first way is to visually compare the general shapes of the semivariogram models. Questions to consider here include: 1) are the semivariogram models similarly structured in terms of the nugget, sill, and range; 2) are the slopes of the semivariogram models comparable; and 3) what is the relative placement of the semivariogram models to one another. The semivariogram structure will provide information on whether the similar features are being identified in the DEMs. The slope of the variogram models will provide insight into the overall rate of change in attribute resolution across multiple

scales within the DEMs. The relative placement of the semivariogram models in relation to one another will suggest the appropriateness of the generalization by comparing the similarity of spatial dependency at a given lag distance. The second method to compare the semivariograms will be to compute the overlap of the semivariogram envelopes. This will provide an empirical way to compare the similarity of the semivariograms. If the envelopes overlap with a rate of 100%, they will be considered to be identical in terms of spatial dependency within each DEM.

3.5 Assessing Vertical Data Integration: Conflation Analysis

The effects of cartographic generalization are often unknown before generalization and tend to be much more serious than the effects caused by model generalization (João, 1995). To understand and quantify these effects, many types of generalization evaluation tools have been developed. Mackaness and Ruas (2007) divide evaluation tools into three categories, including evaluation for tuning (before), controlling (during), or assessing (after) the generalization process. Because this thesis is devoted to understanding the repercussions of iteratively filtering terrain, an assessment tool will be used to explore the generalized data's fitness for use.

A final requirement of terrain on a map is the ability to vertically integrate with other datasets, or how well multiple data layers, for example hydrography or transportation, synchronize with terrain. Filtering data and changing attribute resolution will slightly alter the position of landscape features. This could be exemplified by a minor shift in a ridgeline that forces a stream headwater to start on one side of a ridge and flow to the other side. This shift in position may corrupt the alignment of overlaid vector layers (transportation, hydrography, contours) that may have been generated at a different spatial resolution. It is important to

understand how topology is changing and to what degree vertical data integration problems are introduced by filtering in the various landscape types.

Positional distortion will be measured by extracting vector streams from the filtered terrain and applying a conflation metric to compare extracted, or elevation-derived, streams with a vector benchmark at standard mapping scales. A comparison of the elevation derived streams (EDS) from filtered DEMs to benchmark NHD streams will estimate the degree of successful data integration. The conflation metric to be applied is the Coefficient of Line Correspondence (CLC) (Stanislawski, 2009), which is an analytical form of vector overlay, analogous to the Coefficient of Areal Correspondence (CAC) (Taylor, 1977). The CAC measures the percentage of polygon overlap between two datasets. Similarly, CLC measures the percent match between two polyline datasets.

Conflation was examined using the CLC toolbox developed, researched, and distributed by Buttenfield et al. (2011). Specifically, CLC measures the length of matching confluence-to-confluence stream channels as a proportion of omissions and commissions. Omissions are defined as channels that are present in the benchmark NHD but not the elevation derived streams layer; commissions are the channels that are present in the elevation derived streams layer but not in the benchmark NHD dataset. The coefficient is computed as follows:

$$CLC = \frac{\sum conflations}{\sum conflations \ + \sum(omissions + commissions)}$$

Where:

conflations is the length of matching channels
omissions is the length of channels in benchmark but not in test data
comissions is the length of channels in test data but not in benchmark

The first step of the conflation assessment is to extract EDS from the filtered DEMs. These streams will be compared against the NHD high and medium resolution flowlines. To

ensure consistency, the EDS are extracted to have similar characteristics (i.e. total length and number of confluence-to-confluence features). Filtered DEMs have sinks removed and flow direction computed. A weighted flow accumulation is then created and tailored to preserve physiographic variation in hydrology (Buttenfield et al., 2011; Stanislawski et al., in press). Stream lines are then iteratively extracted from the flow accumulation until their characteristics are within a given threshold of the benchmark lines. The EDS are then enriched with stream order, confluence identifier, and upstream drainage area. Short first-order tributaries are pruned to remove excessive detail and simplified to reduce aliasing from the raster to vector conversion.

The second step of the vertical integration evaluation is to compute the CLC between the NHD benchmark and the EDS streams layer. Line segments will be defined as matching if they are within a given buffer area of one another. This buffer distance conforms to USGS accuracy standards (USGS, 1999) of 0.5 millimeter, at scale, which is approximately 12 meters on either side of the line for a 1:24,000 map or 50 meters for a 1:100,000 map. Confluence-to-confluence features that are more than 50% within this buffer distance are considered to be matches. Mismatches can be categorized based on omissions or commissions.

Filter iterations that have been identified to match the attribute resolution of the 10-meter benchmark DEM will have the CLC performed using the high resolution (12-meter) NHD benchmark at a mapping scale of 1:24,000. Filter iterations that have been identified to match the attribute resolution of the 30-mter benchmark DEM will have the CLC performed using the medium resolution (50-meter) NHD benchmark at a mapping scale of 1:100,000. While the anticipated DEM attribute resolution doesn't exactly match that of the NHD benchmarks, they are sufficiently close to be used for comparison.

The CLC metric ranges between 1.0 (perfect line match) and 0.0 (no line match). CLC values of 0.7 and better have been acknowledged to be an acceptable level of consistency (Buttenfield et al., 2011; Buttenfield et al., 2010), but the metric lacks a known distribution for inferential purposes. For this reason, CLC can be computed for a sample of points within 200 grid cells overlaid on the study area to support a bootstrap computation that permits computation of a confidence interval. This additional step has not been undertaken in this analysis and thus the evaluation is exploratory rather than confirmatory. The CLC metric will identify the degree of conflation between the NHD benchmark streams and the valley lines within the filtered DEMs. The rate of vertical integration will provide a sense of appropriateness of the generalized DEMs at matching the benchmark DEMs.

Because the CLC metric is being used for exploratory purposes, mapping the spatial distribution of conflations, omissions, and commissions will assist in manual interpretation of matches and mismatches. By visualizing the results, spatial patterns of omissions and commissions can be observed. Many factors can influence the CLC results including NHD benchmark compilations, presence of complex hydrographic features (braided streams, pipelines, agricultural ditches, etc.), and complete containment of natural watershed boundaries. The mapped streams that match and mismatch and can be further categorized into such groups and better describe and understand the resulting CLC values.

3.6 Summary

This chapter has laid out the framework of the methodology used in this thesis to determine attribute resolution change and fitness for use of generalized products. A 3-meter DEM will be iteratively filtered with a 3x3 cell focal window using a weighted (Gaussian) mean.

The filtered datasets will be compared coarser spatial resolution DEMs from the U.S. Geological Survey's National Elevation Dataset. To determine if the attribute resolution of a filtered dataset has become similar to that of the coarser spatial resolutions, focal standard deviation and semivariogram analyses will be used to determine filtering iterations that are most similar. The filtered DEM's fitness for use, vertical data integration, will be explored using the Coefficient of Line Correspondence to measure the degree of conflation between stream features derived from the filtered DEM to an NHD benchmark dataset at a known and similar spatial resolution.

The next chapter will explore the results of filtering and examine how smoothing alters DEM attribute resolution. These results will supply evidence to answer the key questions of this thesis including the rate of attribute resolution change and vertical integration with other vector datasets.

Chapter 4. Results

4.1 Overview of the Analysis

In Chapter 1, two research questions were posed about the impacts of DEM filtering on attribute resolution:

1. What is the rate of attribute resolution change during filtering and how does it differ between various landscape characteristics? Is the rate of change constant for all filtering iterations, or do certain iterations exist where dramatic changes occur?
2. How well does the filtered dataset integrate with other vector layers?

In the last chapter, the methodologies for analysis were discussed to address these questions and examine attribute resolution change. This chapter reports on results of the analysis. In order to examine how DEM attribute resolution is affected by generalization, data was iteratively smoothed 100 times. A number of metrics were applied to assess the change in attribute resolution and compare it to independently compiled benchmarks of equal accuracy. These methods include a focal standard deviation, semivariogram, and conflation analysis. The analyses will determine how the generalization process is altering the DEM's attribute resolution locally and globally as well as how the resulting DEM may integrate with other datasets.

The remainder of this chapter will present results of the analysis. These results will ultimately provide information for matching generalization through filtering to a specific spatial resolution and an appropriate mapping scale.

4.2 Benchmark Datasets

Attribute resolution can be difficult to measure. However, attribute and spatial resolutions are intrinsically related. As DEMs are filtered, a disconnect occurs between spatial

and attribute resolutions. This disconnect was measured by systematically comparing a filtered DEM (of unknown attribute resolution) to a benchmark dataset (of known spatial resolution) to identify how many filtering iterations bring the DEM to an attribute resolution most similar to the benchmark data's spatial resolution.

Raster and vector benchmarks were used throughout the analysis. The raster benchmark was taken from the National Elevation Dataset (NED) (top panels of Figure 4.1). Though the NED consists of several products of varying spatial resolution, only two were used as benchmarks, including the 1/3 arc-second and 1 arc-second, or 10- and 30-meter DEMs respectively. These spatial resolutions were compiled independently using photogrammetric methods and Digital Line Graph interpolations. They are hydrologically enforced and conform to vertical and horizontal mapping accuracy standards (USGS, 1999). The NED benchmarks will be used to directly compare a filtered DEM to known spatial resolutions. This will be done using the standard deviation and semivariogram analyses.

The vector benchmark was taken from the National Hydrography Dataset (NHD) (bottom panels of Figure 4.1). "The NHD is a comprehensive set of digital spatial data that represents the surface water of the United States using common features such as lakes, ponds, streams, rivers, canals, stream gages, and dams." (Simley and Carswell, 2009 p.1) As such, it consists of point, line, and polygon datasets and is mainly used for mapping and analysis due to its rich attribute detail. The NHD is currently available in two spatial resolutions, known as high resolution, based on a 1:24,000 topographic mapping scale, and medium resolution, based on a 1:100,000 topographic mapping scale (Simley and Carswell, 2009; USGS, 2000). In 1999, full coverage for the conterminous United States was made available for these two spatial resolutions. Currently, a local scale resolution is becoming available in select areas and is intended for use at

a 1:5,000 mapping scale. This is frequently a densification of the high resolution data and has been compiled at scales ranging from 1:2,400 to 1:12,000 (Simley, 2012; Simley, 2011). Like the NED benchmarks, the NHD also conforms to horizontal and vertical mapping accuracy standards. The NHD benchmarks will be used to assess the degree of conflation between the filtered DEM and an existing vector dataset to measure vertical integration. Only a subset (flowlines) of the NHD feature layers will be used during this analysis.

Figure 4.1 shows the benchmark data for Jay Peak, VT (see Appendix A for the other study sites). Upon close comparison of the two upper panels, the 10-meter benchmark shows more detail than the 30-meter benchmark due to the difference in spatial resolutions. This can be identified through the slight blurriness of the 30-meter benchmark. The lower two panels show the vector benchmarks. The lower left map is of the 1:24,000 compilation (high resolution) flowlines. The lower right map is of the 1:100,000 compilation (medium resolution) flowlines. The high resolution flowlines have a finer detail because more stream features are represented. Medium resolution streams tend to lack headwater channels for included streams (relative to the high resolution data), and this is due in part to the compilation process. Additionally, when flowlines are represented in both benchmarks, the high resolution features often have more geometric complexity (vertices) in the lines, or show variations in the number of vertices across any quadrangle. Additional vertices reflect local density variations in the stream channels and are evident in the high resolution NHD but largely missing from the medium resolution.

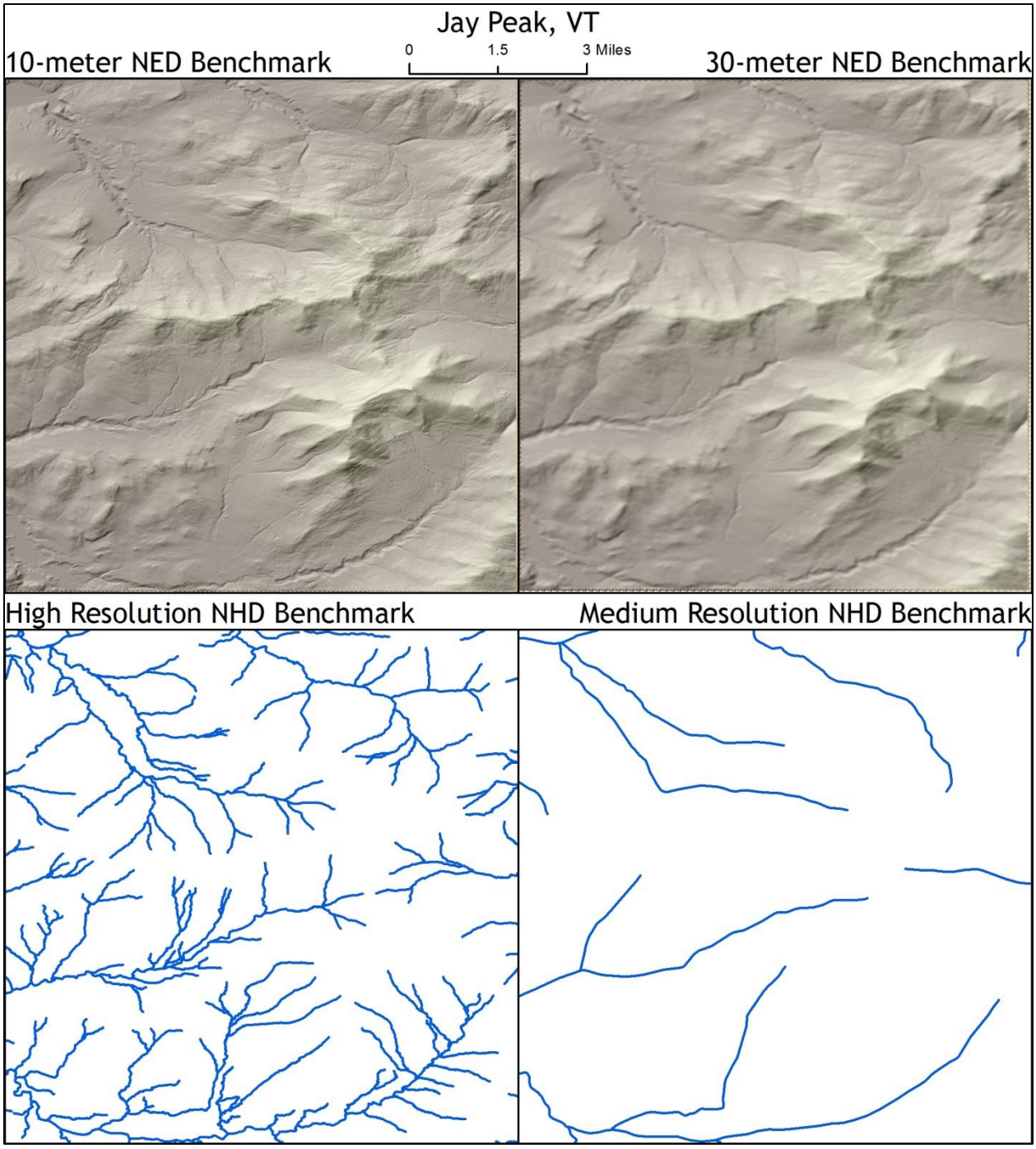

Figure 4.1: Raster and vector benchmark datasets.

4.3 Using focal standard deviation to estimate attribute resolution of filtered DEMs

A focal standard deviation was calculated for each DEM filter iteration on the premise that as smoothing iterations continue, elevation values will more closely approximate a local average. Standard deviations will drop as values become more similar, and the terrain surface

will more closely approximate a terrain surface compiled at a coarser spatial resolution. In order to estimate attribute resolution, the filtered data was compared to National Elevation Dataset (NED) benchmark DEMs of 10-meter and 30-meter spatial resolution. Two focal standard deviations were computed on the filtered 3-meter DEMs. The first is a 10x10 cell window, which covers the same ground size as a 3x3 cell window for the 10-meter DEM. The second is a 30x30 cell window, which covers the same ground size as a 3x3 cell window for the 30-meter DEM.

Table 4.1 shows the focal standard deviations for the benchmark DEMs. When examining the 3x3 cell focal window calculations of all DEMs, the focal standard deviation for the 3-meter DEM is always lower than the 10-meter benchmark, which is always lower than the 30-meter benchmark. The reason for this result is the areal coverage of a 3x3 cell window that has been applied to each DEM. The areal extent of a 3x3 cell window over the 30-meter benchmark DEM is much larger than the 3x3 cell areal coverage of a 3-meter DEM. It is obvious that the terrain will experience more change over a larger area and potentially have a larger range in data values, especially for rugged terrain.

By modifying the area of the focal window, the standard deviation can be standardized and compared more easily with the two benchmark DEMs. A 10x10 cell window used on the 3-meter DEM covers the same areal extent as the 3x3 window for the 10-meter benchmark DEM. Likewise, a 30x30 cell window used on the 3-meter DEM covers the same areal extent as the 3x3 window for the 30-meter benchmark DEM.

Table 4.1: Local standard deviation values of the source (i.e., unfiltered) and benchmark DEMs.

Quadrangle Location	3-m DEM (3x3 cell window; 9m ground size)	10-m DEM (3x3 cell window; 30m ground size)	3-m DEM (10x10 cell window; 30m ground size)	30-m DEM (3x3 cell window; 90m ground size)	3-m DEM (30x30 cell window; 90m ground size)
Granby, CO	0.44	1.28	1.49	3.62	4.23
Strawberry Lake, CO	0.77	2.27	2.65	6.51	7.60
Bryceland, LA	0.19	0.52	0.60	1.34	1.54
Sailes, LA	0.18	0.51	0.59	1.33	1.53
Falkland, NC	0.07	0.17	0.20	0.42	0.48
Greenville, NC	0.07	0.16	0.19	0.34	0.39
Los Griegos, NM	0.14	0.25	0.41	0.72	0.98
Volcano Ranch, NM	0.16	0.35	0.47	0.92	1.16
Six Corners, OR	0.42	1.22	1.43	3.52	4.10
Wolf Mountain, OR	0.53	1.58	1.84	4.56	5.32
Brady South, TX	0.12	0.31	0.37	0.85	1.00
Voca, TX	0.15	0.41	0.48	1.11	1.30
Jay Peak, VT	0.61	1.78	2.08	5.10	5.97
Richford, VT	0.35	0.99	1.16	2.77	3.24
Blackbird Knob, WV	0.49	1.45	1.69	4.15	4.90
Maysville, WV	0.51	1.51	1.76	4.26	5.01

To understand why the focal window sizes need to be modified, examine the focal standard deviations for Blackbird Knob, WV. The standard deviation for the 3-meter test DEM using a 3x3 cell window is 0.49. The standard deviation for the 10-meter benchmark DEM using a 3x3 cell window is 1.45. The 10-meter benchmark standard deviation is much larger than that of the 3-meter DEM but these two values are not comparable due to the differences in areal extent of the window sizes. A 3x3 cell window on a 3-meter DEM covers 81 square meters. A 3x3 cell window on a 10-meter DEM covers 900 square meters. By increasing the focal window size to 10x10 cells for the 3-meter DEM, the focal area now covers 900 square meters and produces a standard deviation value of 1.69 for a comparable focal window size. The standard

deviation of the 3-meter DEM is now greater than that observed in the 10-meter benchmark. Again, this is an expected result since the 3-meter DEM has a higher attribute resolution.

Now that a comparison baseline has been established between resolutions of source and benchmark DEMs, the next objective is identifying rates of attribute resolution change. As the 3-meter DEM is filtered, the two focal standard deviations (10m and 30m) are calculated. The focal standard deviations of each filter iteration were compared to the benchmark DEMs (columns 3 and 5 in Table 4.1) to identify when the filtered attribute resolution approaches the benchmark spatial resolution. When the focal standard deviation of the 3-meter DEM exceeds that of the benchmarks, the attribute resolution will be considered to be finer. When the focal standard deviation of the 3-meter DEM is less than that of the benchmarks, the attribute resolution will be considered to be coarser.

Figure 4.2 compares the standard deviation after each filtering iteration of the 3-meter DEM (solid line) against the benchmark DEMs (dashed line) for Blackbird Knob, WV (See Appendix B for the other study sites). The benchmark spatial resolution lines are flat because this data isn't filtered, that is, these are only intended to be used as a baseline to identify when the filtered 3-meter DEM standard deviation intersects the benchmark standard deviations. These graphs have been separated because they show very different data. As described earlier, the areal extent being examined in each case is different, making comparison difficult between the two graphs' standard deviation values and apparent slopes. What can be compared between the graphs are general trends. In all observed cases, the standard deviation of the 3-meter DEM behaves similarly as the number of iterations increase. The filtering initially removes significant attribute detail (observed by quickly decreasing standard deviation values). However, this trend gradually decays (shown by a flattening curve). This indicates that the rate of decreasing

standard deviation is slowing down or terminating altogether. It is likely that the rate of attribute resolution change would eventually reach zero and that the DEM would become a homogeneous set of elevation values, but this would require an immense amount of filtering, well beyond the scope of this thesis.

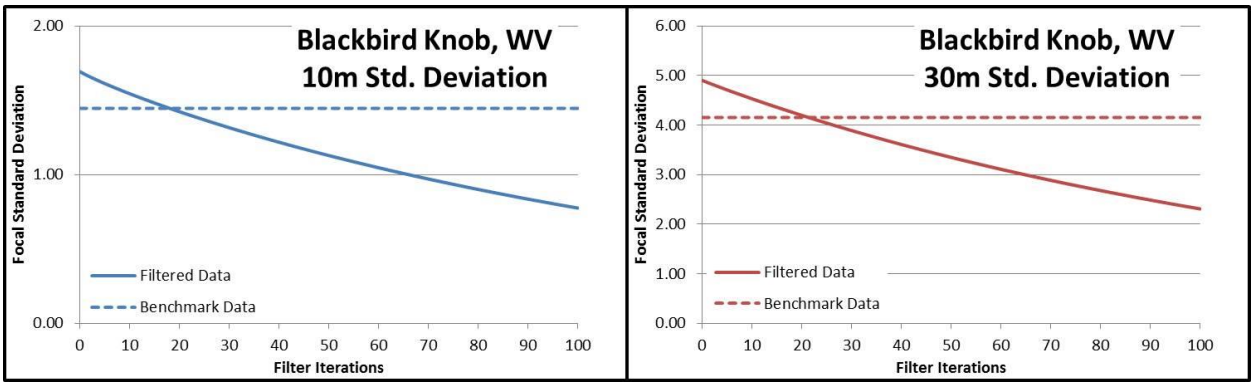

Figure 4.2: Plot of the changing focal standard deviation of the 3-meter DEM through filtering iterations.

Where the two lines cross, the filtered DEM standard deviation is similar to the benchmark value, meaning the attribute resolutions can be associated with a coarser spatial resolution.

Table 4.2 shows all of the study sites ranked by the order in which the attribute resolution is comparable to the 10-meter and 30-meter benchmark spatial resolutions. While the number of filtering iterations required for the 3-meter DEM to match the spatial resolution of the 10-meter benchmark vary (from 5 iterations to 29 iterations), the number of additional filtering required to match the 30-meter benchmark are relatively small. On average, the number of additional filtering iterations for the 3-meter DEM to be comparable to the 30-meter benchmark is 3.25. The two Texas study sites need the most filtering iterations for the 3-meter DEM with a 10-meter attribute resolution to match the 30-meter attribute resolution. However, they only need 5 (Voca, TX) or 7 (Brady South, TX) more iterations. This suggests that, initially, the rate of attribute resolution change is increasing through filtering iterations.

Overall, the flat landscape types approach their 10 meter spatial resolution counterparts in fewer filter iterations than the rugged landscapes. However, there is no clear division in the number of filtering iterations required for an attribute resolution change between flat or rugged landscapes. Two exceptions to the observed trend are the pair of New Mexico study sites (defined as flat and dry), which require the largest number of filtering iterations to match the 10 meter benchmark. The Los Griegos study site also matches the 10- and 30-meter benchmark's spatial resolution at the same filtering iteration. This result may reflect the ways in which the benchmark datasets were generated in that the landscape may not contain landscape features of a size which can be differentiated when generalized from a 10-meter to 30-meter dataset.

Table 4.2: The number of filtering iterations required for a 3-meter DEM to match a coarser attribute resolution.

Climate	Terrain	Quadrangle Location	Standard Deviation matches 10-m DEM (# of filter iterations)	Standard Deviation matches 30-m DEM (# of filter iterations)	Order Displacement
humid	flat	Greenville, NC	5	7	---
humid	flat	Falkland, NC	7	11	---
humid	flat	Bryceland, LA	10	14	---
humid	flat	Sailes, LA	11	15	---
dry	flat	Voca, TX	12	17	---
dry	flat	Brady South, TX	12	19	-2
humid	rugged	Richford, VT	14	18	+1
dry	rugged	Granby, CO	15	18	+1
humid	rugged	Maysville, WV	17	20	---
humid	rugged	Jay Peak, VT	17	21	-1
dry	rugged	Strawberry Lake, CO	18	20	+1
dry	rugged	Six Corners, OR	18	21	---
dry	rugged	Wolf Mountain, OR	19	21	---
humid	rugged	Blackbird Knob, WV	19	22	---
dry	flat	Volcano Ranch, NM	20	22	---
dry	flat	Los Griegos, NM	29	29	---

The last column in Table 4.2, "Order Displacement" is the relative change in order if the data were sorted based on matching the 30-meter benchmark attribute resolution. The order remains fairly consistent with what was observed for the 10-meter rankings. The dry, flat study site of Brady South, TX becomes similar to its 30-meter spatial resolution counterpart after several of the rugged study sites. The lack of major order displacements indicates that the filtering is being applied consistently through the filtering iterations across all the study sites. This result also suggests that all study sites are experiencing equivalent rates of attribute resolution change.

The other aspect to the question of the rate of change is how this may differ across physiographic regions. Figure 4.3 illustrates the standard deviation curves for all study areas through the first 100 filtering iterations. The focal standard deviations for all study sites are plotted and colored according to landscape characteristic (dry/humid and rugged/flat). This shows a clear trend with focal standard deviation for rugged study sites consistently higher than for flat sites, and a muddied trend intermixing focal standard deviations among humid and dry study sites. The reader is cautioned that y axes are not comparable in the left and right panels.

The dramatic differences in trends between rugged and flat terrain becomes apparent in Figure 4.3: rugged areas are characterized by higher standard deviation values for both 10m and 30m spatial resolutions. The plots of rugged study areas also display a much greater overall change in standard deviation rate (2 to almost 4 meters difference for 30m cells, versus less than 1 meter difference for any flat DEM). Conversely, the slope of the standard deviations for flat areas levels off after only a few filtering iterations. This indicates that the rate of attribute resolution change is greater for rugged areas. However, this should be qualified with earlier

observations that rugged areas generally have to undergo a larger change in attribute resolution before matching that of a coarser spatial resolution benchmark.

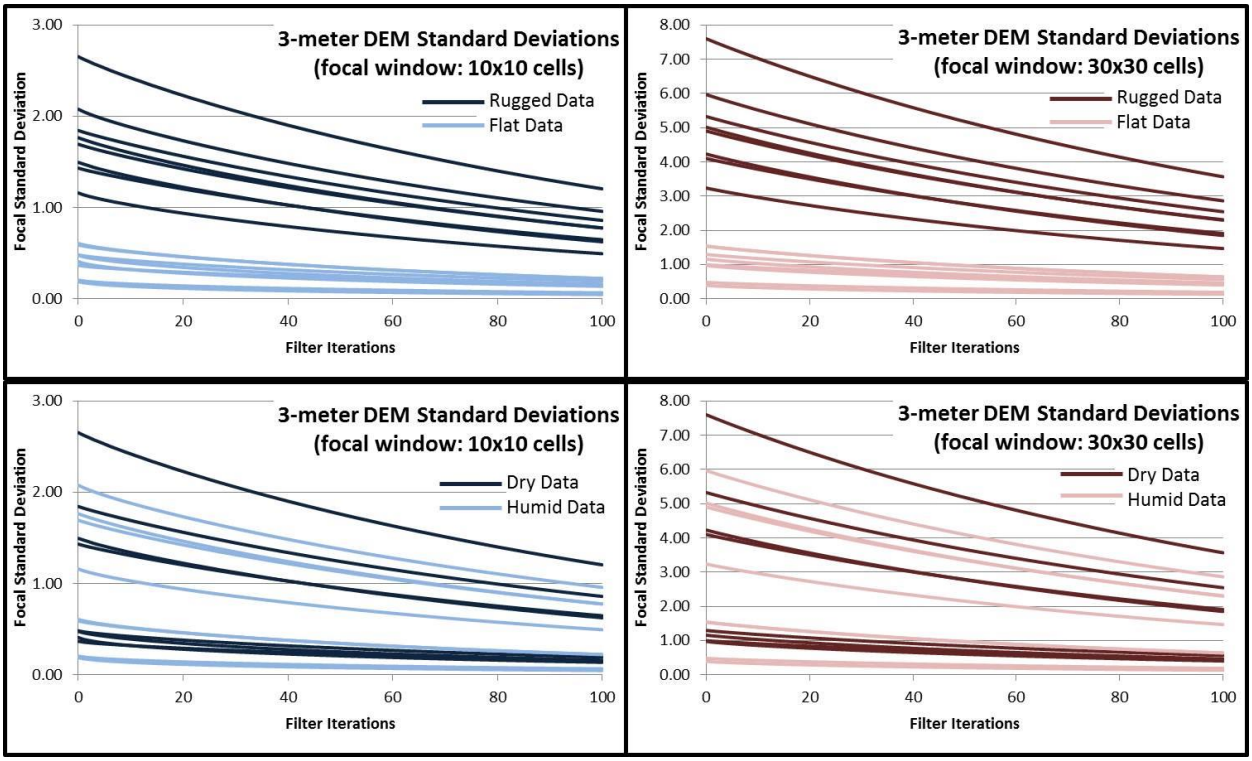

Figure 4.3: Comparison between the focal standard deviations for all study sites grouped by terrain characteristics.

Climatic variables such as precipitation have often been included when modeling and characterizing terrain. By categorizing the lower panels of Figure 4.3 into humid and dry conditions, some interesting insights can be identified. First, the mixing of plotted lines for 10m and 30m plots implies that wet or dry conditions have little distinguishing effect on the filtering process for rugged terrain. Climatic conditions have a much larger impact on the characteristics of flat terrain. The two DEMs for flat study areas with the highest standard deviation in lower panels are the Louisiana study sites. This region is extremely dendritic with well-defined flow channels. This characteristic creates a large local standard deviation for changing attribute resolution during filtering. In the remaining three flat study areas (TX, NM and NC), the hydrographic landscape isn't as dendritic. There appears to be a strong impact from these

climatic characteristics in transforming the landscape, similar to flash flood channelization of arid regions. This suggests that while climatic conditions may have a profound effect on the characteristics of the landscape, and thus on the expected rate of attribute resolution change through generalization, the effect can often be distorted in the presence of other prevailing characteristics.

4.4 Measuring the scope of attribute change in a DEM using semivariograms

The semivariance of a dataset describes the autocorrelation in the data set. In this thesis, semivariograms are used to compare the filtered DEM to the benchmark DEMs after the number of filtering iterations identified by the standard deviation. The semivariance describes how the generalization process affects DEM variance at various lag distances. It will help to answer the rates of attribute resolution change and whether iterative filtering only affects a localized area or if the impacts of filtering can have global implications on the resulting DEM resolution.

The semivariogram analysis was calculated for the two filtering iterations identified by the standard deviation analysis. Two sets of semivariograms were generated for the specified filtering iterations. The first was within the focal standard deviation window. This is important because it demonstrates the effects of filtering at a local scale. The second was across the entire study site to demonstrate the effects of filtering at a global scale. The need to create two semivariograms is required because of the scale at which trends can be observed. The effects of the filtering within the focal standard deviation window (maximum of 90 meters) will not be able to be seen when the semivariogram is created across the entire DEM (about 16,000 meters)

Five hundred (500) experimental semivariograms were calculated for each DEM, with 10,000 point pairs being used at each lag distance. A lag distance of 1 cell (3 meters, 10 meters,

or 30 meters depending on the DEM being used) was used to create the semivariograms within the focal standard deviation window. This causes 90 or 30 lags for the 3-meter DEM and 3 lags for the other benchmark DEMs. Conversely, a lag distance of 170 meters was used when creating a semivariogram across the entire study site. This equates to 50 lags.

The maximum and minimum semivariance values for each lag distance were used to create an envelope of possible realizations of the true semivariogram, analogous to a confidence interval. This envelope is useful for examining how well the semivariance of the filtered 3-meter DEM replicates the semivariance of a benchmark DEM at the iterations specified in the standard deviation analysis. In all cases, the distribution of the 10,000 semivariance values at each lag distance for each of the 500 semivariograms created was normally distributed.

Figure 4.4 shows the semivariograms calculated within the focal standard deviation windows. The red lines represent the semivariance envelope for the benchmark DEM. The blue lines represent the semivariance envelope for the filtered DEM. Note that the lag distances (x-axis) of each graph vary and comparisons direct comparisons cannot be made between the two panels.

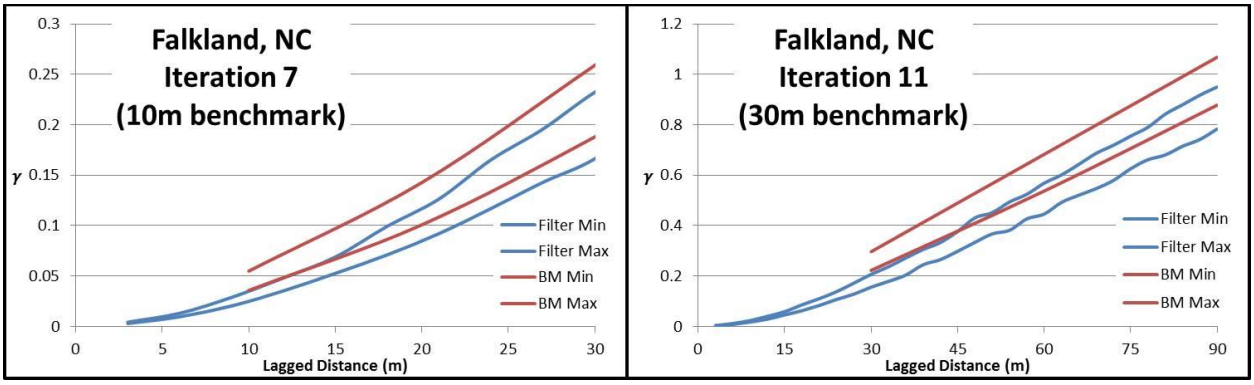

Figure 4.4: Semivariogram plots of DEM elevation values within the focal standard deviation window.

Figure 4.4 shows the semivariances within the standard deviation filtering window for Falkland, NC (see Appendix C for the other study sites). The nugget for the 3-meter DEM that

has been filtered 7 times is 0.003 and 0.002 for the 11th filtering iteration. The nugget for the 10-meter benchmark is 0.036 and for the 30-meter benchmark is 0.222. The nugget is an artifact of the DEM's spatial resolution and is greater for the benchmark DEMs because the variance measured at a smaller distance would be 0.0 since the pixel value would be compared against itself. Figure 4.4 demonstrates that the iterative filtering has appropriately altered the attribute resolution of the Falkland, NC, DEM to match that of the benchmark DEMs because the semivariogram envelopes overlap. However, the overlap with the 30-meter benchmark isn't as large and the data is more likely to be over generalized. The filtered DEMs can be identified that it is over generalized because the semivariance is less than that of the benchmark.

In fact, for many of the study sites, the 3-meter DEM is shown to be over generalized (see Appendix C). Few of the study sites are considered to be possible realizations of a coarser 10-meter attribute resolution with a high degree of semivariance envelope overlap. These results suggest that the DEMs have been systematically over generalized which contradict the findings of the standard deviation analysis. However, it is important to remember that the standard deviation is only a snapshot at one scale. The semivariograms of 10 of the 16 study sites intersect the 10-meter DEM semivariance at a lag distance of 30 meters (the focal standard deviation window size), some of which just slightly intersecting. Only 6 of the 16 study sites intersect the 30-meter semivariogram envelope at a lag distance of 90 meters.

Despite localized fluctuations in the slopes of the semivariogram lines, the shapes and patterns remain consistent between the filtered DEM and its benchmark. While the semivariograms do not perfectly match, there are no instances where the slope of one semivariogram greatly deviates from that of the semivariogram it is being compared to. While

this seems like a trivial observation, it suggests that the filtering process is maintaining the key characteristics of the data.

Now that the semivariograms have been examined within the filtering window, the next step is to examine semivariograms over a larger distance to see if overlap occurs beyond the focal window. This would demonstrate how far-reaching the filtering impacts are on the filtered DEMs. Figure 4.5 shows the semivariograms up to 8000 meters (170 meter lag distance, 50 lags, and half the diagonal distance of each study site). Appendix D shows the semivariograms of the remaining study sites. Note that these cover a much larger distance than what was shown in Figure 4.4. The semivariograms shown in Figure 4.4 cover a small portion of the lag distances in Figure 4.5.

The relationship between the filtered DEM and the benchmark can differ dramatically from what was observed when examining the semivariance within the focal windows shown in Figure 4.4 (see Richford, VT or Los Griegos, NM in Appendix D). Only the North Carolina study sites (Falkland, NC shown in Figure 4.5) have filtered DEM semivariances that continue to match the benchmark resolutions through the 8000 meter distance. Several other study sites also show close resemblances between filtered DEM semivariograms and benchmark semivariograms. In many other cases, the filtered DEMs appear to be overgeneralized and none show possible under generalization. Unlike the short lag distance semivariance slopes, the semivariance of the filtered DEM can differ dramatically from the observed semivariance of the benchmark resolution. This result suggests that iteratively filtering in a small window can dramatically affect the global characteristics of the DEM.

The parts of the semivariograms can also describe the data and help define how different landscapes may behave differently or similar. The first part of the semivariogram to check for is

a sill which will describe the size of the features represented in the DEMs. Only five study sites reach a sill. Jay Peak, VT, for example, approaches a sill at approximately 7,500 meters. This suggests that size of the features captured by the semivariogram is about this size. This is likely the large valley that runs from the northwest corner to about the center of the study site. Other study sites that show interesting semivariogram characteristics include Falkland, NC, and Sailes, LA. In both of these study sites, a pseudo-sill is encountered and can be observed by a change in the semivariance slope. This type of a features suggests that multiple scales of features can be observed in the data.

The second characteristic used to compare the semivariograms is the maximum semivariance values. For example, Jay Peak, VT, and Bryceland, LA, have very similar semivariogram shapes. However, the maximum semivariance value of Jay Peak is 600,000 meters. The maximum semivariance value of Bryceland is only 600 meters. The maximum semivariance is indicative of the relative relief seen in the DEMs. It also implies a scaling factor for landscape features. The semivariograms are suggesting that even though these two study areas are defined differently in terms of landscape relief, the structure of the terrain is similar.

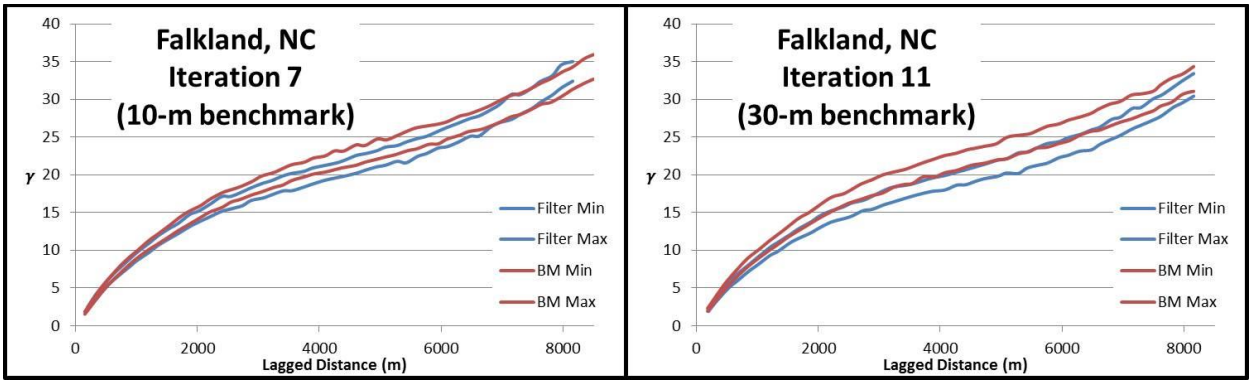

Figure 4.5: Semivariogram plots of DEM elevation values across half of the study site.

Table 4.3 explores the interaction between the two semivariance envelopes by examining the percentage of overlap. If the filtered DEM's attribute resolution exactly matches that of the

benchmark, the overlap should be a 100% match. The maximum overlap observed when comparing to a 10-meter DEM was 87% (Greenville, NC). The majority of the mismatch in this study site occurs at larger lag distances, suggesting that the filtering process is having a global effect on the DEM. Overall, the flat study sites have higher overlaps between the semivariograms than the rugged study sites. There is no clear trend in semivariogram overlap between climatic regimes.

Table 4.3: The measured overlap between the filter and benchmark semivariograms that span half of a study site.

Climate	Terrain	Quad Location	10-m Variogram Overlap	30-m Variogram Overlap
flat	humid	Greenville, NC	86.74%	66.99%
flat	humid	Falkland, NC	74.08%	20.84%
flat	dry	Brady South, TX	64.67%	0.00%
flat	dry	Voca, TX	55.98%	2.59%
flat	humid	Bryceland, LA	52.05%	0.00%
rugged	humid	Richford, VT	47.24%	0.00%
flat	dry	Los Griegos, NM	45.75%	25.54%
flat	dry	Volcano Ranch, NM	35.43%	18.01%
rugged	dry	Granby, CO	34.88%	0.00%
flat	humid	Sailes, LA	34.05%	0.00%
rugged	humid	Maysville, WV	19.68%	0.00%
rugged	dry	Wolf Mountain, OR	10.65%	0.00%
rugged	humid	Blackbird Knob, WV	10.14%	0.00%
rugged	dry	Six Corners, OR	0.00%	0.00%
rugged	humid	Jay Peak, VT	0.00%	0.00%
rugged	dry	Strawberry Lake, CO	0.00%	0.00%

Additionally, only four of the study sites have overlap greater than 2.6% when comparing the 30-meter semivariograms. This is consistent with examination of the semivariograms within the focal standard deviation window. Filtering to match a target attribute resolution that is very different from the source attribute resolution may lead to results that greatly deviate from the intended attribute resolution. It is evident that iterative filtering is more effective when slightly

modifying the attribute resolution. When a large change in attribute resolution is required, alternative methods of generalization may be more appropriate.

4.5 Conflation analysis to test vertical integration

Conflation will be assessed using a Coefficient of Line Correspondence (CLC) (Stanislawksi, 2009) to measure the vertical integration of the terrain with vector streams. Elevation derived streams (EDS) are extracted from the filtered DEMs that were identified in the standard deviation analysis and compared with National Hydrography Dataset (NHD) benchmark flowlines of similar spatial resolution. The CLC metric measures how well corresponding flowlines in the two datasets (EDS and NHD) match. CLC ranges between values of 0.0 to 1.0 where 0.0 indicates no match and 1.0 indicates a perfect match. From a cartographic perspective, higher rates of vertical integration (values closer to 1.0) will result in better cartographic products. From an analytic perspective, higher rates of conflation indicate a better match between datasets and a model output that is has less systematic error.

The filtering iterations that were designated to match 10-meter spatial resolution were compared to the NHD high resolution (24K) flowlines. The filtering iterations that were designated to match the 30-meter spatial resolution were compared to the NHD medium resolution flowlines. This was done because the high resolution flowlines were compiled at a spatial resolution of 12 meters while the medium resolution flowlines were compiled at a spatial resolution of 50 meters (Tobler, 1988; Simley and Carswell, 2009). The resolutions do not match exactly, but are close enough to be used together.

Tables 4.4 and 4.5 show the results of the CLC analysis between the filtered dataset and the NHD benchmarks. The CLC values in Table 4.4 range from 0.24 to 0.82. Previous research

has identified a CLC greater than 0.70 to demonstrate an acceptable tolerance for vertical integration (Buttenfield et al., 2011). This threshold value was identified when measuring the CLC value over an entire hydrologic subbasin, which can range from about 2 times to 70 times the size of the study areas used in this thesis. Therefore, it is likely that acceptable CLC values will range slightly due to the quality of NHD data being more consistent (better or worse quality) through the 7.5 minute quadrangle. Nonetheless, there appears to be a natural division between high and low CLC values at about 0.65. This suggests that 11 of the 16 study sites have a high degree of vertical integration with the high resolution NHD benchmark.

In all cases, the CLC values are lower for the filtered DEMs that match a 30-meter benchmark than the filtered DEMs that match a 10-meter benchmark. While this appears to reinforce the prior findings that the 3-meter DEM with 30-meter attribute resolution performs poorly, this is not completely true. Lower values are partially an artifact of the higher degree of spatial resolution mismatch between the 30-meter elevation derived streams to the 50-meter NHD benchmark. As discussed earlier in this chapter, the 100K NHD lacks variations in local feature density that would be resolved in the 3-m DEM, and the lower CLC could also be indicative of the lack of natural feature density differences in the medium resolution benchmark. There is a natural division between high and low CLC values between 0.61 and 0.56.

When examining the CLC of the filtered DEMs with 10-meter attribute resolution, no clear trend is apparent between climatic or terrain characteristics yielding a higher or lower CLC value. A trend between terrain characteristics does emerge in the CLC values of the filtered DEMs with 30-meter attribute resolution (Table 4.5). Here, the rugged study sites generally exhibit higher CLC values. This is likely due to the filtering process eroding small ridges and valleys that would be more prominent in the flat study sites. Because many of the flowlines in

the rugged study areas are located in well-defined valleys, these areas will be less affected by the generalization and therefore preserved.

Table 4.4: CLC results of conflation of the 10-meter filtered DEM compared to the 24K (12m) flowline benchmark.

Climate	Terrain	Quad Location	Filtering Iteration	Matching Length(km)	Commission Length(km)	Omission Length(km)	CLC
dry	rugged	Six Corners, OR	18	212.10	24.26	22.76	0.82
dry	flat	Brady South, TX	12	215.99	30.43	12.29	0.79
dry	flat	Voca, TX	12	273.67	44.90	43.89	0.76
dry	rugged	Wolf Mountain, OR	19	170.17	38.19	14.48	0.75
humid	flat	Sailes, LA	11	221.80	62.48	35.53	0.73
humid	rugged	Richford, VT	14	216.52	70.31	41.30	0.69
humid	rugged	Maysville, WV	17	168.53	43.86	23.21	0.68
humid	rugged	Jay Peak, VT	17	189.73	51.93	28.49	0.67
humid	flat	Bryceland, LA	10	210.15	71.66	49.84	0.67
humid	rugged	Blackbird Knob, WV	19	134.72	29.60	23.49	0.66
dry	rugged	Strawberry Lake, CO	18	152.44	49.21	34.52	0.65
dry	rugged	Granby, CO	15	167.47	95.66	71.26	0.54
humid	flat	Falkland, NC	7	184.11	100.55	87.14	0.51
dry	flat	Volcano Ranch, NM	20	90.25	108.15	42.81	0.38
humid	flat	Greenville, NC	5	165.15	203.57	185.42	0.31
dry	flat	Los Griegos, NM	29	106.02	187.86	112.88	0.26

Table 4.5: CLC results of the 30-meter filtered DEM compared to the 100K (50m) flowline benchmark.

Climate	Terrain	Quad Location	Filtering Iteration	Matching Length(km)	Commission Length(km)	Omission Length(km)	CLC
dry	rugged	Strawberry Lake, CO	20	71.84	17.34	1.42	0.72
humid	rugged	Blackbird Knob, WV	22	95.33	13.84	4.52	0.67
humid	rugged	Maysville, WV	20	112.32	34.62	12.20	0.64
humid	rugged	Richford, VT	18	63.69	24.67	4.42	0.64
dry	rugged	Wolf Mountain, OR	21	101.21	39.89	6.12	0.63
dry	rugged	Six Corners, OR	21	107.57	43.36	14.05	0.62
humid	flat	Falkland, NC	7	118.56	26.86	25.72	0.61
dry	rugged	Granby, CO	18	102.46	38.95	16.49	0.56
humid	flat	Bryceland, LA	14	67.81	27.77	19.38	0.56
dry	flat	Brady South, TX	19	82.37	40.77	3.40	0.55
humid	flat	Sailes, LA	15	60.32	22.50	6.23	0.53
dry	flat	Voca, TX	17	86.81	47.83	21.04	0.51
humid	rugged	Jay Peak, VT	21	51.90	28.44	3.44	0.51
humid	flat	Greenville, NC	7	142.55	84.13	63.99	0.50
dry	flat	Los Griegos, NM	29	113.68	147.66	41.61	0.32
dry	flat	Volcano Ranch, NM	22	39.75	72.99	16.75	0.24

The results of the CLC analysis are mapped in Figure 4.6 and in Appendix E, where reasons for high and low CLC values are described in further detail for other DEMs. Figure 4.6 shows the CLC results of Los Griegos, NM, which has one of the lowest CLC values. A braided stream runs through the southeastern corner of the map. This feature causes an inappropriate increase to the total length of flowlines to be extracted from the DEM. However, the process of extracting elevation derived streams isn't well suited to extracting braided features, so excessive headwater channels are extracted. The red lines show many of the braided channels that were missed in the EDS extraction. The length of braids was then extracted from the western part of the DEM. Due to the presence of the braided stream, EDS were poorly extracted which caused a low CLC value to be calculated. Similar artifacts are caused in channelized, urban areas (see Greenville, NC in Appendix E) or from poor benchmark compilations (see Voca, TX in Appendix E).

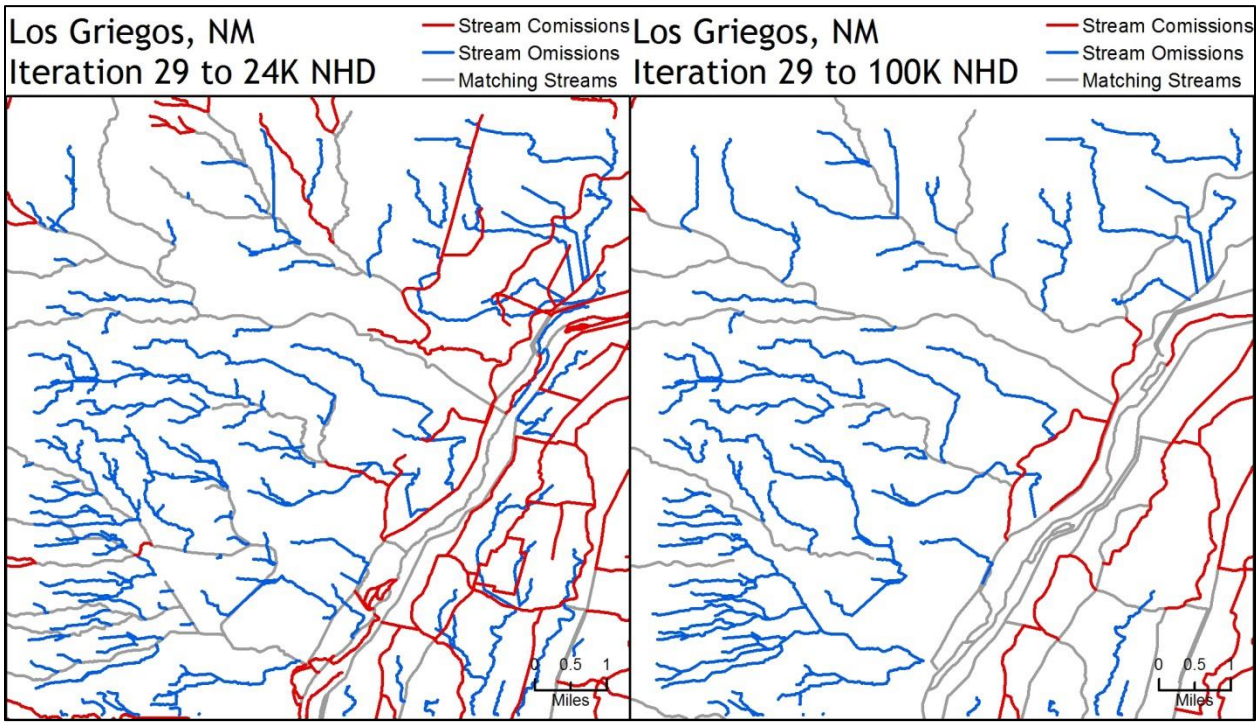

Figure 4.6: Map of the stream matches, omissions, and commissions between the elevation derived streams and the NHD benchmark flowlines.

Frequently, the study sites with low CLC values demonstrate poor vertical integration for the reasons given above. Higher CLC values demonstrate better feature conflation, and better integration of terrain with hydrographic data layers. Despite the semivariogram analysis suggesting that the filtering has widespread global impact, the CLC analysis identifies that the generalized DEMs are still suitable for vertical integration and the impacts of filtering aren't altering the terrain's local structure.

4.6 Summary

This analysis of iterative filtering results has incorporated several measures to assess the relationship of low-pass filtering with attribute resolution. The standard deviation metric identified that rugged areas require more filtering to achieve an attribute resolution similar to a benchmark than do flat areas. However, the semivariogram analysis showed that the rugged study sites appeared to be over-generalized relative to flat areas when compared with the benchmark DEMs. The rugged study sites also had a smaller degree of overlap when examining the semivariograms across a larger lag distance. While this doesn't precisely contradict the results of the standard deviation, caution should be used and the two metrics should be considered together rather than in isolation.

The semivariogram analysis shows that the filtering process has maintained key characteristics of the DEM. It was also identifies a large impact on global attribute resolution when performing many filtering iterations. As the number of filtering iterations increases, the discrepancy in attribute resolution increases between the filtered datasets and benchmark DEMs. Because of this, it appears that iterative filtering is most effective for small changes in attribute resolution.

The conflation analysis with NHD benchmark flowlines has shown that iterative low-pass filtering of DEMs preserves large and smaller features required for vertical integration with independently compiled datasets. Highest values of CLC were identified to range from about 0.61 to 0.65 for 11 of the 16 study sites when filtered to a 10-meter spatial resolution. Only 7 of the 16 study sites conflated at this CLC level when filtered to a 30-meter spatial resolution. Some low CLC values can be argued to be artifacts of inappropriately extracting complex features (braided channels or urban channelization), data compilation problems of the NHD benchmark, or poor boundary definitions where a single quadrangle crosses multiple watersheds.

Overall, the flat study areas achieved a coarser attribute resolution after fewer filtering iterations. Within flat study sites, the climatic characteristics seem to have a much more profound effect on the filtering process, with humid areas achieving a benchmark attribute resolution before the dry areas. This suggests that while climatic conditions can have a strong effect on the characteristics of the landscape, these effects can be augmented in the presence of other landscape characteristics, such as relative relief. Rugged terrain types have generally higher rates of vertical integration with vector benchmarks. This suggests that the filtering process is affecting the underlying structure of the flat study areas. Since the flat areas have a smaller local relief, these minor ridges and valleys are becoming homogenized such that flow patterns are being distorted.

The next chapter will discuss the implications of this analysis. The results identified here will be expanded upon to discuss what was learned and how these results may affect DEM generalization for cartographic display. The discussion will conclude by exploring ways in which this thesis can be expanded and improve.

Chapter 5: Implications of Results

5.1 Introduction

In the previous section, results of the standard deviation, semivariogram, and conflation analysis were identified as useful tools for identifying how attribute resolution changes as a DEM is iteratively filtered. The CLC shows that even though the attribute resolution was reduced, it did not corrupt the data's structure and ability to integrate with other vector datasets.

In this chapter, the implications of these results will be discussed. The first thing discussed will be the lessons that can be taken away from this research by expanding upon the results identified in the previous chapter. Next, possible applications of this work will be identified and how these results can be implemented into real world mapping scenarios. Some weaknesses of this thesis will also be documented. The thesis will then conclude with future work and how to expand upon the methodology presented in this thesis.

5.2 Implications of the research

The work in this thesis confirmed the known limitation of spatial filtering which is that it is most applicable for a small change in scale. While the focal standard deviation identified filtering iterations that match the attribute resolution of a benchmark resolution DEM, the semivariograms showed that this generates results which become increasingly overgeneralized when performing a larger change in attribute resolution. A different generalization approach (resampling instead of filtering) is likely more appropriate for generalizing with a larger scale or resolution change in mind.

The topic of star and ladder generalization strategies is rooted in this observation (Stoter, 2005), something that has been omitted earlier from this document. In a star-based

generalization, data is aggressively generalized to reach a target resolution. A ladder based strategy gradually alters data through several incremental generalization steps. This thesis uses a ladder based approach that iteratively generalizes an intermediate dataset until a target resolution is reached. The semivariogram and CLC analyses determined that the filtering can perform poorly when compared to a known benchmark that is designed to be used at a target resolution that is much coarser than the source scale. This finding suggests that when a large change is required, a star based approach may be more useful to match the characteristics of the known benchmark (i.e. through resampling).

Generally, all study sites in this thesis achieved the next coarser spatial resolution (10-meter) by 20 filtering iterations, with flat areas achieving this by 12 filtering iterations. Similar trends are identified when the data is filtered to an even coarser attribute resolution (30-meter). To do this, the number of filtering iterations required is only slightly higher. The flat study areas take up to 20 iterations to achieve the 30-meter attribute resolution; the rugged study sites require up to 22 iterations. The focal standard deviation plots demonstrate that the rate of generalization initially happens at a fast rate, gradually decaying through later filtering iterations. However, the opposite trend appears when the filtered DEM matches the benchmark DEM. This is likely due to the same compilation source of the benchmark DEMs. This point should be explored further, perhaps by using other data sources for the benchmark DEMs.

As noted in the previous chapter, the filtering process modifies the attribute resolution of flat study areas at a faster rate than rugged study areas because the local relief in these areas is smaller. The CLC results reinforce this argument because the conflation between NHD flowlines and elevation derived flow (EDS) is lower in flat areas. Conversely, the filtering

process preserves the valleys and streams in rugged areas because of the higher relief and well-defined valley lines.

These results suggest that flat study areas are more susceptible to significant landscape alterations through the filtering process. The addition of breaklines or stream burning prior to the generalization process may improve the rate of vertical integration of vector datasets. However, this strategy applies a heuristic generalization approach that may be difficult for cartographers to implement programmatically. Therefore, care should be taken when filtering data with low relief, as locally important landscape characteristics may be negatively impacted.

Often, climate characteristics play an important role when performing model generalization. The results indicate that climate conditions play a negligible role in filtering rugged areas. However, climatic characteristics play a stronger role in flat areas. Dry, flat study areas behave similarly to what has been observed when filtering rugged areas. Channelization in dry areas creates a higher local relief that better defines flow lines. This can also be seen in the CLC rates for the 10-meter attribute resolution. For example, the Texas study sites have a higher conflation than do the highly dendritic Louisiana sites.

5.3 Applications of this work

5.3.1 Landscape Characterization

As expected, the global and local relief of the DEM was a prevailing factor in identifying differences among the effects of filtering. For example, the standard deviation values were higher, the semivariograms had a higher degree of mismatch, and the CLC showed higher conflation errors. The study sites used in this thesis were selected based on pre-existing landscape partitions that might not be readily available to all cartographers. A question arises as

how to characterize data so it can be appropriately filtered. This thesis demonstrated that a semivariogram can be useful in identifying features and landscape characteristics of a DEM. Other researchers have argued a similar point (see for example O'Sullivan and Unwin, 2010; Goodchild and Proctor, 1997).

The range, sill, and slope of the semivariogram model permit several inferences about the landscape. The range indicates of the size of features that are observed in the study area. However, some study sites in this thesis arguably contain more than one sill, or a partial sill. Sailes, LA, demonstrates a sill at about 2000 meters; the semivariance increases dramatically at about 7000 meters. Heterogeneity in the DEM (many small features and valleys) exists in the terrain of Sailes, LA. The semivariogram picks up on this detail. The larger trend valleys (running from the west to east and from the southwest towards the north east) aren't picked up as readily because their length exceeds the maximum lag distance. Therefore, the range of the semivariograms provides an estimate of the generalization decisions to be made based on feature size.

The sill provides information about the DEM's ruggedness. The sill is the point where the spatial dependence in the data stops and is noted by the semivariance coming into equilibrium, or the maximum semivariance observed when no equilibrium is reached. Rugged landscapes have sills at a higher semivariance than flat landscapes. Despite the apparent difference in semivariance values, landscapes can share similar structures in terms of spatial dependence (for example, compare Bryceland, LA, with Jay Peak, VT). The relief differs dramatically between the study sites. However, the relative shapes of the semivariograms mimic one another. Although the Bryceland, LA, semivariograms are more similar when comparing the filtered and benchmark envelopes, filtering process augmented the spatial dependence equally

within these sites. This result suggests that generalization decisions can be based on the size of features to be maintained instead of the relief.

5.3.2 Relating attribute resolution to spatial resolution

The results of this work will aid cartographers in generalizing DEM data to an appropriate resolution for display or analysis at a target scale. Several methods exist to convert data's spatial resolution to map scale, but can become complicated when generalizing raster attribute resolution through filtering. This complication can be avoided by changing the spatial resolution of a raster through resampling. However, this strategy sometimes maintains too much attribute detail or performs poorly in tandem with the landscape granularity or the display resolution of the map. Spatial filtering simplifies the appearance of a DEM and maintains the source cell size. The characteristics of a landscape help a cartographer to understand how filtering a DEM will alter the attribute resolution and thus, its performance as a base map. The relationship between attribute and spatial resolution of a generalized DEM assists in identification of a target scale.

In addition, the results of this thesis can assist in decision making for intermediate scale level-of-detail (LoD) datasets. The U.S. Geological Survey (USGS) currently makes large scale maps with fine spatial resolution DEMs through *The National Map* and small scale maps with coarser spatial resolution through *The National Atlas*. Historically, the USGS made intermediate scale maps (e.g. 100K, 250K), which are still available but are no longer being updated (USGS, 1985). A user requirement has demanded data availability for elevation datasets at many intermediate scales (Sugarbaker et al., 2009). The rate of attribute resolution change through

generalization provides guidelines on generalizing current DEMs to match a desired LoD that integrates with existing vector datasets.

The attribute resolution of a DEM can be efficiently implemented into the construction of a Multi-Resolution Database (MRDB). An MRDB is a spatial database that contains data with several levels of detail (LoD) in order to represent data across a wide variety of scales. An MRDB portray data appropriate for several given scales and integrate with other data layers that may have been generated at different scales (Bobzien et al., 2008). The generalization process may augment the degree of vertical integration. Appropriate vertical data integration leads to the successful construction and implementation of MRDBs. A seamless transition of data through scales is accomplished by precisely relating the attribute resolution of raster data to a given spatial resolution which increases the level of integration and is tied to specific mapping scales.

5.4 Weaknesses and Limitations of the thesis

This thesis identifies attribute resolution change by comparing data to a benchmark DEM having a known spatial resolution. The original intent of this thesis was to identify how DEM attribute resolution may change through low-pass filtering. The direct results of this thesis are applicable by helping a cartographer to understand what terrain types may be more or less affected by the generalization process and how aggressively these data need to be generalized.

A methodological concern arises when comparing the semivariograms. A striking similarity exists between the semivariance envelope values of the benchmark DEMs. More research is required to understand this problem, but is likely an artifact of the DEM compilation. The benchmark DEM compilation methods both used DRG contour lines to interpolate elevation values. The contours may not have been sparse or dense enough to create truly independent

datasets. This hypothesis can be evaluated by using a DEM from a different data source as another benchmark. The Global Digital Elevation Model (GDEM), which is offered in a 30-meter spatial resolution, can be used as a control to provide another estimation of the spatial dependence at this spatial resolution. If the semivariograms are drastically different, the results derived from the standard deviation analysis may be biased. The standard deviation identified that more filtering iterations are required to match a 3-meter attribute resolution DEM to a 10-meter benchmark's spatial resolution than to match the 10-meter attribute resolution (filtered 3-meter DEM) to a 30-meter spatial resolution. The 90-meter SRTM DEM could be used as a third benchmark to evaluate how the attribute resolution of the filtered DEM compares to another spatial, coarser resolution.

This thesis lacks of any examination of terrain derivatives. The generalization process affects various terrain derivatives (see Kienzle, 2004; Chang and Tsai, 1991). For a cartographic purpose, the DEM is most often present used on a map to provide a hypsometric tint. This feature layer is less susceptible to resolution derived problems because it is symbolized using a continuous, monochromatic color ramp. Changes in resolution augment the representation of terrain derivatives, such as shaded relief or slope and aspect, because they rely on some type of classification. While the hillshade layer relies on a monochromatic color ramp, it is divided into areas of illumination or shade. In areas of complex relief change (i.e. the frequent, rugged valleys in Strawberry Lake, CO), raster pixels coalesce and can create a poor map quality when attribute resolution is too fine. This thesis has not performed any analysis on the terrain derivatives and future research could perform some of the standard deviation metrics on the hillshade instead of the DEM. It would be interesting to see if the results agreed or contradicted those discussed here.

One limitation that was overlooked in this thesis was the lack of widespread availability of 3-meter DEMs provided in the NED. This impacted the ability to select study sites. Additionally, the lack of data impacted some of the analysis conducted in this thesis, most notably the conflation analysis. Figure 5.1 shows the data availability of the 3-meter DEMs. The top image shows the data availability in October, 2011, which was around the time initial study sites were selected. The lower image shows the data availability in October, 2013. The lower image shows that new patches in dry regions were added including all of Iowa.

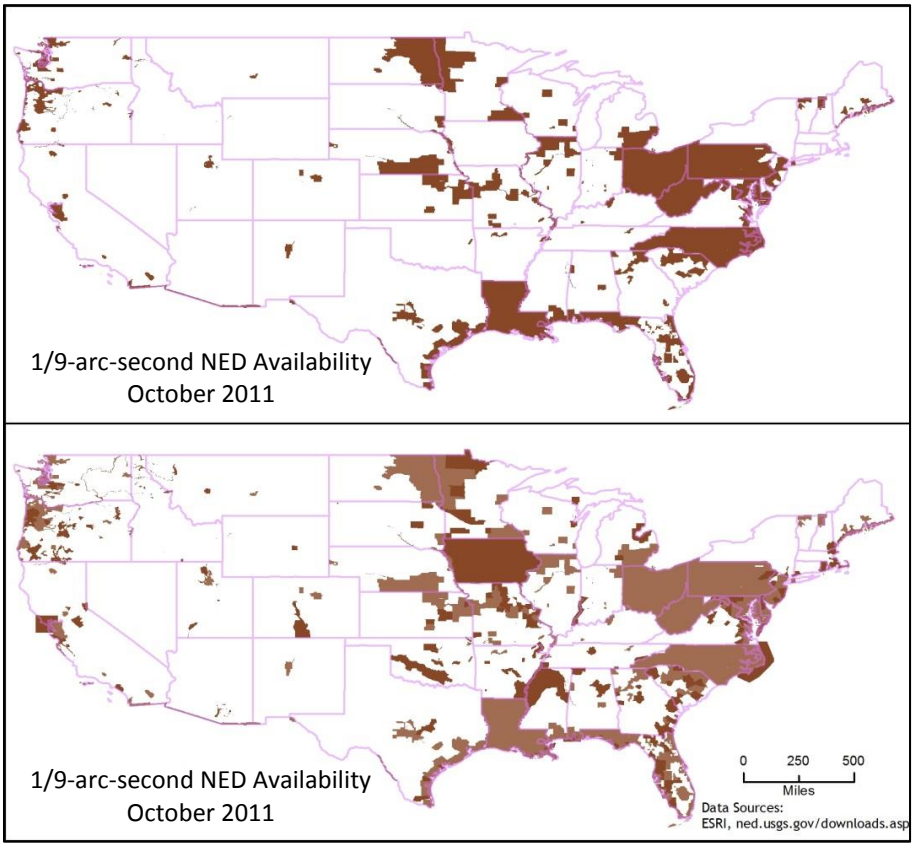

Figure 5.1: 3-meter NED availability at the start and conclusion of this thesis.

5.5 Continuation of work

5.5.1 Expansion of Research Design

This thesis filtered data using a Gaussian kernel. The Gaussian filter is a common spatial filter and has a unique ability to cascade. Iteratively filtering data can be computationally

expensive and often cartographers filter once with a large window. The cascading ability of the Gaussian kernel allows a cartographer to relate the number of filtering iterations used in this thesis with a given window size to a single filter of a larger window size. However, some GIS systems don't offer the Gaussian kernel out-of-the-box, and frequently a focal mean is used instead. Unlike the Gaussian kernel, the focal mean kernel treats all neighboring cells with equal weight. It is important to understand how other filters alter the rate of attribute resolution change as was identified here. In the future, research should replicate the methodology proposed in this thesis with using alternative filtering algorithms to examine how and why different filters may alter the rate of attribute resolution change. It is unlikely that different filters will generate identical results, but it is unknown if the general rates of attribute resolution change will remain similar (i.e. flat study areas experience a faster rate of attribute resolution change, etc.).

Another possible method of analysis incorporates a star generalization approach as discussed above. This thesis demonstrated that the filtered DEM's spatial dependencies can become quite different from that seen in the benchmark DEMs at large lag distances. To test the star based approach, a resampling of the 3-meter DEM should be applied so that it matches the benchmark DEM's spatial resolution. At this point, the focal standard deviation and semivariogram analysis can be conducted to compare the attribute resolution of the resampled DEM to the benchmark. As identified earlier, large changes in resolution may require this type of generalization.

A final expansion of the research design conducts a comparison of the terrain derivatives of the filtered DEMs to the coarser spatial resolution DEMs. As mentioned in the previous section, the main reasons for generalizing the attribute resolution of a DEM are for the display of terrain derivatives. However, this thesis never directly examined any terrain derivatives. Results

of performing this analysis on the terrain derivatives would have generated a stronger argument to support the appropriateness of the attribute resolution for use at a smaller mapping scale.

5.5.2 Improvements of CLC analysis

Some of the study sites experienced very low CLC values. As described in the last chapter, some of these low values can be defended due to several factors that can affect the metric (e.g., the presence of braided streams). The CLC analysis depends upon extracting stream features from the DEM, preferably from an entire watershed where the flow is expected to be contiguous. Some study sites overlapped multiple Hydrologic Unit Codes (HUCs). This fragmentation and focus in headwater regions caused elevation derived stream extraction to be negatively impacted. To compensate, the CLC analysis needs to be expanded to include elevation data that surrounds the study area. Due to 3-meter DEM availability limitations, this was not possible for some study sites.

The elevation derived streams were extracted based on data characteristics of the NHD flowlines. The flowlines contain many types of features including perennial and intermittent streams, canals, pipelines, connectors, artificial paths, etc. Some of these latter examples are difficult to model because they are not truly present in the landscape (e.g. underground conduit or pipeline; seen in Strawberry Lake, CO) or are too small to be identified in the course spatial resolutions DEMs (e.g small agricultural or urban canals as seen in Greenville, NC). Removing these complex features from the NHD benchmark will improve the efficacy of the CLC metric.

The CLC analysis matched a 10-meter attribute resolution DEM to 12-meter spatial resolution hydrographic features. This is a very close match and likely to be used in a real work scenario. However, the 30-meter attribute resolution DEM was compared to 50-meter spatial

resolution hydrographic features. The difference between these spatial resolutions augments this result because both terrain and hydrography are widely acknowledged to be sensitive to scale and resolution changes. Minimizing the difference between vector and raster benchmark spatial resolutions will improve the results of the conflation analysis. This could be fit into the above discussion of resampling DEMs or identifying an external DEM dataset that more closely matches a 50-meter spatial resolution. Alternatively, implementing third hydrographic flowline benchmark can bolster the results of the conflation analysis. *The National Atlas* hosts a hydrographic dataset at a scale of 1:1,000,000, or with a 500-meter spatial resolution (The National Atlas, 2012). Some elevation datasets exist at this spatial resolution. Under the scope of this thesis, filtering a 3-meter DEM to match a 500-meter attribute resolution was impractical. A star-based generalization approach makes this a more reasonable objective.

5.5.3 Data Validation

This thesis failed to perform any data validation on the generalized products. It is still unknown how filtering may augment the vertical and horizontal positional accuracy. The American Society for Photogrammetry and Remote Sensing defines the vertical accuracy of DEMs to be one third the indicated contour interval at scale (ASPRS, 1990). The National Standard for Spatial Data Accuracy determines if elevation values conform to accuracy standards by calculating the RMSE error of the data points (NSSDA, 1998). A difference grid derived from the filtered 3-meter and unfiltered 3-meter DEM would help to address the accuracy augmentation. A 95% confidence interval for RMSE error can be calculated and applied to the intended mapping scale. If the accuracy remains within the standard's thresholds, the DEM can be certified to conform to national mapping accuracy standards. However, if the RMSE does not

conform to national mapping accuracy, the filtering process needs to be re-evaluated or the data used with caution that it may not be the best representation on a map. If the accuracy is inappropriate, other methods of generalization should be considered that will maintain proper horizontal and vertical accuracy.

5.6 Summary

The theoretical contribution of this thesis is rooted in a deep literature pool for cartographic generalization. In this context, data are modified to improve a map's message and is determined on a map's purpose, scale, target audience, and data complexity (Weibel, 1987; Robinson and Sale, 1969). Frequently, cartographers relate a minimum mapping unit or spatial resolution directly to a mapping scale (Demers, 2002; Tobler, 1988) in order to meet appropriate cartographic renderings. Spatial filtering is a common method to simplify the appearance of a DEM. However, filtering causes a disconnection between the attribute and spatial resolutions and makes determining a scale that matches the filtered DEM's fitness for use ambiguous.

This thesis explored the effects of generalization on attribute resolution change and how this change can relate back to a target mapping scale. This was done by comparing smoothed DEMs to benchmark datasets within the NED and NHD. A standard deviation and semivariogram analysis were conducted to evaluate the rate of attribute resolution change and how the filtering affects the spatial dependency of elevation values within the filtered DEM. A conflation analysis measured the degree of vertical integration with NHD vector stream.

The results demonstrated the ability to relate the attribute resolution of a filtered DEM back to a known spatial resolution, and therefore a target mapping scale. Additionally, the effects of generalization across various physiographic landscapes were explored. The standard deviation and semivariogram analysis demonstrated that the rate of attribute resolution change

increases through filtering iterations. This is contrary to what would have been expected and may have been a result of the benchmark DEMs used. The rate of attribute resolution change is faster for flat landscapes and more aggressive filtering is required to change the attribute resolution of a rugged landscape. Climatic characteristics impacted the rate of attribute resolution change, but were muddied by other prevailing characteristics. The semivariogram analysis demonstrated that filtering is adequate for a small change in scale or resolution because large deviances in spatial dependencies appear when a DEM is aggressively smoothed. The conflation analysis demonstrated that the filtering process has not altered the spatial structure of the DEM and that vertical integration is maintained between vector datasets of similar spatial resolutions. However, low relief areas experience lower rates of vertical integration because locally significant landscape structures can be eroded through the filtering process.

The main weaknesses and limitations noted in this thesis are drawn from the sole use of NED elevation data. Small and infrequent patches of 3-meter DEMs across the United States limited the ability to test a wide range of physiographic characteristics and have directly impacted the results of the conflation analysis. Additionally, the benchmark NED datasets were specifically chosen because of their independent compilations and conformity to national mapping accuracy standards. Due to their shared source information, a truly independent compilation may not have been truly accurate, as seen in the semivariogram analysis.

The next steps of this work include modifying the methodology to include a comparison of multiple smoothing methods. Most GIS software packages use a focal mean as the default filtering algorithm. This is fundamentally different from the weighted Gaussian kernel used in this thesis. By comparing filtering methods, specific filtering algorithms can be compared and contrasted and differences in the implications on a DEM surface can be identified.

Bibliography

Ai, T. and Li, J. (2009) A DEM Generalization by Minor Valley Branch Detection and Grid Filling. *ISPRS Journal of Photogrammetry and Remote Sensing*, 65, pp. 198-207.

American Society for Photogrammetry and Remote Sensing (ASPRS) (1990) ASPERS Accuracy Standards for Large-Scale Maps. *Photogrammetric Engineering & Remote Sensing*, Annual Reports, pp. 1068-1070.

Anderson, J. R., Hardy, E. E., Roach, J. T., and Witmer, R. E. (1976) A Land Use and Land Cover Classification System for Use with Remote Sensor Data. *Geological Survey Professional Paper 964*, available <http://landcover.usgs.gov/pdf/anderson.pdf> Last visited 11/18/2013.

ASTER GDEM Validation Team (2011) ASTER Global Digital Elevation Model Version 2 – Summary of Validation Results, available <http://www.jspacesystems.or.jp/ersdac/GDEM/ver2Validation/Summary_ GDEM2_validation_ report_final.pdf> Last visited 1/11/13.

Barber, P. B. and Shortridge, A. (2005) LiDAR Elevation Data for Surface Hydrologic Modeling: Resolution and Representation Issues. *Cartography and Geographic Information Science*, 32, 4, pp. 401-410.

Bard, S. (2004) Quality Assessment of Cartographic Generalisation. *Transactions in GIS*, 8, 1, pp. 63-81.

Beard, K. and Mackaness, W. A. (1991) Generalization Operations and Supporting Structures. *Proceedings of AutoCarto 10*, Baltimore, Maryland, March, pp. 29-45.

Bobzien, M., Burghardt, D., Petzold, I., Neum, M., and Weibel, R. (2008) Multi-representation Databases with Explicitly Modeled Horizontal, Vertical, and Update Relations. *Cartography and Geographic Information Science*, 35, 1, pp. 3-16.

Bolstad, P. (2008) *GIS Fundamentals: A first text on geographic information system*, 3rd ed. White Bear Lake, MN: Eider Press.

Brassel, K. (1974) A Model for Automatic Hill-Shading. *The American Cartographer*, 1, 1, pp. 15-27.

Brassel, K. and Weibel, R. (1988) A Review and Conceptual Framework of Automated Map Generalization. *International Journal of Geographical Information Systems*, 2, 3, pp. 229-244.

Brewer, C. A. and Buttenfield, B. P. (2007) Framing Guidelines for Multi-Scale Map Design Using Databases at Multiple Resolutions. *Cartography and Geographic Information Science*, 34, 1, pp. 3-15.

Brewer, C. A. and Buttenfield, B. P. (2010) Mastering Map Scale: Balancing Workloads Using Display and Geometry Change in Multi-Scale Mapping. *Geoinformatica*, 14, 2, pp. 221-239.

British National Committee for Geography (1966) *Glossary of Technical Terms in Cartography*. London: The Royal Society Press.

Burrough, P. and McDonnell, R. (1998) *Principles of Geographic Information Systems*. London: Oxford Press.

Burt, J. E., Barber, G. M., and Rigby, D. L. (2009) *Elementary Statistics for Geographers*, 3rd ed. New York, NY: The Guilford Press.

Buttenfield, B. P. (1995) Object-Oriented Map Generalization: Modeling and Cartographic Considerations in *GIS and Generalization: Methodology and Practice*, Müller, J.-C., Lagrange, J.-P., and Weibel, R. (eds.). Bristol, Pennsylvania: Taylor & Francis Publishers, pp. 91-105.

Buttenfield, B. P. and Mark, D. M. (1991) Expert Systems in Cartographic Design in *Geographic Information Systems: The microcomputer and modern cartography*, Taylor, D. (ed.). Elmsfor, NY: Pergamon Press.

Buttenfield, B. P., Stanislawski, L. V., and Brewer, C. A. (2010) Multiscale Representations of Water: Tailoring Generalization Sequences to Specific Physiographic Regimes. *Proceedings of GIScience 2010*, Zurich, Switzerland, September.

Buttenfield, B. P., Stanislawaski, L. V., and Brewer, C. A. (2011) Adapting Generalization Tools to Physiographic Diversity for the USGS National Hydrography Dataset. *Cartography and Geographic Information Science*, 38, 3, pp. 289-301.

Carter, J. R. (1992) The Effect of Data Precision on the Calculation of Slope and Aspect using Gridded DEMs. *Cartographica*, 29, 1, pp. 22-34.

Chang, K.-T. and Tsai, B.-W. (1991) The Effect of DEM Resolution on Slope and Aspect Mapping. *Cartography and Geographic Information Science*, 18, 1, pp. 69-77.

Chaudhry, O. Z. and Mackaness, W. A. (2010) DTM Generalisation: Handling Large Volumes of Data for Multi-Scale Mapping. *The Cartographic Journal*, 47, 4, pp. 360-370.

Chilès, J-P. and Delfiner, P. (1999) *Geostatistics: Modeling Spatial Uncertainty*. New York, NY: John Wiley & Sons.

Clarke, K. C. (1988) Scale Based Simulation of Topographic Relief. *The American Cartographer*, 15, 2, pp. 173-181.

Clarke, K. C. and Cloud, J. G. (2000) On the Origins of Analytical Cartography. *Cartography and Geographic Information Science*, 27, 3, pp. 195-204.

Clarke, K. C. and Lee, S. J. (2007) Spatial Resolution and Algorithm Choice as Modifiers of Downslope Flow Computed from Digital Elevation Models. *Cartography and Geographic Information Science*, 43, 3, pp. 215-230.

Cressie, N. A. C. (1993) *Statistics for Spatial Data*. New York, NY: John Wiley & Sons.

Danielson, J. J. and Gesch, D. B. (2011) Global Multi-resolution Terrain Elevation Data 2010 (GMTED2010). *U. S. Geological Survey Open File Report 2011-1073*, available <http://pubs.usgs.gov/of/2011/1073> Last visited 1/11/13.

DeMers, M. N. (2002) *GIS Modeling in Raster*. London, England: John Wiley & Sons, Inc.

Dent, B., Torguson, J., and Hodler, T. (2009) *Cartography: Thematic Map Design*, 6th ed. New York, NY: McGraw-Hill.

Diez-Roux, A. V. (2003) The Examination of Neighborhood Effects on Health in *Conceptual and Methodological Issues Related to the Presence of Multiple Levels of Prganization in Neighborhoods and Health*, Kawachi, I. and Berkman, L. F. (eds.), New York, NY: Oxford University Press, pp. 45-64.

Eckert, M. (1908) On the Nature of Maps and Map Logic, translated by Joerg, W. *Bulletin of the American Geographical Society*, 40, 6, pp. 344-351.

Evans, I. S. (1972) General Geomorphometry, Derivations of Altitude and Descriptive Statistics in *Spatial Analysis in Geomorphology*, Chorley, R. J. (ed.). New York, NY: Harper & Row, Publishers, pp. 17-90.

Farr, T. G., Rosen, P. A., Caro, E., Crippen, R., Duren, R., Hensley, S., Korbrick, M., Paller, M., Rodriguez, E., Roth, L., Seal, D., Shaffer, S., Shimada, J., Umland, J., Werner, M., Oskin, M., Burbank, D., and Alsdorf, D. (2007) The Shuttle Radar Topography Mission. *American Geophysical Union*, available <www2.jpl.nasa.gov/srtm/SRTM_paper.pdf> Last visited 1/11/13.

Fotheringham, A. S. and Rogerson, P. A. (1993) GIS and Spatial Analytical Problems. *International Journal of Geographical Information Systems*, 7, 1, pp. 3-19.

Frank, A. U. and Timpf, S. (1994) Multiple Representations for Cartographic Objects in a Multi-Scale Tree: An Intelligent Graphical Zoom. *Computers and Graphics Special Issue on Modeling and Visualization of Spatial Data in GIS*, 18, 6, pp. 823-829.

Frankel, K. L. and Dolan, J. F. (2007) Characterizing Arid Region Alluvial Fan Surface Roughness with Airborne Laser Swath Mapping Digital Topographic Data. *Journal of Geophysical Research: Earth Surface*, 112, 2, pp. 14.

Franklin, W. R. (2000) Applications of Analytical Cartography. *Cartography and Geographic Information Science*, 27, 3, pp. 225-237.

Ge, Y. and Cheng, Q. (2007) Boundary Effect Reduction in Image Filtering. *Journal on Image and Video Processing*, 7, 2, pp. 17-25.

Gesch, D. (2007) The National Elevation Dataset in *Digital Elevation Model Technologies and Applications: The DEM Users Manual*, Maune, D. (ed.), 2ed. Bethesda, Maryland: American Society for Photogrammetry and Remote Sensing, pp. 99-118.

Gesch, D., Evans, G., Mauck, J., Hutchinson, J., and Carswell, W. J. Jr. (2009) The National Map – Elevation. *U. S. Geological Survey Fact Sheet 2009-3053*, available <http://pubs.usgs.gov/fs/2009/3053> Last visited 2/5/2013.

Gesch, D., Oimoen, M., Greenlee, S., Nelson, C., Steuck, M., and Tyler, D. (2002) The National Elevation Dataset. *Photogrammetric Engineering and Remote Sensing*, 68, 1, pp. 5-11.

Goodchild, M. F. and Proctor, J. (1997) Scale in a Digital Geographic World. *Geographical and Environmental Modeling*, 1, 1, pp. 5-23.

Griffith, D. A. (1980) Towards a Theory of Spatial Statistics. *Geographical Analysis*, 12, 4, pp. 325-339.

Grohmann, C. H., Smith, M. J., and Riccomini, C. (2010) Multiscale Analysis of Topographic Surface Roughness in the Midland Valley, Scotland. *IEEE Transactions on Geoscience and Remote Sensing*, 99, pp. 1-14.

Heller, M. (1990) Triangulation Algorithms for Adaptive Terrain Modeling. *Proceedings of the 4th International Symposium on Spatial Data Handling*, Zurich, Switzerland, pp. 163-174.

Homer, C. H., Fry, J. A., and Barnes, C. A. (2012) The National Land Cover Database, available <http://pubs.usgs.gov/fs/2012/3020/> Last visited 1/27/13.

Imhof, E. (2007) *Cartographic Relief Presentation*. Redlands, CA: ESRI Press.

International Cartographic Association (ICA) (1973) *Multilingual Dictionary of Technical Terms in Cartography*, Franz, Germany: Steiner Verlag.

Isaaks, E. H. and Srivastava, R. M. (1989) *Applied Geostatistics*. New York, NY: Oxford University Press.

Jain, R., Kasturi, R., and Schunck, B. G. (1995) *Machine Vision*. New York, NY: McGraw-Hill.

Jenny, B. and Hurni, L. (2006) Swiss-Style Colour Relief Shading Modulated by Elevation and by Exposure to Illumination. *The Cartographic Journal*, 43, 3, pp. 198-207.

João, E. M. (1995) The Importance of Quantifying the Effects of Generalization in *GIS and Generalization: Methodology and Practice*, Müller, J.-C., Lagrange, J.-P., and Weibel, R. (eds.). Bristol, Pennsylvania: Taylor & Francis Publishers, pp. 183-193.

Kienzle, S. (2004) The Effect of DEM Raster Resolution on First Order Second Order, and Compound Terrain Derivatives. *Transactions in GIS*, 8, 1, pp. 83-111.

Kilpeläin, T. and Sarjakoski, T. (1995) Incremental Generalization for Multiple Representations of Geographical Objects in *GIS and Generalization: Methodology and Practice*, Müller, J.-C., Lagrange, J.-P., and Weibel, R. (eds.). Bristol, Pennsylvania: Taylor & Francis Publishers, pp. 209-218.

Kimerling, J. (2011) DEM Resolution, Output Map Pixel Density, and Largest Appropriate Map Scale. *ESRI Mapping Center Blog*, available <http://blogs.esri.com/esri/arcgis/2011/02/28/dem-resolution-output-map-pixel-density-and-largest-appropriate-map-scale/> Last visited 8/12/12.

Lee, Y. C. (1991) Cartographic Data Capture and Storage in *Geographic Information Systems: The microcomputer and modern cartography*, Taylor, D. (ed.). Elmsfor, NY: Pergamon Press.

Leonowicz, A. M. and Jenny, B. (2011) Generating Hypsometric Layers from GTOPO30 for Small-Scale Mapping. *Proceedings of the 6th ICA Mountain Cartography Workshop: Mountain Mapping and Visualization*, pp. 139-146.

Leonowicz, A. M., Jenny, B., and Hurni, L. (2010a) Automated Reduction of Visual Complexity in Small-Scale Relief Shading. *Cartographica*, 45, 1, pp.64-74.

Leonowicz, A. M., Jenny, B., and Hurni, L. (2010b) Terrain Sculptor: Generalizing Terrain Models for Relief Shading. *Cartographic Perspectives*, 67, pp. 51-60.

Lillesand, T. M., Kiefer, R. W., and Chipman, J. W. (2007) *Remote Sensing and Image Interpretation*, 6th ed. New York, NY: Wiley & Sons.

Longley, P. A., Goodchild, M. F., Maguire, D. J., and Rhind, D. W. (2005) *Geographic Information Systems and Science*, 2nd ed. London, England: John Wiley & Sons Ltd.

MacEachren, A. M. (1995) *How Maps Work: Representation, Visualization, and Design*. New York, NY: Guilford.

Mackaness, W. A. and Ruas, A. (2007) Evaluation in the Map Generalisation Process in *Generalisation of Geographic Information: Cartographic Modeling and Applications*, Mackaness, W. A., Raus, A., and Sarjakoski, L. T. (eds.). Oxford, United Kingdom: Elsevier, Ltd., pp. 89-111.

Mark, D. M. (1975) Geomorphometric Parameters: A Review and Evaluation. *Geografiska Annaler Series A: Physical Geography*, 57, 3/4, pp. 165-177.

Mark, D. M. (1991) Object Modeling and Phenomenon-Based Generalization in *Map Generalization*, Buttenfield, B. P. and McMaster, R. B. (eds.). New York, NY: John Wiley & Sons, pp. 103-118.

McMaster R. B. and Monmonier, M. (1989) A Conceptual Framework for Quantitative and Qualitative Raster-Mode Generalization. *Proceedings of GIS/LIS 1989*, Orlando, Florida, November, pp. 390-403.

McMaster, R. B. (1989) Introduction to 'Numerical Generalization in Cartography'. *Cartographica*, 26, 1, pp. 1-6.

McMaster, R. B. and Shea, K. S. (1992) *Generalization in Digital Cartography*. Washington D.C.: Association of American Geographers.

Moellering, H. (2000) The Scope and Conceptual Content of Analytical Cartography. *Cartography and Geographic Information Science*, 27, 3, pp. 205-223.

Morrison, J. L. (1974) A Theoretical Framework for Cartographic Generalization with Emphasis on the Process of Symbology. *International Yearbook of Cartography*, 14, pp. 115-127.

National Standard for Spatial Data Accuracy (NSSDA) (1998) Geospatial Positioning Accuracy Standards, Part 3: National Standard for Spatial Data Accuracy. *Federal Geographic Data Committee, FGDC-STD-007.3-1998* , available <http://www.fgdc.gov/standards/projects/FGDC-standards-projects/accuracy/part3/chapter3> Last visited 8/21/2013.

O'Sullivan, D. and Unwin, D. J. (2010) *Geographic Information Analysis*, 2nd ed. New York, NY: John Wiley & Sons.

Openshaw, S. (1983) *The Modifiable Areal Unit Problem: Concepts and Techniques in Modern Geography*. Norwich, England: Geo Books.

Osborn, K., List, J., Gesch, D., Crowe, J., Merrill, G., Constance, E., Mauck, J., Lund, C., Caruso, V., and Kosvich, J. (2001) National Digital Elevation Program in *Digital Elevation Model Technologies and Application: The DEM Users Manual*, Maune, D. (ed.). Bethesda: American Society for Photogrammetry and Remote Sensing, pp. 83-120.

Patterson, T. (2000) A View on High: Heinrich Berann's Panoramas and Landscape Visualization Techniques for the U.S. National Park Service. *Cartographic Perspectives*, 36, 1, pp. 38-65.

Patterson, T. (2001) DEM Manipulation and 3-D Terrain Visualization: Techniques Used by the U.S. National Park Service. *Cartographica*, 38, 1, pp. 89-101.

Patterson, T. (2012) Creating Web Map Shaded Relief, Shaded Relief: Ideas and techniques about relief presentation on maps. *Shaded Relief: Ideas and Techniques about Relief Presentation on Maps*, available <http://www.shadedrelief.com/web_relief/> Last visited 12/1/12.

Patterson, T. and Jenny, B. (2012) ShadedReliefArchive.com – a Digital Repository for Cartographic Relief Art. *World Museums Magazine*, 297, pp. 46-50.

Patterson, T. and Vaughn Kelso, N. (2004) Hal Shelton Revised: Designing and Producing Natural-Color Maps with Satellite Land Cover Data. *Cartographic Perspectives*, 47, pp. 28-53.

Pike, R. J. and Thelin, G. P. (1990) Mapping the Nation's Physiography by Computer. *Cartographic Perspectives*, 8, pp. 15-24.

Piwowar, J. M., LeDrew, E. F., and Dudycha, D. J. (1990) Integration of Spatial Data in Vector and Raster Formats in a Geographic Information System Environment. *International Journal of Geographical Information Systems*, 4, 4, pp. 429-444.

Raisz, E. J. (1931) The Physiographic Method of Representing Scenery on Maps. *Geographical Review*, 21, 2, pp. 297-304.

Raisz, E. J. (1962) *Principles of Cartography*. New York, NY: McGraw-Hill.

Robinson, A. H. and Thrower, N. J. W. (1957) A New Method of Terrain Representation. *Geographical Review*, 47, 4, pp. 507-520.

Robinson, A. and Sale, R. (1969) *Elements of Cartography*, 3rd ed. New York, NY: John Wiley & Sons, Inc.

Robinson, W. S. (1950) Ecological Correlations and the Behavior of Individuals. *American Sociological Review*, 15, 3, pp. 351-357.

Rodríguez, E., Morris, C. S., Belz, J. E., Chapin, E. C., Martin, J. M., Daffer, W., and Hensley, S. (2005) An Assessment of the SRTM Topographic Products. Technical Report JPL D-31639, *Jet Propulsion Laboratory*, available <www2.jpl.nasa.gov/srtm/SRTM_D31639.pdf> Last visited 1/11/13.

Simley, J. D. (2011) USGS National Hydrography Dataset Newsletter – August 2011. *NHD Newsletters*, 10, 10, available <nhd.usgs.gov/newsletter_list.html> Last visited 1/27/13.

Simley, J. D. (2012) USGS National Hydrography Dataset Newsletter – January 2012. *NHD Newsletters*, 11, 3, available <nhd.usgs.gov/newsletter_list.html> Last visited 1/27/13.

Simley, J. D. and Carswell, W. J., Jr. (2009) The National Map: Hydrography. *U. S. Geological Survey Fact Sheet 2009-3054*, available <http://pubs.usgs.gov/fs/2009/3054> Last visited 12/1/12.

Slocum, T., McMaster, R., Kessler, F., and Howard, H. (2009) *Thematic Cartography and Geovisualization*, 3rd ed. Upper Saddle River, NJ: Pearson.

Stanislawski, L. V. (2009) Feature Pruning by Upstream Drainage Area to Support Automated Generalization of the United States National Hydrography Dataset. *Computers, Environment and Urban Systems*, 33, pp. 325-333.

Stanislawski, L. V. and Buttenfield, B. P. (2011) Hydrographic Generalization Tailored to Dry Mountainous Regions. *Cartography and Geographic Information Society*, 38, 2, pp. 117-125.

Stanislawski, L. V., Briat, M. O., Punt, E., Howard, M. Brewer, C. A., and Buttenfield, B. P. (2012 a) Density Stratified Thinning of Road Networks to Support Automated Generalization for The National Map. *Proceedings of the 15th Workshop of the International Cartographic Association Commission on Generalisation and Multiple Representation*, Istanbul, Turkey, September.

Stanislawski, L. V., Doumbouya, A. T. Miller-Corbett, C. D., Buttenfield, B. P., and Arundel-Murin, S. T. (2012 b) Scaling Stream Densities for Hydrologic Generalization. *Proceedings of GIScience 2012 Short Paper*, Columbus Ohio, September.

Stanislawski, L. V., Finn, M. P., and Buttenfield, B. P. (in press) Integrating Hydrographic Generalization Over Multiple Physiographic Regimes in *Generalization and Data Integration*, Mackaness, W. A., and Buttenfield, B. P. (eds).

Stanislawski, L. V., Raposo, P., Howard, M. and Buttenfield, B. P. (2012 c) Automated Metric Assessment of Line Simplification in Humid Landscapes. *Proceedings of Auto-Carto 12*, Columbus, Ohio, September.

Steward, H. J. (1974) Cartographic Generalization: Some Concepts and Explanation. *Cartographica*, 11, 1, pp. 1-50.

Stoter, J. E. (2005) Generalisation within NMA's in the 21st Century. *Proceedings of the 22nd International Cartographic Conference*, Coruna, Spain.

Sugarbaker, L. J. and Carswell, W. J., Jr (2011) The National Map. *U.S. Geological Survey Fact Sheet 2011-3042*, available <http://pubs.usgs.gov/fs/2011/3042> Last visited 12/1/12.

Sugarbaker, L., Coray, K. E., and Poore, B. (2009) The National Map Consumer Requirements: Findings from Interviews and Surveys. *U. S. Geological Survey Open File Report 2009-1222*, available <http://pubs.usgs.gov/of/2009/1222/> Last visited 12/1/12.

Taylor, P. J. (1977) *Quantitative Methods in Geography: An Introduction to Spatial Analysis*. Boston, MA: Houghton Mifflin.

The National Atlas (2012) One Million-Scale Streams. *National Atlas of the United States*, available <http://nationalatlas.gov> Last visited 8/19/13.

Tobler, W. D. (1976) Analytical Cartography. *The American Cartographer*, 3, 1, pp. 21-31.

Tobler, W.R. (1987) Measuring Spatial Resolution. *Proceedings of the International Workshop on Geographical Information Systems*, Beijing, P.R.C., 25-28 May 1987, pp. 42-47.

Tobler, W. D. (1988) Resolution, Resampling, and All That in *Building Data Bases for Global Science*, Mounsey, H. and Tomlinson, R. (eds.). London, England: Taylor and Francis, pp. 129-137.

Tomlinson, R. (2003) *Thinking About GIS: geographic information system planning for managers*. Redlands, CA: ESRI Press.

Tóth, T. (2010) Accidental cARTographer. *Cartographic Perspectives*, 67, pp. 19-28.

Tyner, J. (2010) *Principles of Map Design*. New York, NY: The Guilford Press.

U. S. Fish and Wildlife Service (2004) National Standards and Quality Components for Wetlands, Deepwater, and Related Habitat Mapping. *U.S. Fish and Wildlife Service Division of Habitat and Resource Conservation*, available <www.fws.gov/stand/standards/dl_wetlands_WWW.html> Last visited 1/27/13.

U. S. Geological Survey (USGS) (1985) Part 1: Series Description, Standards for 1:100,000-Scale Quadrangle Maps. *U. S. Geological Survey National Geospatial Program Standards Documents*, available <http://nationalmap.gov/standards/pdf/100K_Standards_Part1.pdf> Last visited 10/21/2013.

U. S. Geological Survey (USGS) (1999) Map Accuracy Standards. *US Department of the Interior and US Geological Survey, USGS Fact Sheet 171-99*, available <http://pubs.usgs.gov/fs/1999/0171/> Last visited 10/21/2013.

U. S. Geological Survey (USGS) (2000) The National Hydrography Dataset. *Data Users Guide*, available <*http://nhd.usgs.gov/chapter1/chp1_data_users_guide.pdf*> Last visited 10/21/2013.

Usery, E. L., Finn, M. P., and Starbuck, M. (2009) Data Layer Integration for *The National Map* of the United States. *Cartographic Perspectives*, 62, 1, pp. 28-41.

Usery, E. L., Finn, M., Scheidt, D., Ruhl, S., Beard, T., and Bearden, M. (2004) Geospatial Data Resampling and Resolution Effects on Watershed Modeling: A Case Study Using the Agricultural Non-Point Source Pollution Model. *Journal of Geographical Systems*, 6, 3, pp. 289-306.

Wade, T. and Sommer, S. (2006) *A to Z GIS: An illustrated dictionary of geographic information systems*, 2nd ed. Redlands, CA: ESRI Press.

Wang K. and Lo, C.-P. (1999) An Assessment of the Accuracy of Triangulated Irregular Networks (TINs) and Lattices in ARC/INFO. *Transactions in GIS*, 3, 2, pp. 161-174.

Weibel, R. (1987) An Adaptive Methodology for Automated Relief Generalization. *Proceedings of AutoCarto 8*, pp. 42-49.

Weibel, R. (1992) Models and Experiments for Adaptive Computer-Assisted Terrain Generalization. *Cartography and Geographic Information Society*, 19, 3, pp. 133-153.

Wolock, D. M. and McCabe, G. J. (1999) Estimates of runoff using water-balance and atmospheric general circulation models. *Journal of the American Water Resources Association*, 35, 6, pp. 1341-1350.

Wright, J. K. (1942) Map Makers are Human: Comments on the Subjective in Maps. *The Geographical Review*, 32, 4, pp. 527-544.

Wu, S., Li, J., Huang, G. (2005) An Evaluation of Grid Size Uncertainty in Empirical Soil Loss Modeling with Digital Elevation Models. *Environmental Modeling and Assessment*, 10, 1, pp. 33-42.

Zaksek, K. and Podabnikar, T. (2005) An Effective DEM Generalization with Basic GIS Operations. *Proceedings of the 8th ICA Workshop on Generalization and Multiple Representation*, A Coruńa, Spain, July.

Zhou, Q. and Chen, Y. (2010) Generalization of DEM for Terrain Analysis Using a Compound Method. *ISPRS Journal of Photogrammetry and Remote Sensing*, 66, pp. 38-45.

Appendix A: Benchmark Datasets

To achieve the goal of identifying attribute resolution change in a DEM after iterative filtering, data was compared to benchmark data with a known spatial resolution. Attribute resolution can be difficult to measure. However, attribute and spatial resolutions are intrinsically related. As fine spatial resolution DEMs are generalized through smoothing, a disconnect occurs between spatial and attribute resolutions. This disconnect was measured by systematically comparing a filtered data (unknown attribute resolution) to a benchmark dataset (known spatial resolution) to identify how the attribute resolution of the filtered data may match that of a known, coarser spatial resolution.

To accomplish this task, a raster and vector benchmarks were used throughout the analysis. The raster benchmark was taken from the National Elevation Dataset (NED). Though the NED consists of several products of varying resolution, only two were used as benchmarks, including the 1/3 arc-second and 1 arc-second, or 10- and 30-meter DEMs respectively. The NED benchmarks will be used to directly compare a filtered DEM to a benchmark at a known spatial resolution. This will be done using the standard deviation and semivariogram analyses. The vector benchmark was taken from the National Hydrography Dataset (NHD). The NHD is currently available in two resolutions, known as high resolution, based on a 1:24,000 topographic mapping scale, and medium resolution, based on a 1:100,000 topographic mapping scale (Simley and Carswell, 2009; USGS, 2000). The NHD benchmarks will be used to assess the degree of conflation between the filtered DEM and an existing vector dataset to measure the degree of vertical integration. Only a subset (flowlines) of the NHD will be used during this analysis.

In the following graphics, the benchmark data is shown for every study site. All of the maps are shown at a scale of 1:157,000. The upper two images are of the raster benchmarks, taken from the NED. The upper left map is the 10-meter benchmark DEM. The upper right map is the 30-meter benchmark DEM. At first, they look very similar. However, upon closer inspection, the 10-meter benchmark shows more detail (finer attribute resolution) than the 30-meter benchmark due to the difference in spatial resolutions. The lower two images are of the vector benchmarks, taken from the NHD. The lower left map is of the 1:24,000 compilation (high resolution) flowlines. The lower right map is of the 1:100,000 compilation (medium resolution) flowlines. The high resolution flowlines have a finer attribute resolution because more stream features are represented. Additionally, when flowlines are represented in both benchmarks, the high resolution features have more detail (vertices) in the lines. Study sites are ultimately divided into 4 physiographic regimes including rugged/dry, rugged/humid, flat/dry, and flat/humid and driven by the landscape partitions derived by Stanislawski et al. (2011). The terrain ruggedness was identified based on relative relief. The aridity was identified using estimated annual runoff which was considered to be a useful surrogate for precipitation.

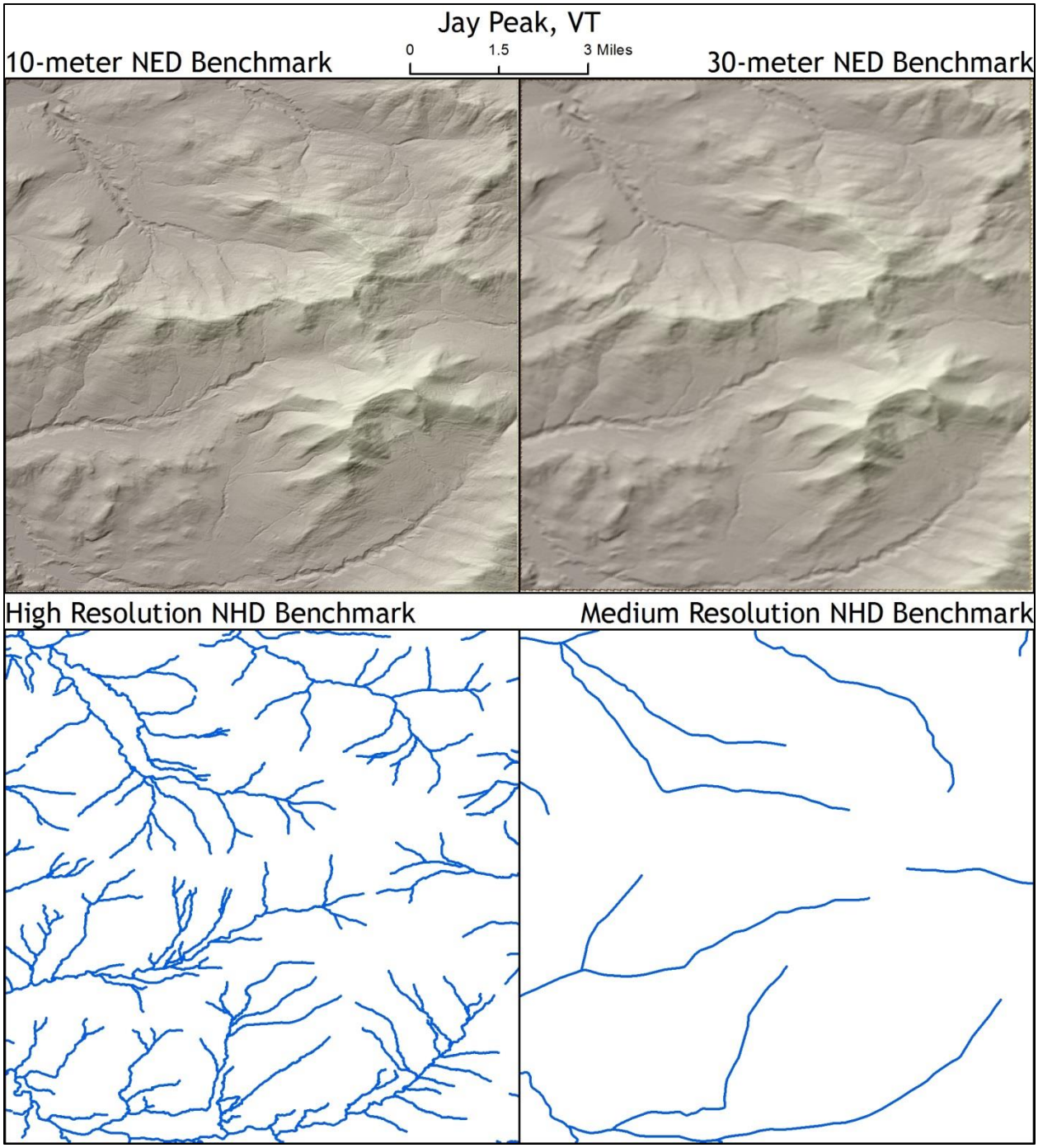

A.1: Semivariogram plots for Jay Peak, VT. This study site is classified as rugged, humid. The relief observed in this study site is 1033.92 meters and the estimated annual runoff is 760 millimeters. The study site only intersects one HUC08 subbasin.

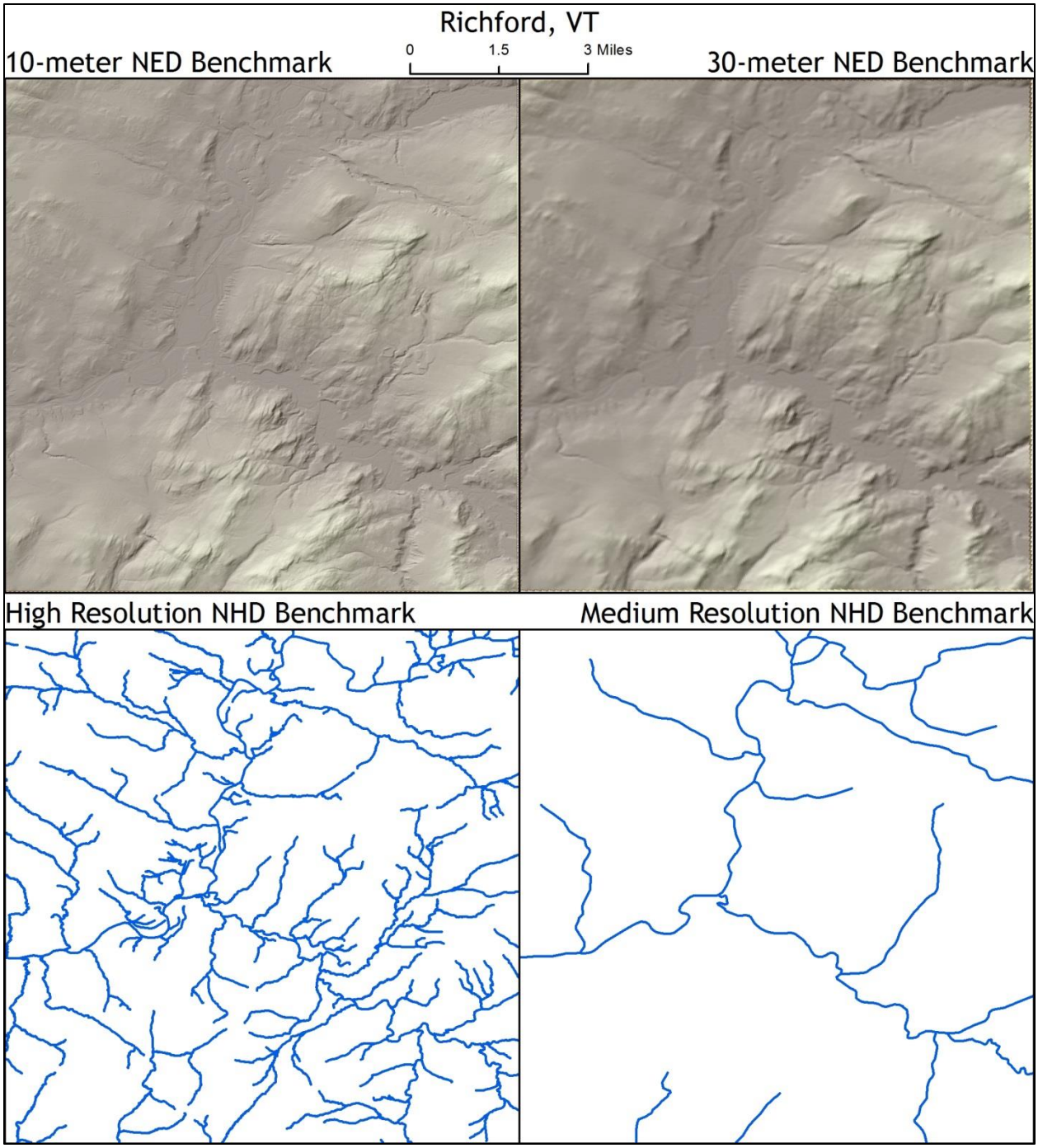

A.2: Semivariogram plots for Richford, VT. This study site is classified as rugged, humid. The relief observed in this study site is 454.67 meters and the estimated annual runoff is 590 millimeters. The study site only intersects one HUC08 subbasin.

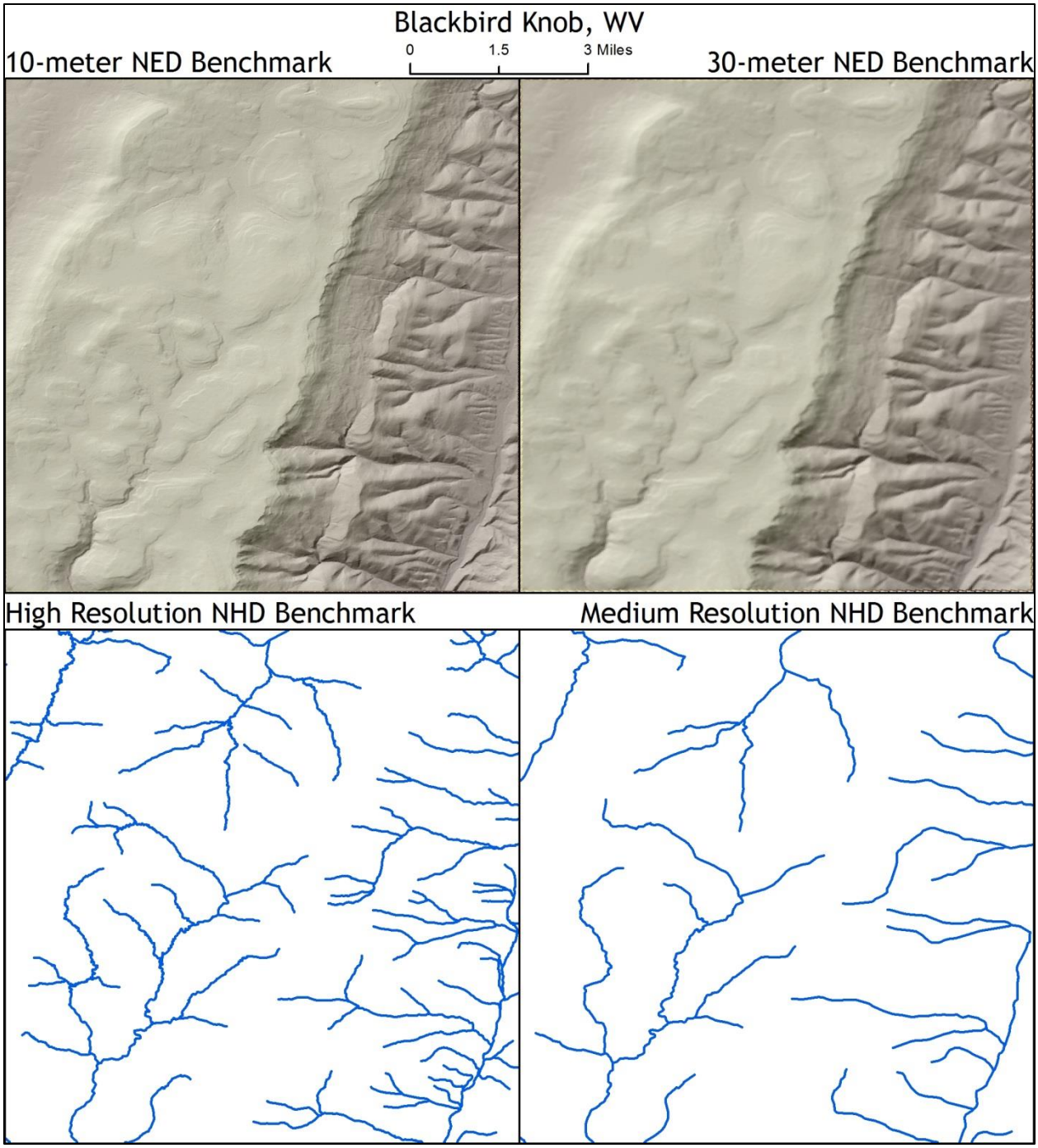

A.3: Semivariogram plots for Blackbird Knob, WV. This study site is classified as rugged, humid. The relief observed in this study site is 879.28 meters and the estimated annual runoff is 567 millimeters. The study site intersects 2 HUC08 subbasins.

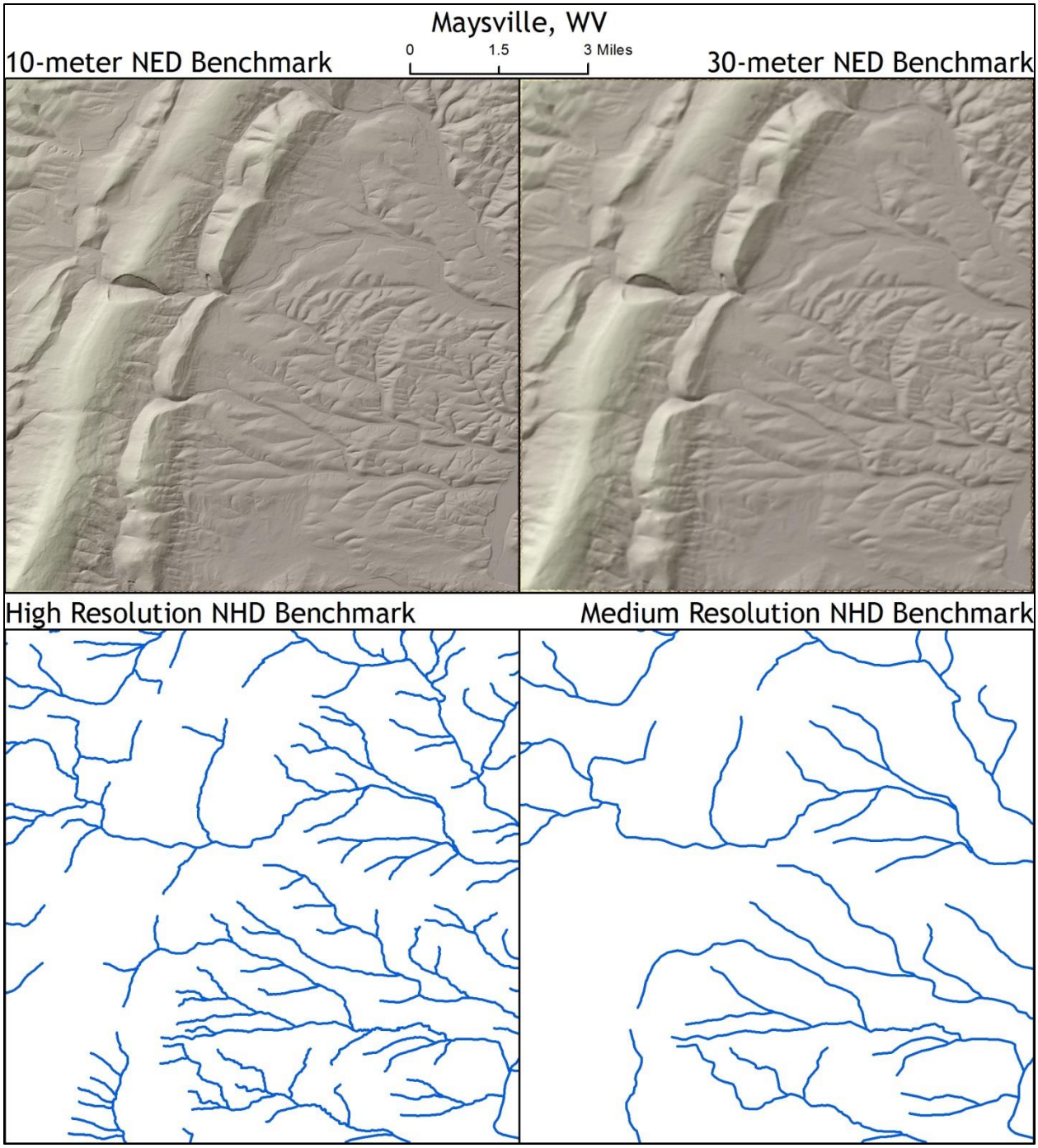

A.4: Semivariogram plots for Maysville, WV. This study site is classified as rugged, humid. The relief observed in this study site is 666.35 meters and the estimated annual runoff is 237 millimeters. The study site only intersects one HUC08 subbasin.

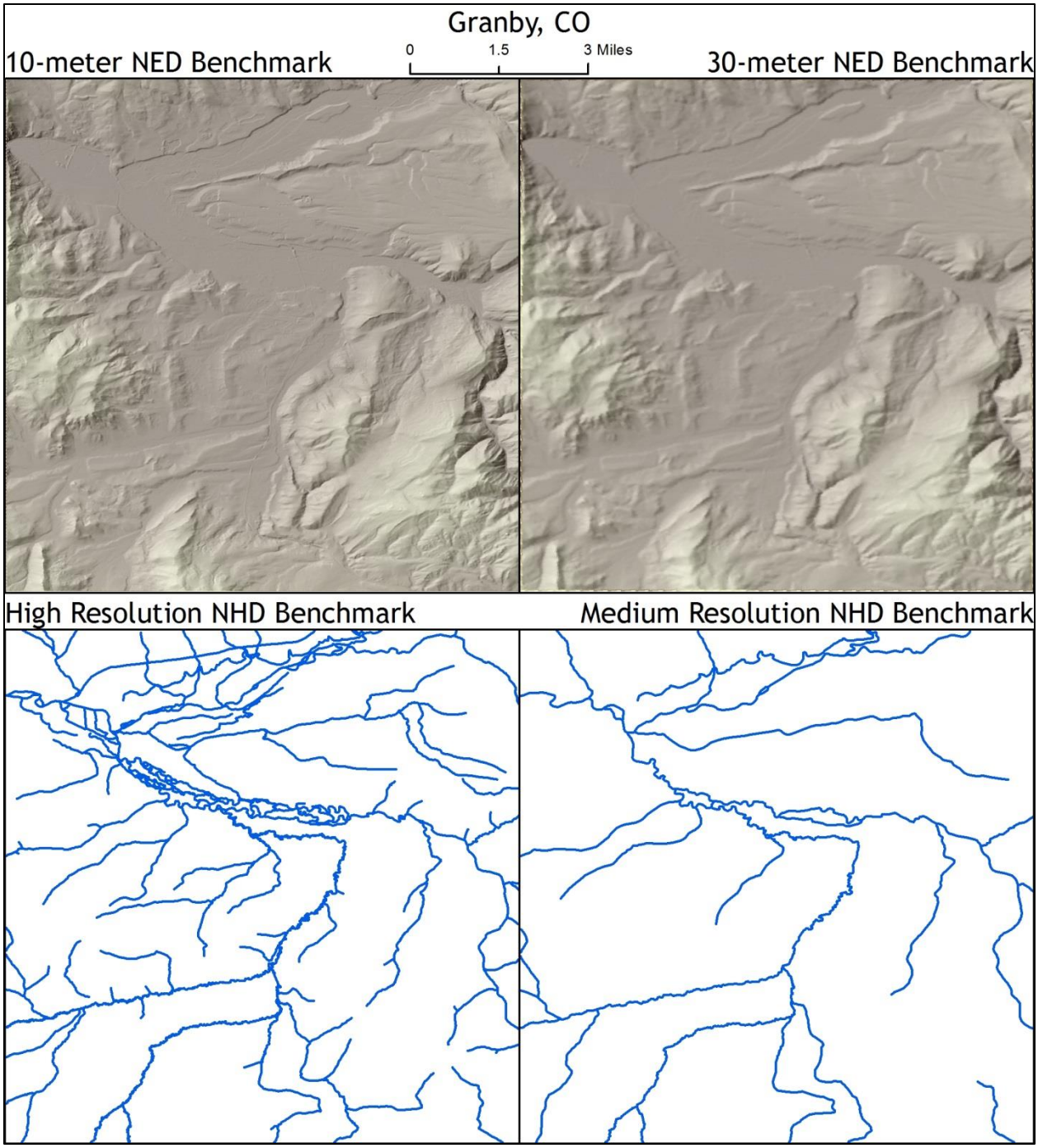

A.5: Semivariogram plots for Granby, CO. This study site is classified as rugged, dry. The relief observed in this study site is 554.86 meters and the estimated annual runoff is 120 millimeters. The study site only intersects one HUC08 subbasin.

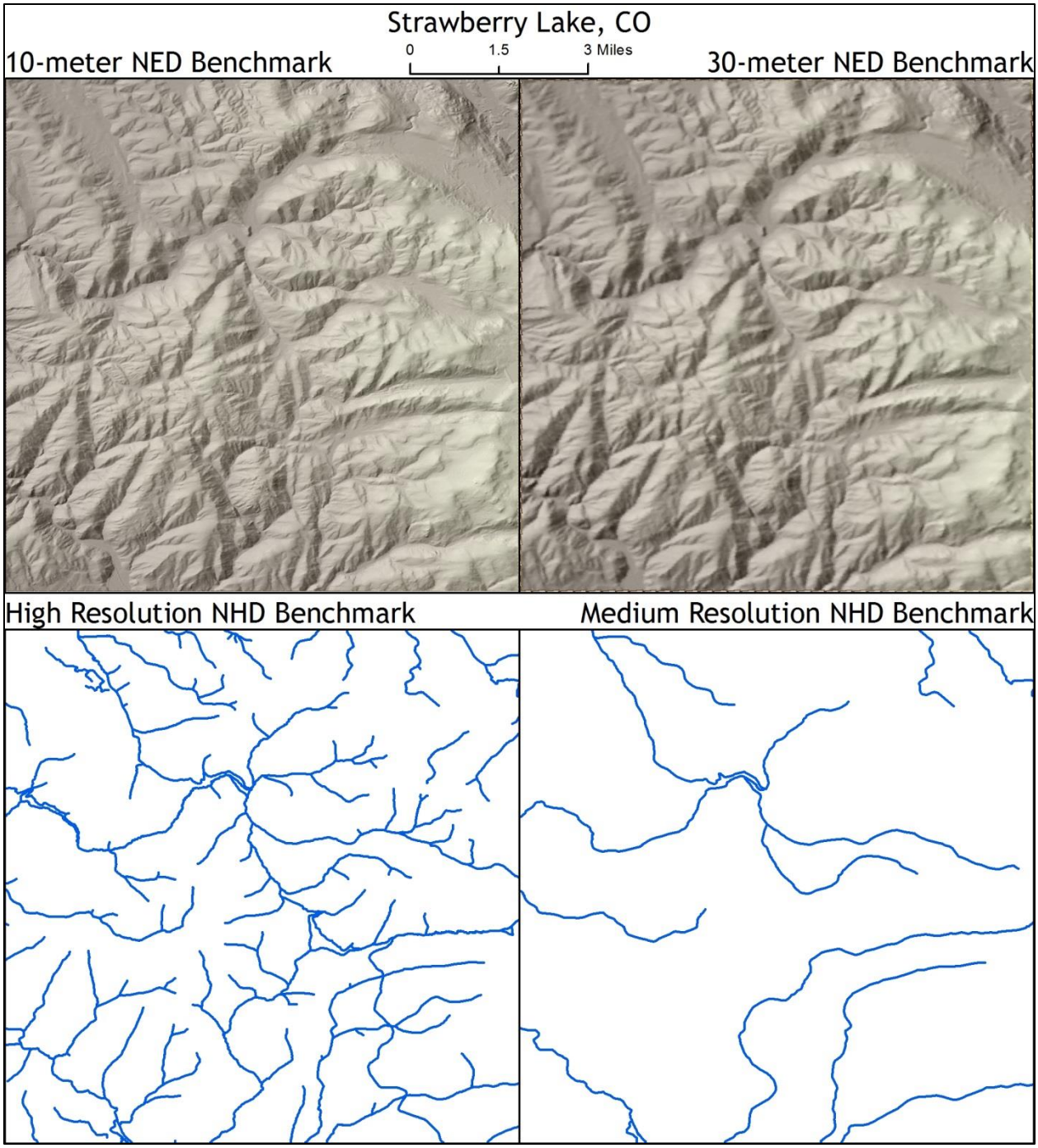

A.6: Semivariogram plots for Strawberry Lake, CO. This study site is classified as rugged, dry. The relief observed in this study site is 836.21 meters and the estimated annual runoff is 155 millimeters. The study site only intersects one HUC08 subbasin.

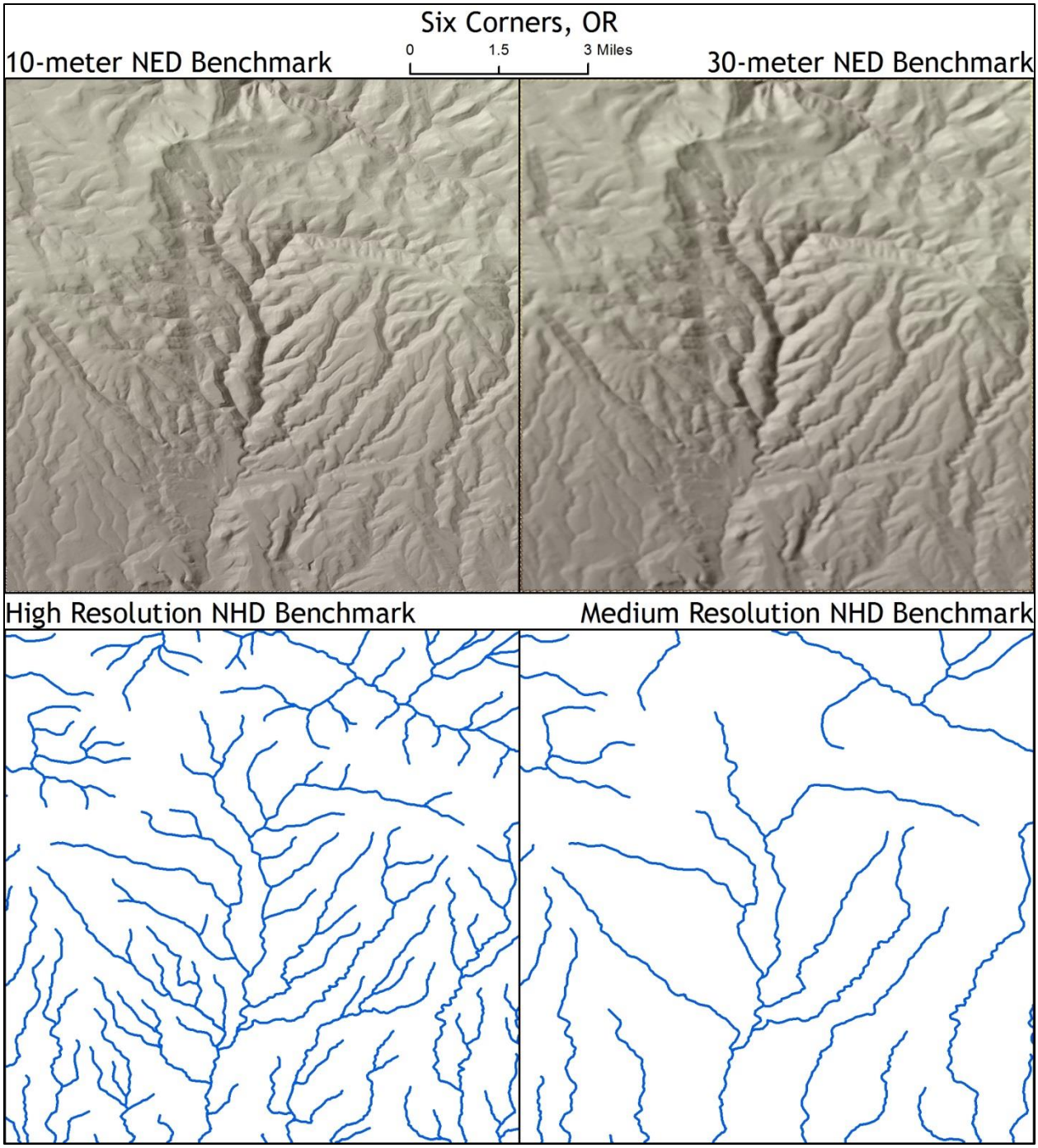

A.7: Semivariogram plots for Six Corners, OR. This study site is classified as rugged, dry. The relief observed in this study site is 671.97 meters and the estimated annual runoff is 110 millimeters. The study site only intersects one HUC08 subbasin.

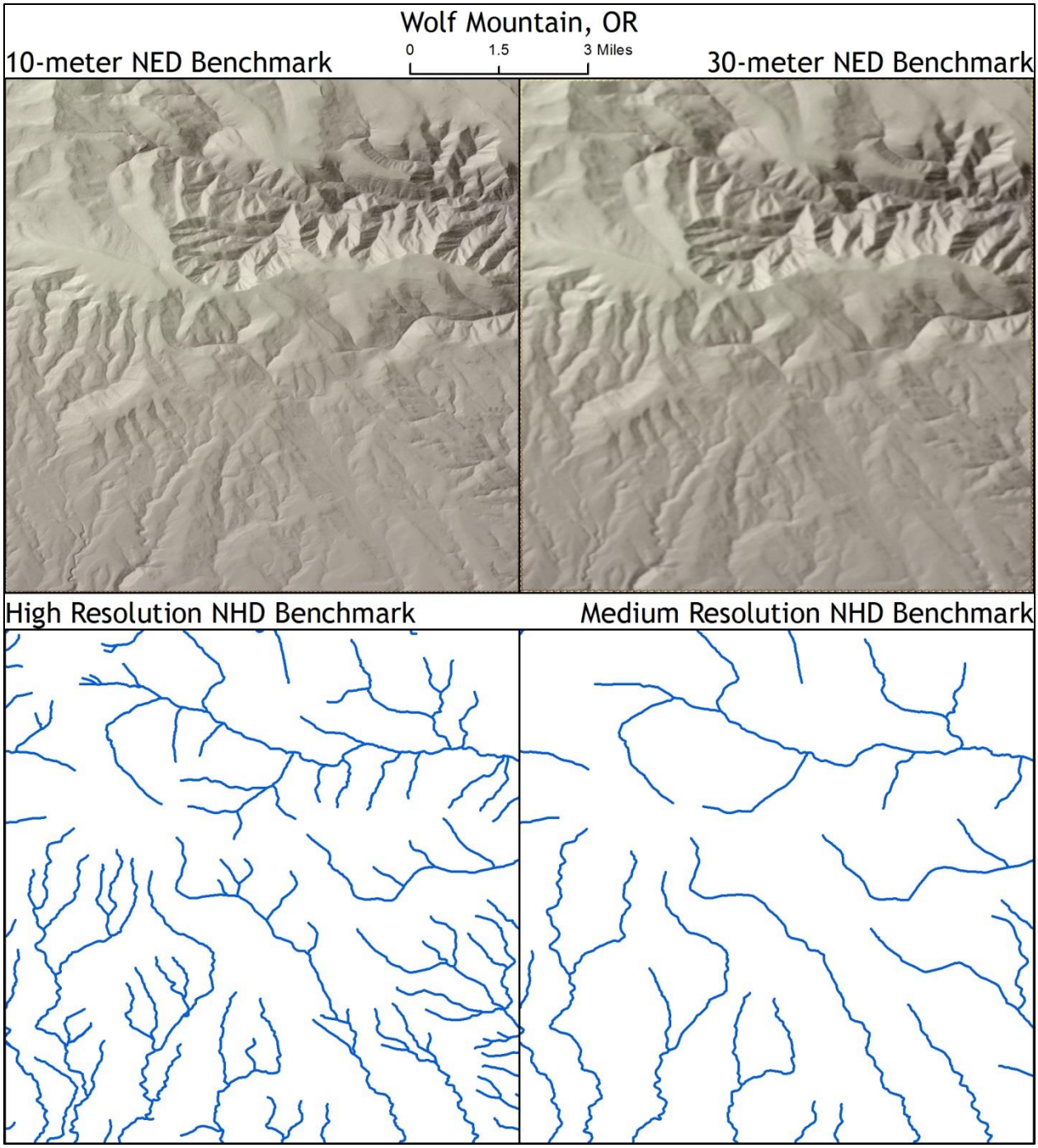

A.8: Semivariogram plots for Wolf Mountain, OR. This study site is classified as rugged, dry. The relief observed in this study site is 917.03 meters and the estimated annual runoff is 107 millimeters. The study site only intersects one HUC08 subbasin.

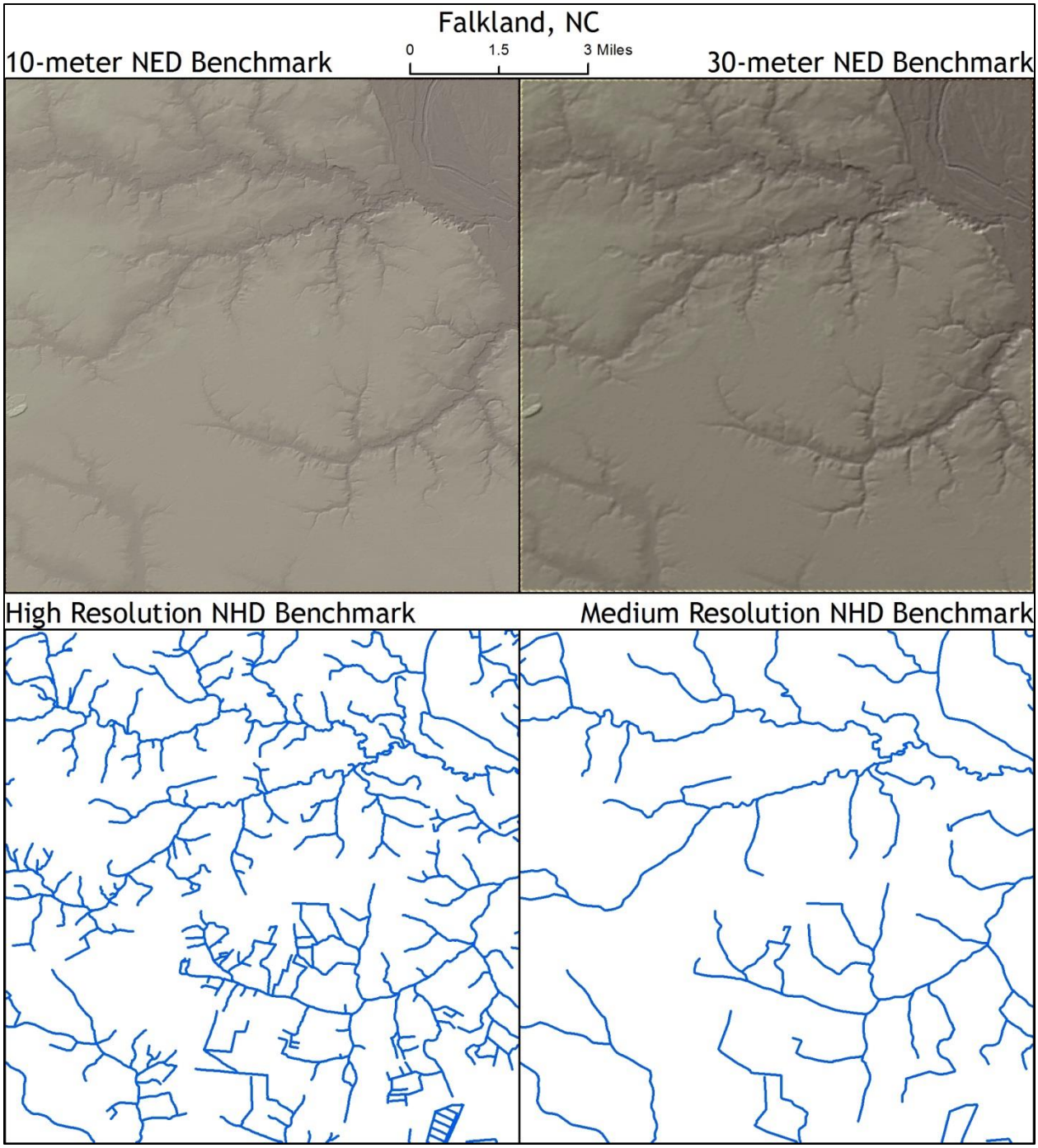

A.9: Semivariogram plots for Falkland, NC. This study site is classified as flat, humid. The relief observed in this study site is 40.38 meters and the estimated annual runoff is 383 millimeters. The study site only intersects one HUC08 subbasin.

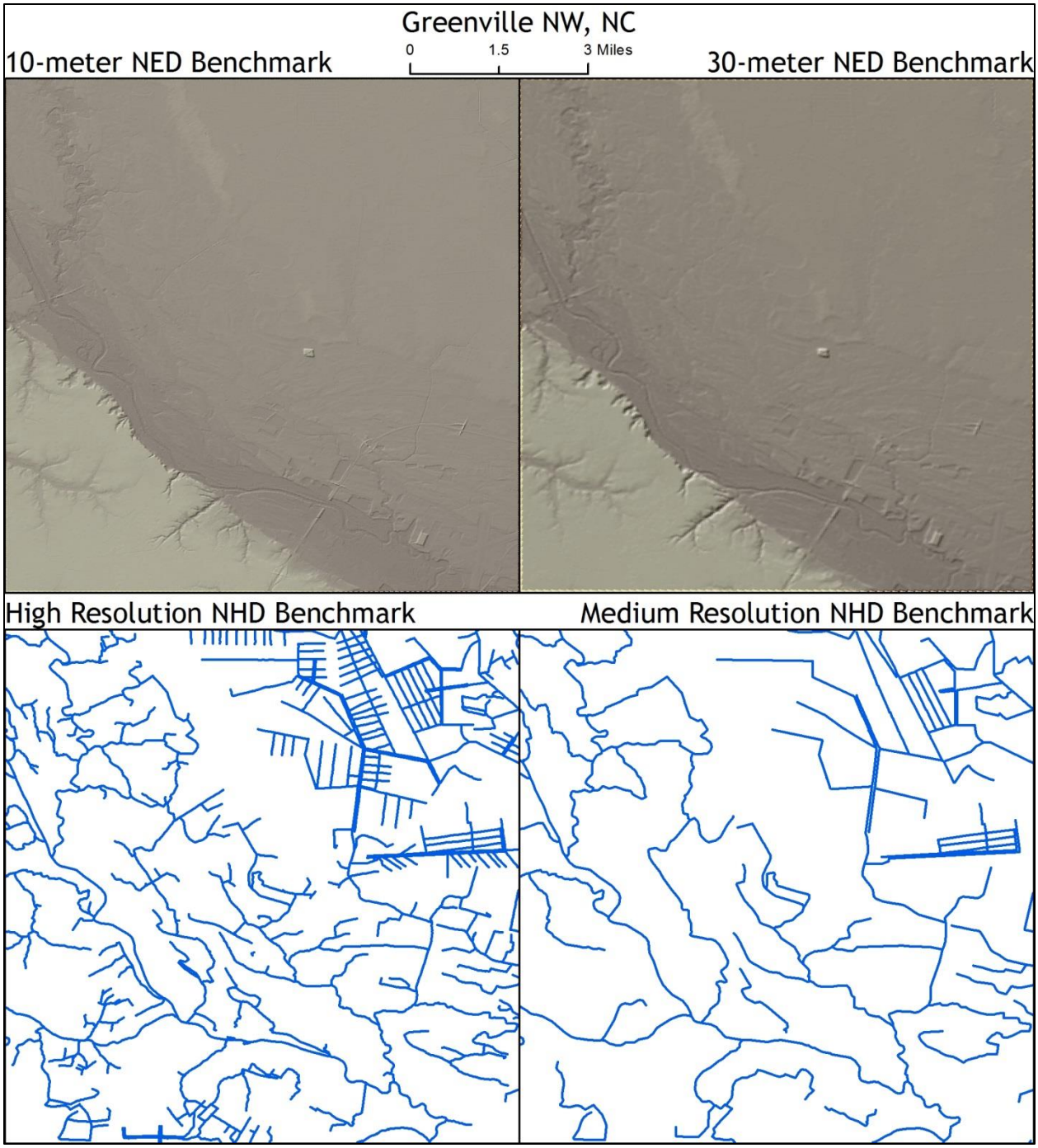

A.10: Semivariogram plots for Greenville, NC. This study site is classified as flat, humid. The relief observed in this study site is 29.36 meters and the estimated annual runoff is 405 millimeters. The study site only intersects one HUC08 subbasin.

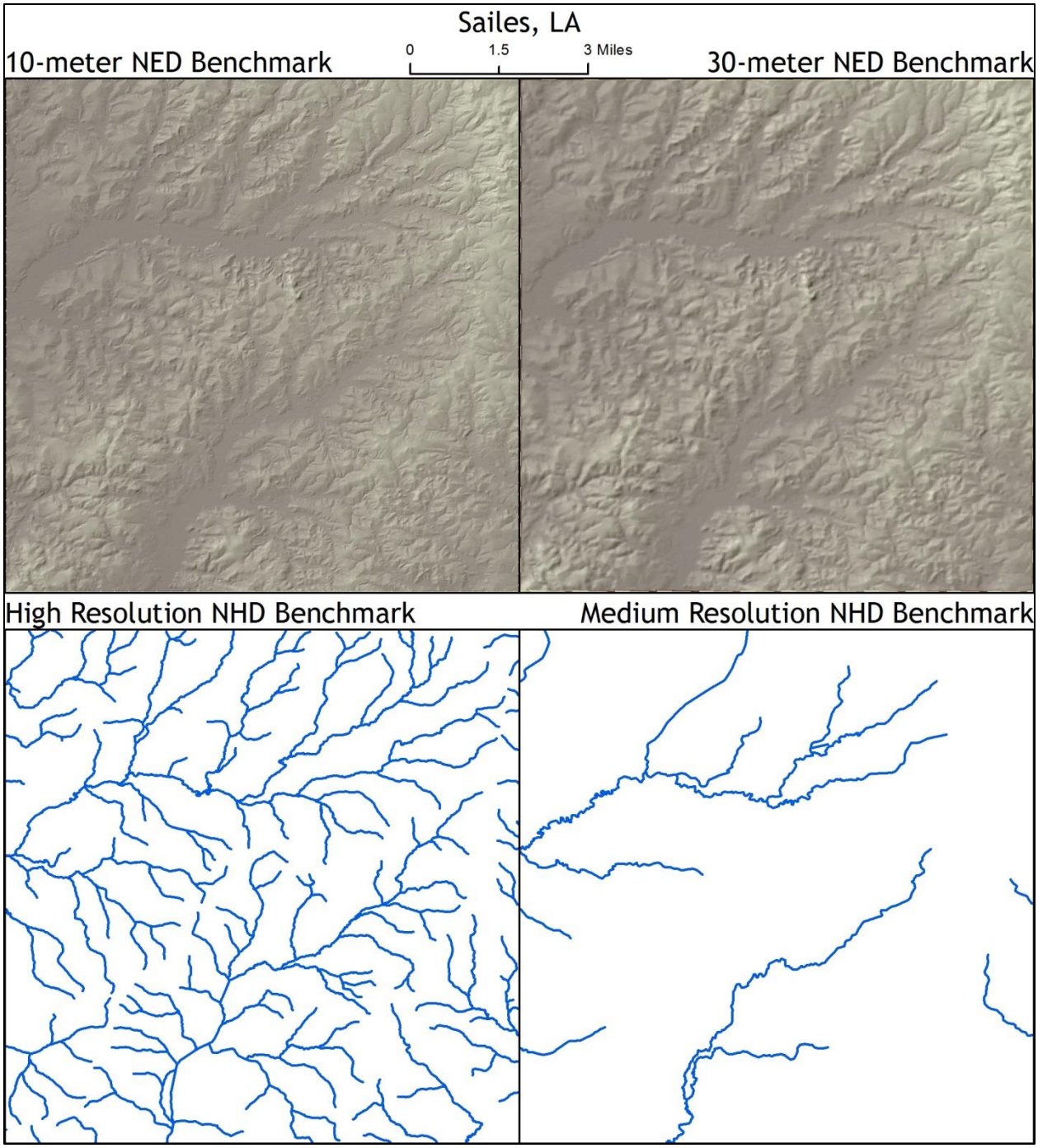

A.11: Semivariogram plots for Sailes, LA. This study site is classified as flat, humid. The relief observed in this study site is 92.72 meters and the estimated annual runoff is 551 millimeters. The study site only intersects one HUC08 subbasin.

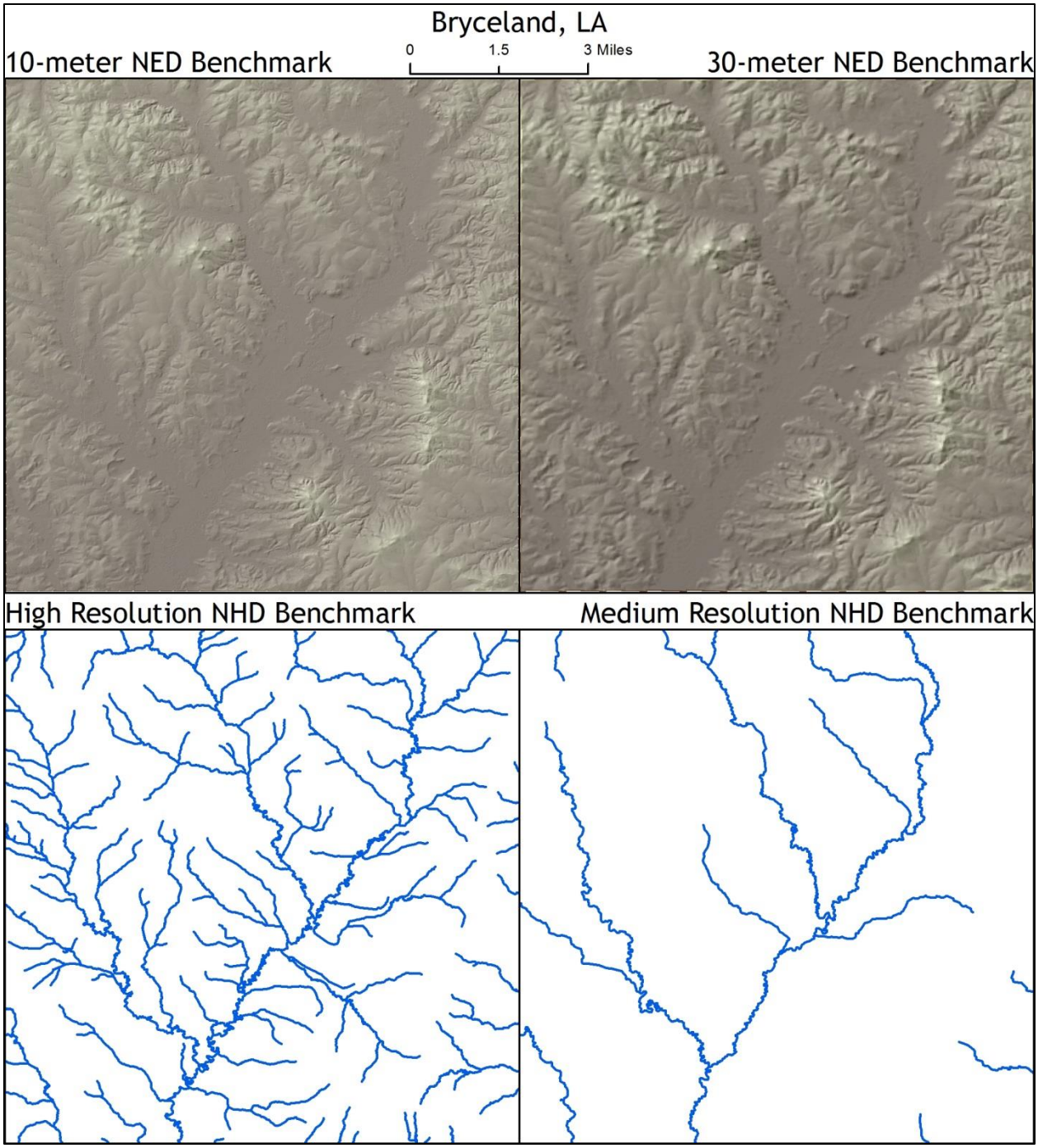

A.12: Semivariogram plots for Bryceland, LA. This study site is classified as flat, humid. The relief observed in this study site is 105.21 meters and the estimated annual runoff is 591 millimeters. The study site intersects 2 HUC08 subbasins.

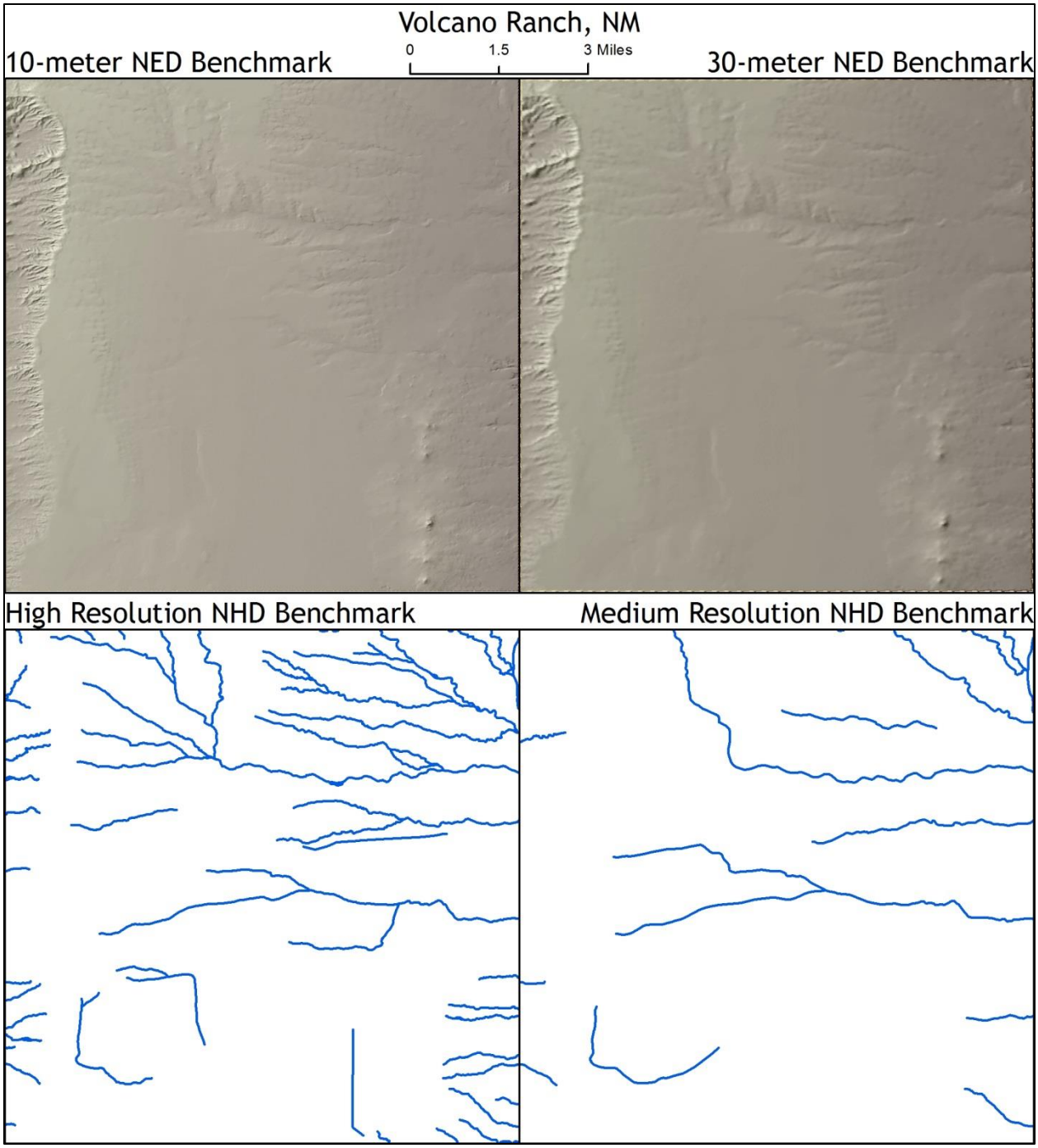

A.13: Semivariogram plots for Volcano Ranch, NM. This study site is classified as flat, dry. The relief observed in this study site is 254.48 meters and the estimated annual runoff is 12 millimeters. The study site only intersects one HUC08 subbasin.

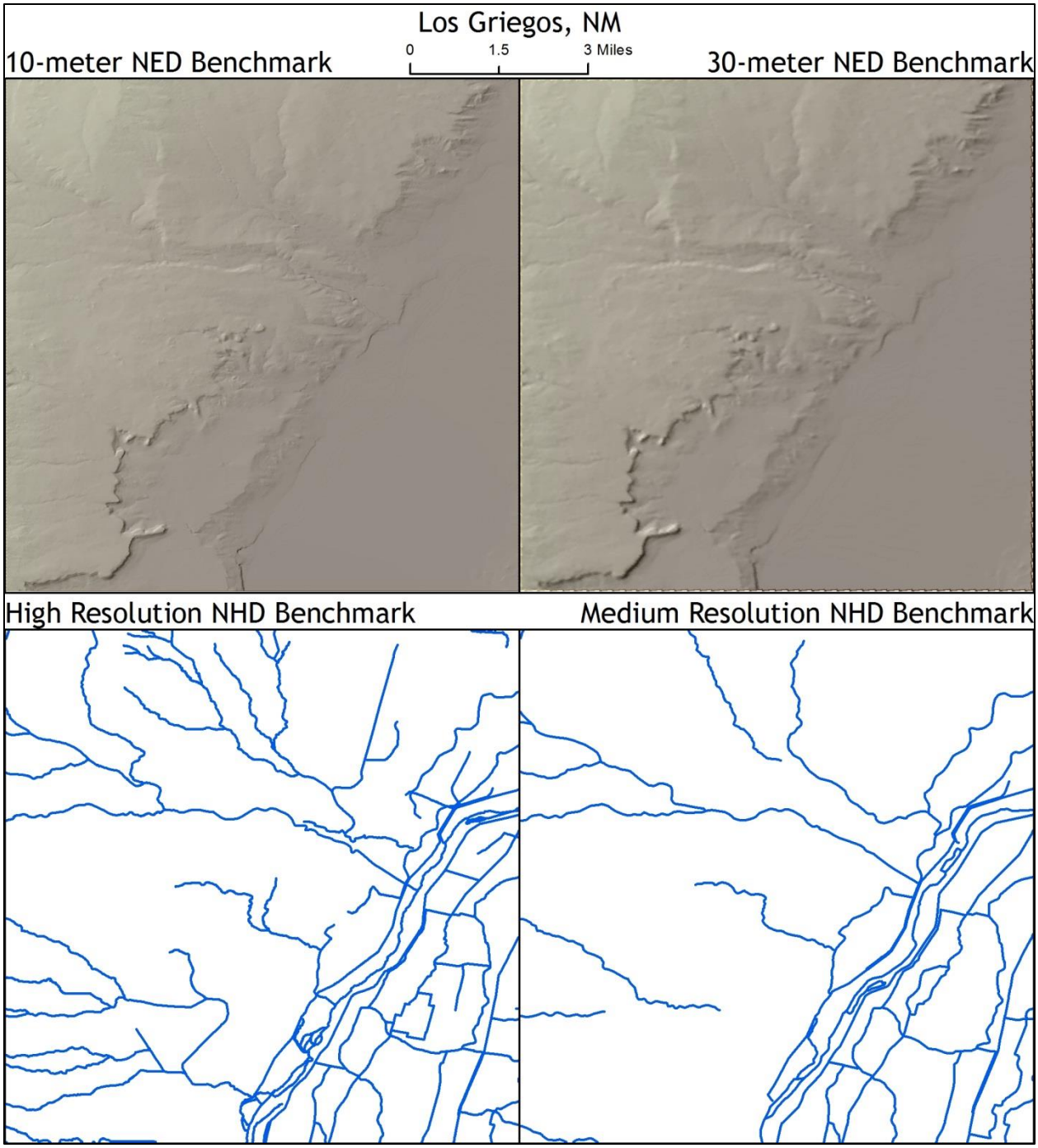

A.14: Semivariogram plots for Los Griegos, NM. This study site is classified as flat, dry. The relief observed in this study site is 221.11 meters and the estimated annual runoff is 11 millimeters. The study site only intersects one HUC08 subbasin.

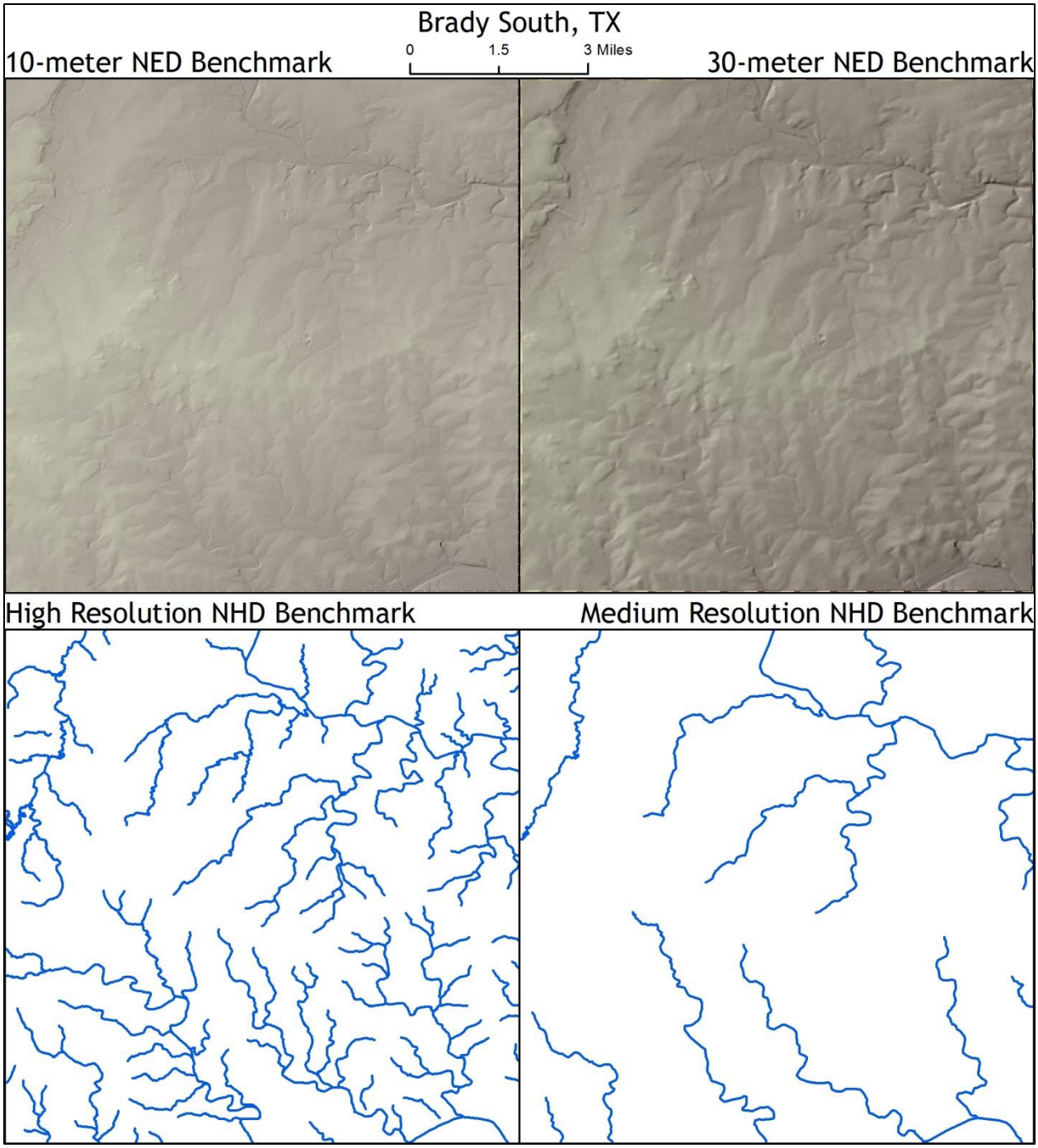

A.15: Semivariogram plots for Brady South, TX. This study site is classified as flat, dry. The relief observed in this study site is 125.46 meters and the estimated annual runoff is 54 millimeters. The study site only intersects one HUC08 subbasin.

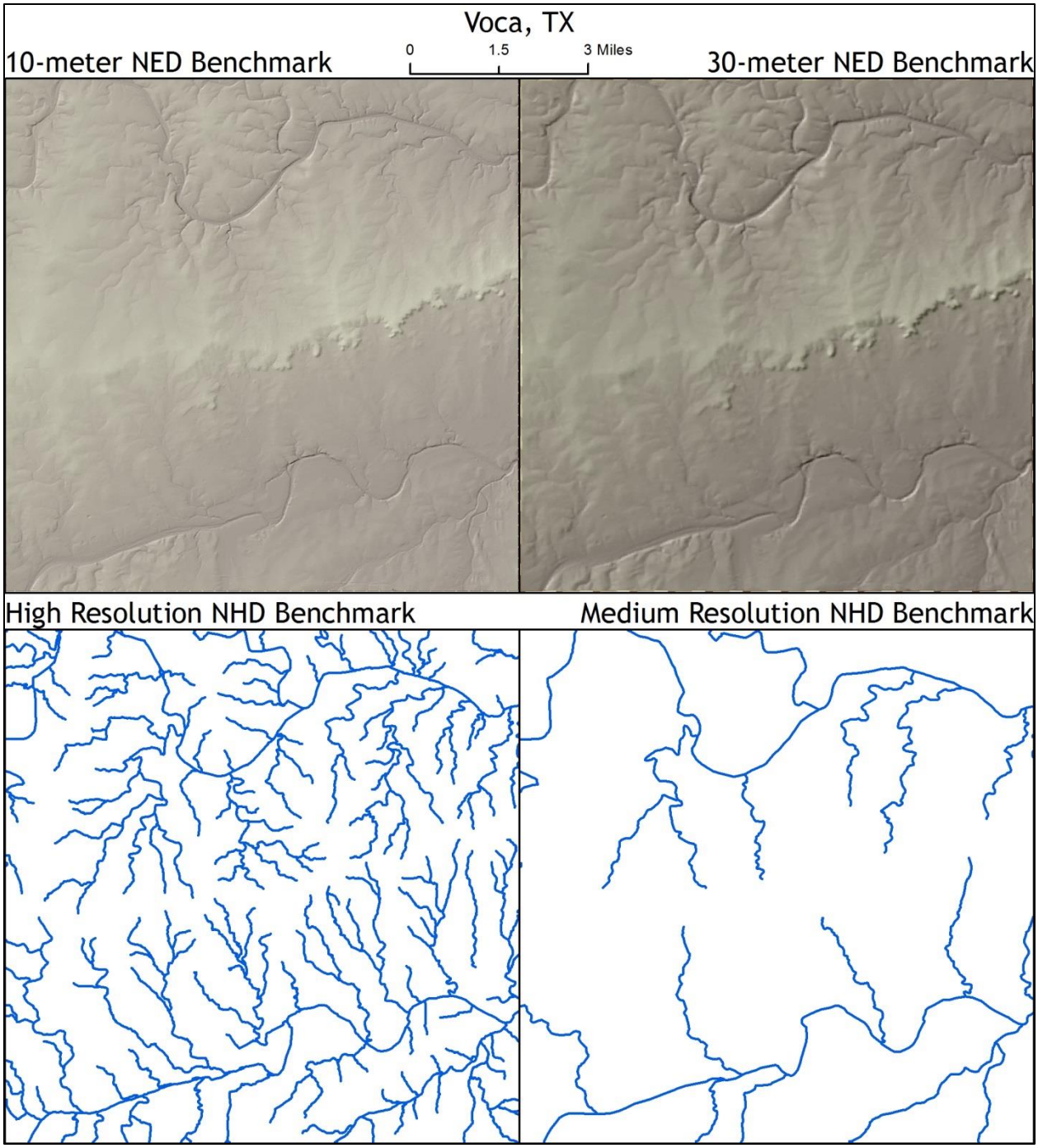

A.16: Semivariogram plots for Voca, TX. This study site is classified as flat, dry. The relief observed in this study site is 111.07 meters and the estimated annual runoff is 54 millimeters. The study site only intersects one HUC08 subbasin.

Appendix B: Standard Deviation Plots for all Study Sites

The first metric used to assess the change of resolution is the local standard deviation. Standard deviation has historically been used as a metric to estimate surface roughness and is a good predictor of how similar values are within a dataset. In this thesis, the standard deviation is used to compare the similarity of a neighborhood of cells in a smoothed DEM to a coarser resolution benchmark DEM. When the local standard deviations are most similar to the benchmark, the resolution of the smoothed DEM will be considered to have approached the benchmark resolution.

A 10x10 cell focal window was applied to the 3-meter filtered DEM in order to compare the standard deviation to the 10-meter benchmark (using a 3x3 cell window). A 30x30 cell focal window was then used on the 3-meter filtered DEM in order to compare the standard deviation to the 30-meter benchmark (using a 3x3 cell window). By altering the sizes of the focal window on the 3-meter DEMs, the areal extent of the windows are equivalent and comparisons can be made easily.

In the following graphics, the solid lines represent the focal standard deviation of the filtered DEM after each filter iteration. The dashed lines represent the focal standard deviation of the benchmark DEM. This line does not decrease or increase because it is computed only once, and meant to only serve as a standard to identify when the filtered DEM is most similar to the benchmark DEMs. The left panel compares the attribute resolution of the filtered DEM to the 10-meter benchmark. The right panel compares the attribute resolution of the filtered DEM to the 30-meter benchmark. It is important to note that the focal standard deviations (y-axis) cannot be compared between the two panels because it is calculated over different areal extents.

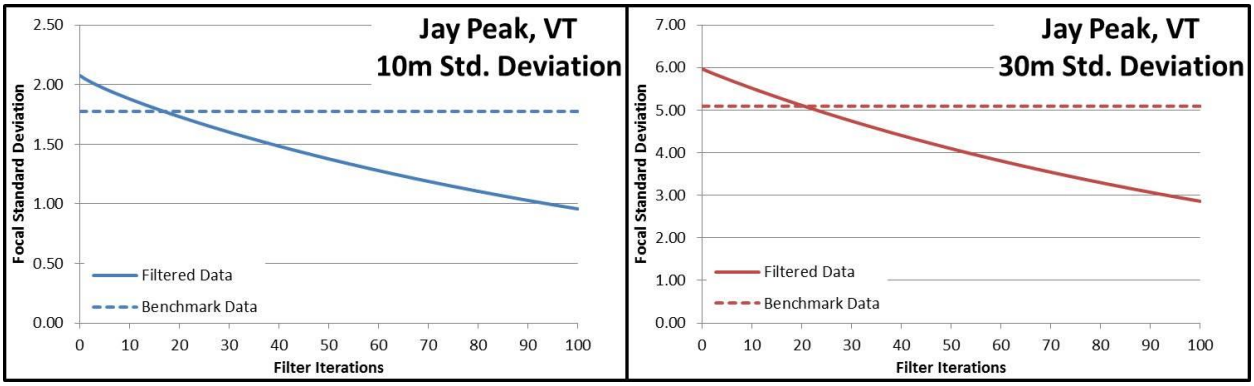

B.1: Standard deviation plot for Jay Peak, VT. This study site is classified as rugged, humid. A standard deviation value for the 3-meter DEM is most similar to the attribute resolution of the 10-meter benchmark after 17 iterations. A standard deviation value for the 3-meter DEM is most similar to the attribute resolution of the 30-meter benchmark after 21 iterations.

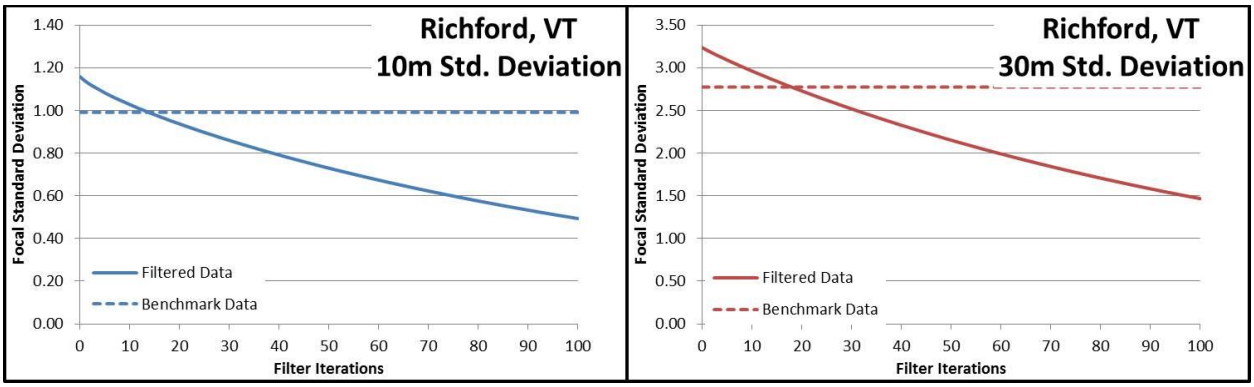

B.2: Standard deviation plot for Richford, VT. This study site is classified as rugged, humid. A standard deviation value for the 3-meter DEM is most similar to the attribute resolution of the 10-meter benchmark after 14 iterations. A standard deviation value for the 3-meter DEM is most similar to the attribute resolution of the 30-meter benchmark after 18 iterations. This study site achieves a coarser attribute resolution before any other rugged study site. This is likely due to the terrain being transitional (mixed low-high relief) and containing a wide river basin.

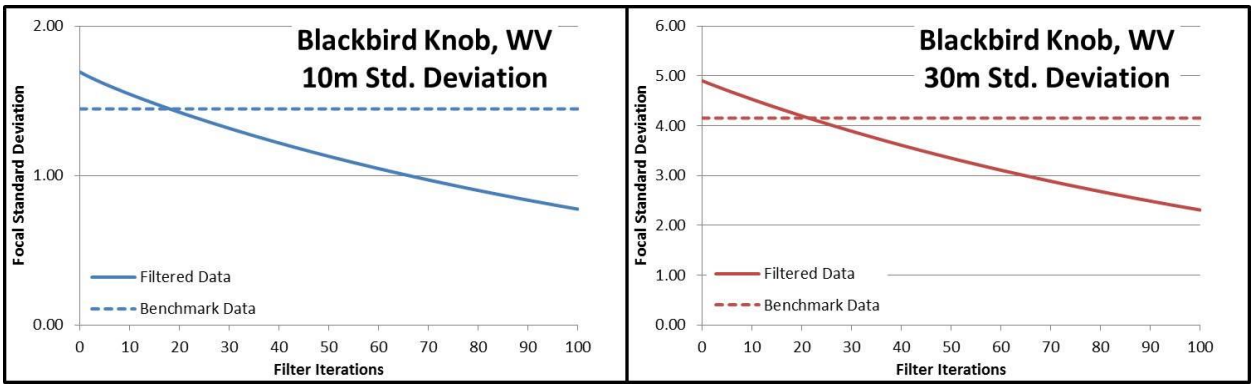

B.3: Standard deviation plot for Blackbird Knob, WV. This study site is classified as rugged, humid. A standard deviation value for the 3-meter DEM is most similar to the attribute resolution of the 10-meter benchmark after 19 iterations. A standard deviation value for the 3-meter DEM is most similar to the attribute resolution of the 30-meter benchmark after 22 iterations. Blackbird Knob, WV requires the highest number of filtering iterations for rugged landscapes.

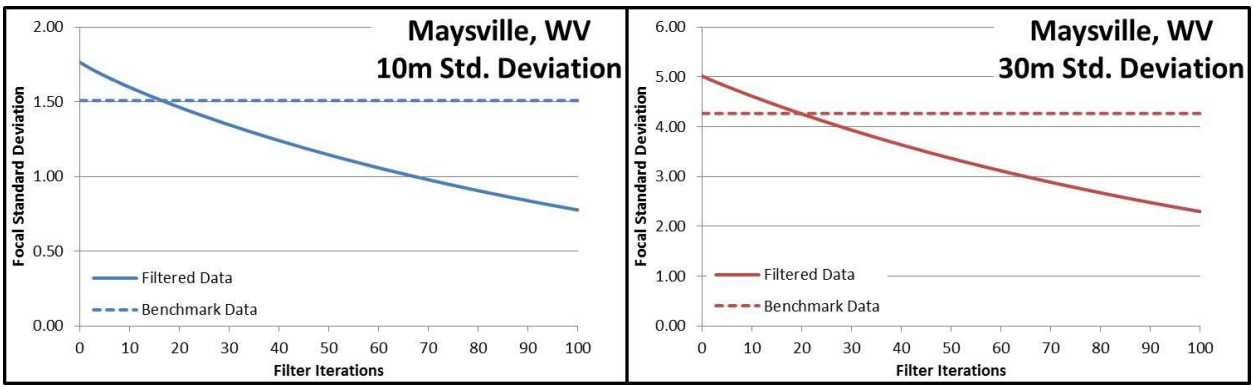

B.4: Standard deviation plot for Maysville, WV. This study site is classified as rugged, humid. A standard deviation value for the 3-meter DEM is most similar to the attribute resolution of the

10-meter benchmark after 17 iterations. A standard deviation value for the 3-meter DEM is most similar to the attribute resolution of the 30-meter benchmark after 20 iterations.

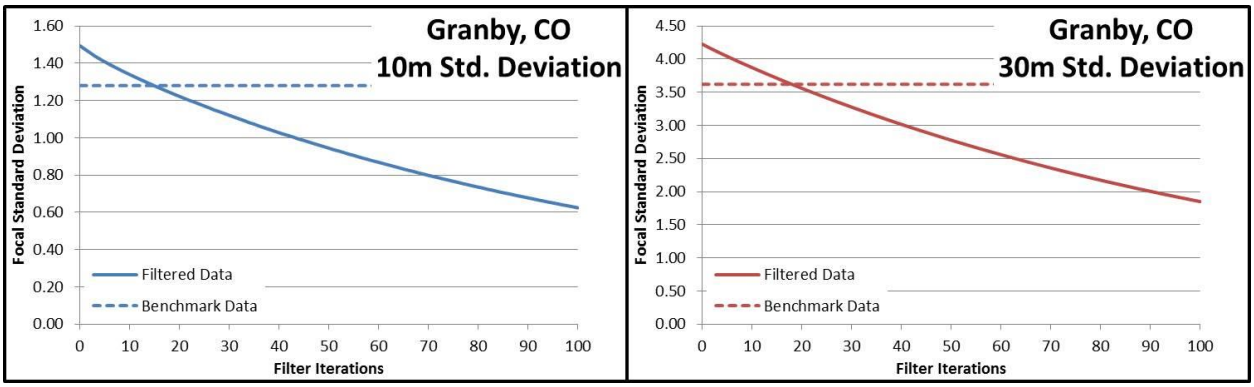

B.5: Standard deviation plot for Granby, CO. This study site is classified as rugged, dry. A standard deviation value for the 3-meter DEM is most similar to the attribute resolution of the 10-meter benchmark after 15 iterations. A standard deviation value for the 3-meter DEM is most similar to the attribute resolution of the 30-meter benchmark after 18 iterations. Granby, CO, achieves a coarser attribute resolution quickly relative to other rugged study sties. Similar to Richford, VT, this study site also has a mixed terrain (low to high relief).

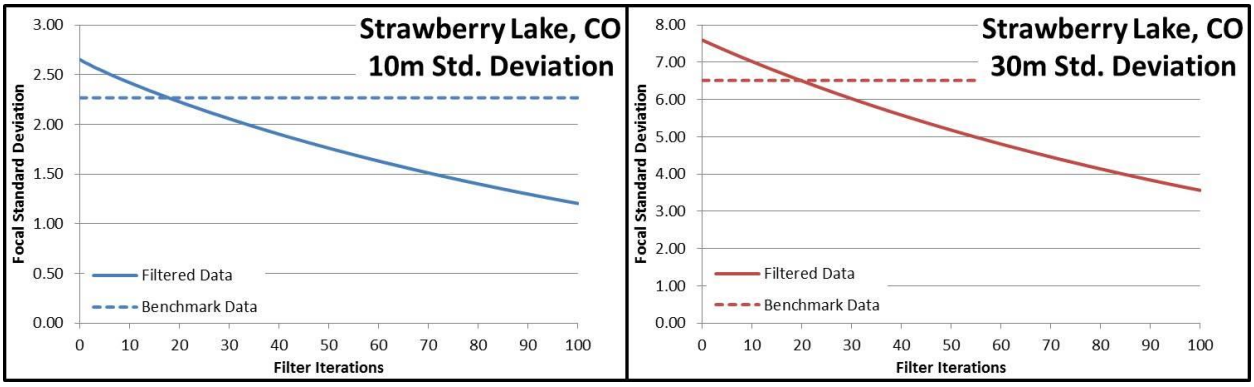

B.6: Standard deviation plot for Strawberry Lake, CO. This study site is classified as rugged, dry. A standard deviation value for the 3-meter DEM is most similar to the attribute resolution of the 10-meter benchmark after 18 iterations. A standard deviation value for the 3-meter DEM is most similar to the attribute resolution of the 30-meter benchmark after 20 iterations.

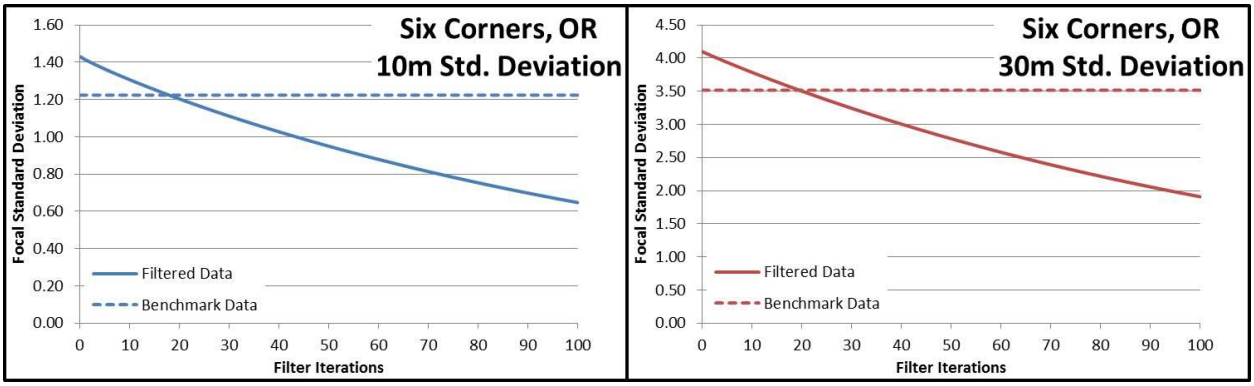

B.7: Standard deviation plot for Six Corners, OR. This study site is classified as rugged, dry. A standard deviation value for the 3-meter DEM is most similar to the attribute resolution of the 10-meter benchmark after 18 iterations. A standard deviation value for the 3-meter DEM is most similar to the attribute resolution of the 30-meter benchmark after 21 iterations.

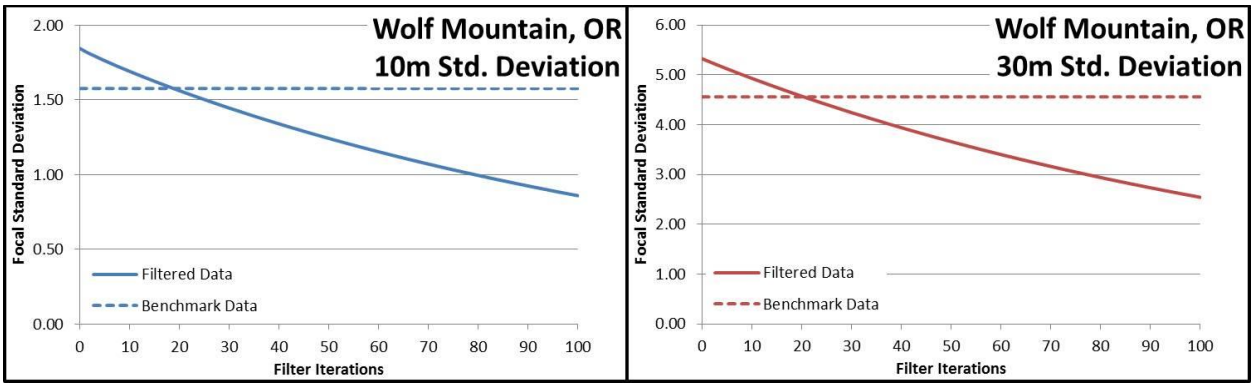

B.8: Standard deviation plot for Wolf Mountain, OR. This study site is classified as rugged, dry. A standard deviation value for the 3-meter DEM is most similar to the attribute resolution of the 10-meter benchmark after 19 iterations. A standard deviation value for the 3-meter DEM is most similar to the attribute resolution of the 30-meter benchmark after 21 iterations.

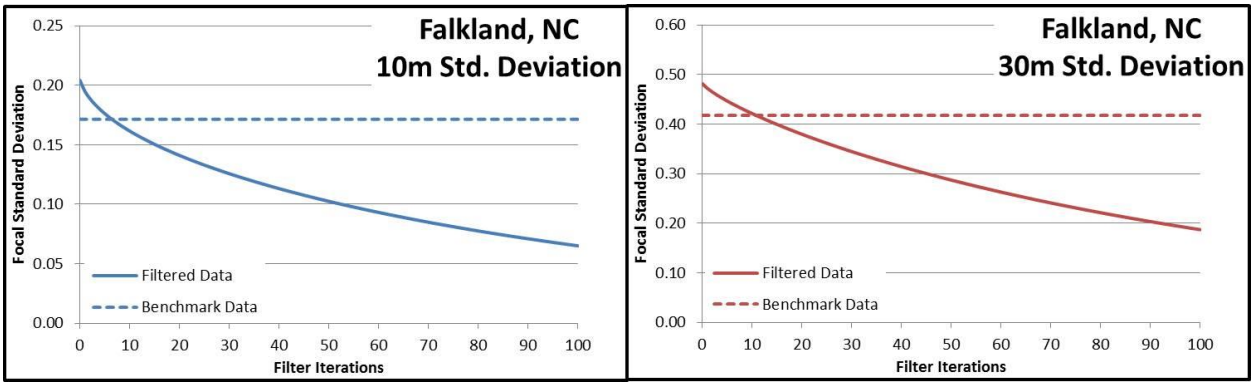

B.9: Standard deviation plot for Falkland, NC. This study site is classified as flat, humid. A standard deviation value for the 3-meter DEM is most similar to the attribute resolution of the 10-meter benchmark after 7 iterations. A standard deviation value for the 3-meter DEM is most similar to the attribute resolution of the 30-meter benchmark after 11 iterations.

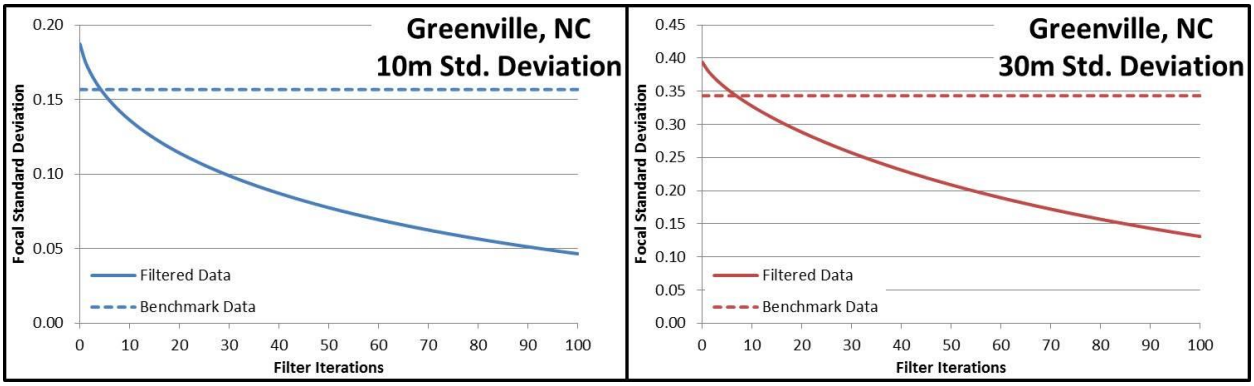

B.10: Standard deviation plot for Greenville, NC. This study site is classified as flat, humid. A standard deviation value for the 3-meter DEM is most similar to the attribute resolution of the 10-meter benchmark after 5 iterations. A standard deviation value for the 3-meter DEM is most similar to the attribute resolution of the 30-meter benchmark after 7 iterations. Greenville, NC, is the first study site to reach a 10-meter attribute resolution. It also reaches the 30-meter attribute resolution before any other study site reaches its 10-meter benchmark Greenville also has the lowest relief of any of the other study sites.

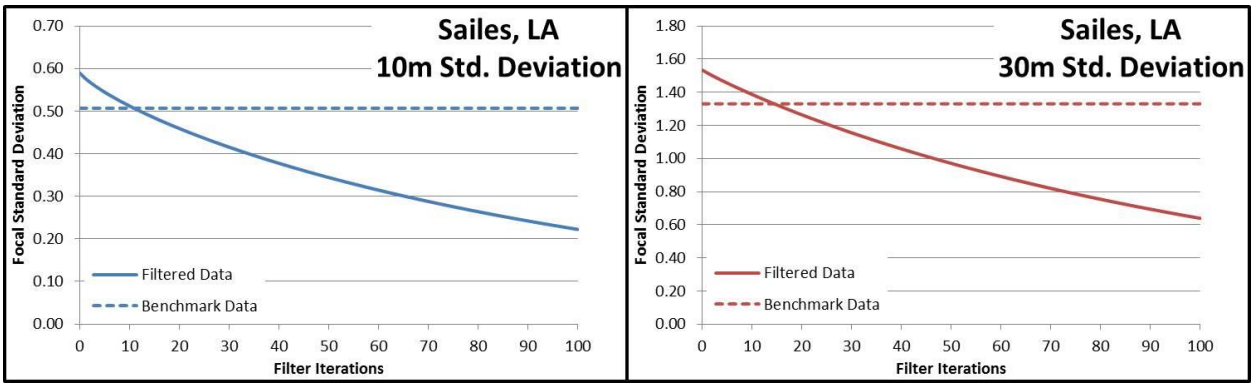

B.11: Standard deviation plot for Sailes, LA. This study site is classified as flat, humid. A standard deviation value for the 3-meter DEM is most similar to the attribute resolution of the 10-meter benchmark after 11 iterations. A standard deviation value for the 3-meter DEM is most similar to the attribute resolution of the 30-meter benchmark after 15 iterations.

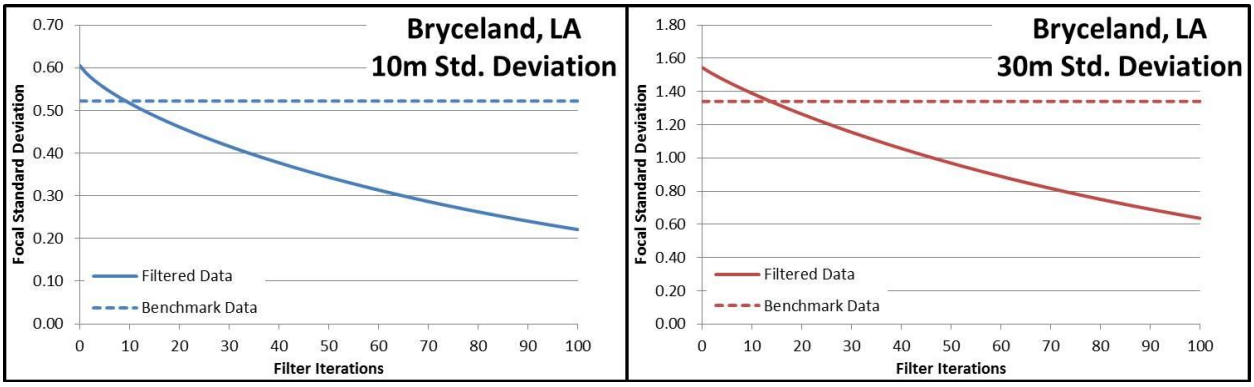

B.12: Standard deviation plot for Bryceland, LA. This study site is classified as flat, humid. A standard deviation value for the 3-meter DEM is most similar to the attribute resolution of the 10-meter benchmark after 10 iterations. A standard deviation value for the 3-meter DEM is most similar to the attribute resolution of the 30-meter benchmark after 14 iterations.

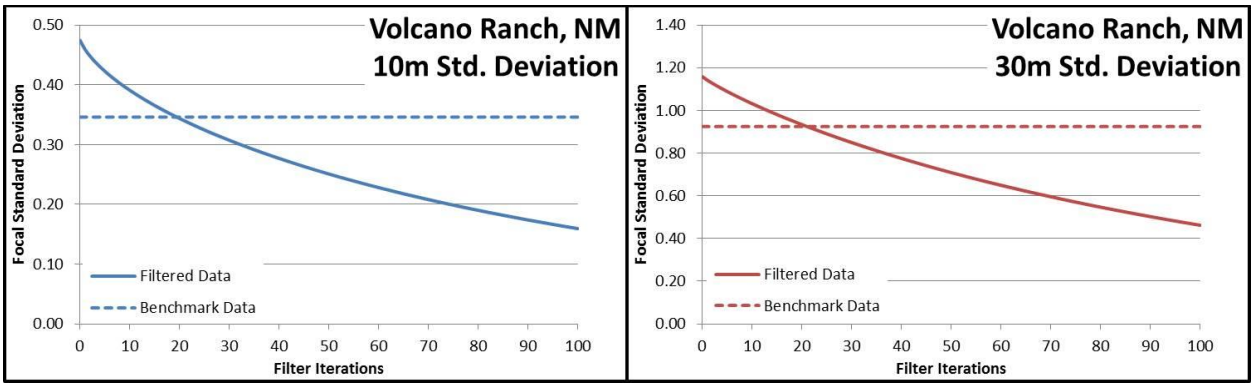

B.13: Standard deviation plot for Volcano Ranch, NM. This study site is classified as flat, dry. A standard deviation value for the 3-meter DEM is most similar to the attribute resolution of the 10-meter benchmark after 20 iterations. A standard deviation value for the 3-meter DEM is most similar to the attribute resolution of the 30-meter benchmark after 22 iterations. Both of the New Mexico study sites are the last to achieve a coarser resolution, which is opposite of trends with the remainder of the flat study sites. This may likely be attributed to a large difference in the landscape features that have been captured by DEM compilation between the 3-meter benchmark and the 10- and 30-meter benchmarks.

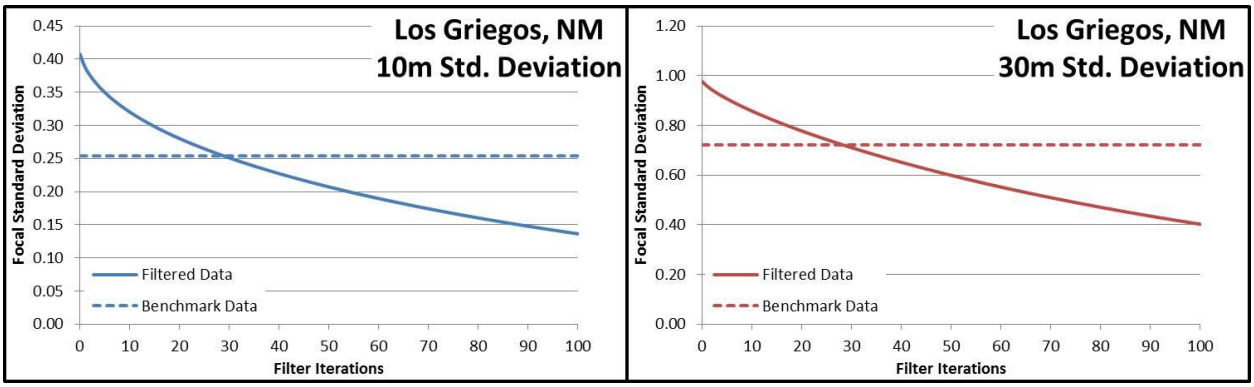

B.14: Standard deviation plot for Los Griegos, NM. This study site is classified as flat, dry. A standard deviation value for the 3-meter DEM is most similar to the attribute resolution of the 10-meter benchmark after 29 iterations. A standard deviation value for the 3-meter DEM is most similar to the attribute resolution of the 30-meter benchmark after 29 iterations. Strangely, this study site reaches the 10-meter and 30-meter benchmarks after the same number of filtering iterations. This suggests that there may not be significant differences between the attribute resolutions of the 10-meter and 30-meter benchmarks.

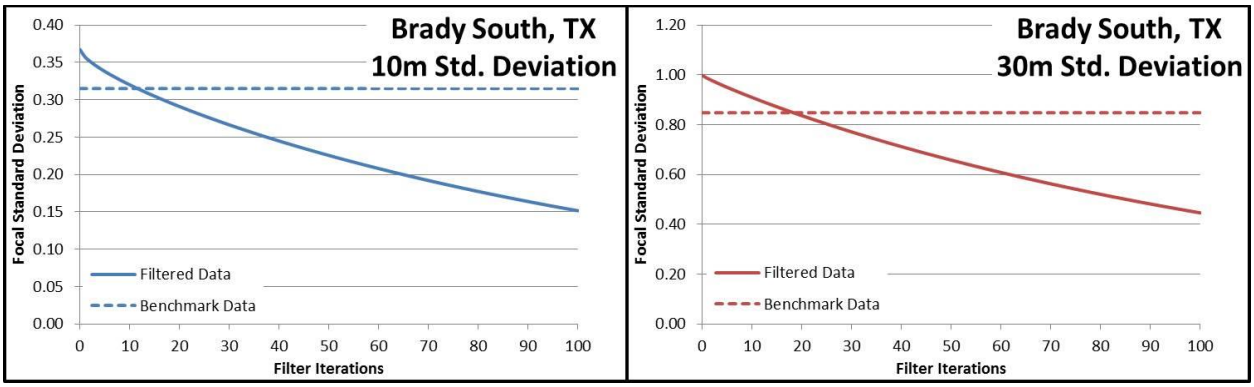

B.15: Standard deviation plot for Brady South, TX. This study site is classified as flat, dry. A standard deviation value for the 3-meter DEM is most similar to the attribute resolution of the 10-meter benchmark after 12 iterations. A standard deviation value for the 3-meter DEM is most similar to the attribute resolution of the 30-meter benchmark after 19 iterations.

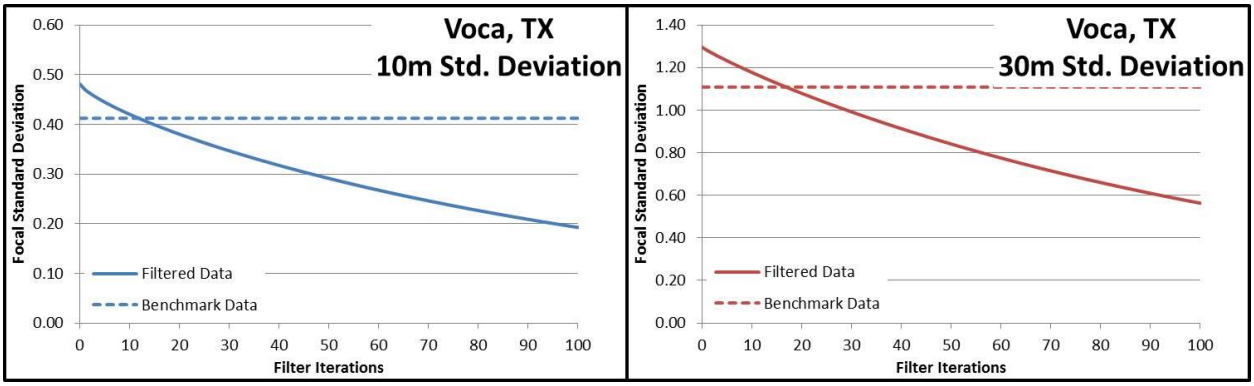

B.16: Standard deviation plot for Voca, TX. This study site is classified as flat, dry. A standard deviation value for the 3-meter DEM is most similar to the attribute resolution of the 10-meter benchmark after 12 iterations. A standard deviation value for the 3-meter DEM is most similar to the attribute resolution of the 30-meter benchmark after 17 iterations.

Appendix C: Semivariograms within the Focal Standard Deviation Window for all Study Sites

Empirical semivariograms are created for the generalized DEM and for the benchmark DEM. These semivariograms demonstrate more precisely how well the resolutions of the two DEMs match locally. Where the semivariance of the generalized DEM is greater than the semivariance of the benchmark DEM, it is considered under-generalized. Conversely, when the semivariance of the generalized DEM is less than that of the benchmark, it is considered overgeneralized. The standard deviation analysis will be a two-part process. The first will examine how the filtering process has affected the DEM within the focal standard deviation window (local effects). The second will examine how the filtering process has affected the DEM across the entire dataset (global effects).

The semivariograms were calculated at a lag distance of one cell, resulting in a lag distance of 3 meters for the 3-meter DEM, 10 meters for the 10-meter DEM and 30 meters for the 30-meter DEM. Five hundred (500) experimental semivariograms were calculated within the focal standard deviation window. Ten thousand (10,000) point pairs were sampled to calculate the semivariance at each lag distance. Within the 500 semivariograms, the semivariance values at each lag distances were normally distributed. The minimum and maximum semivariance values were extracted from each of the 500 semivariograms at each lag distance to create a semivariance envelope, to represent possible realizations of the true semivariance.

In the following graphics, the red lines represent the semivariance envelope of the benchmark (10- or 30-meter DEM). The blue lines represent the semivariance envelope of the filtered DEM after the listed filtering iteration. The left panel shows the semivariance envelope interaction between the filtered DEM and the 10-meter benchmark and has a maximum lag distance of 30 meters. The right panel shows the semivariance envelope interaction between the filtered DEM and the 30-meter benchmark and ha a maximum lag distance of 90 meters. It is important to note that the semivariance (x-axis) between the panels is not the same because of the difference in lag distances between the panels.

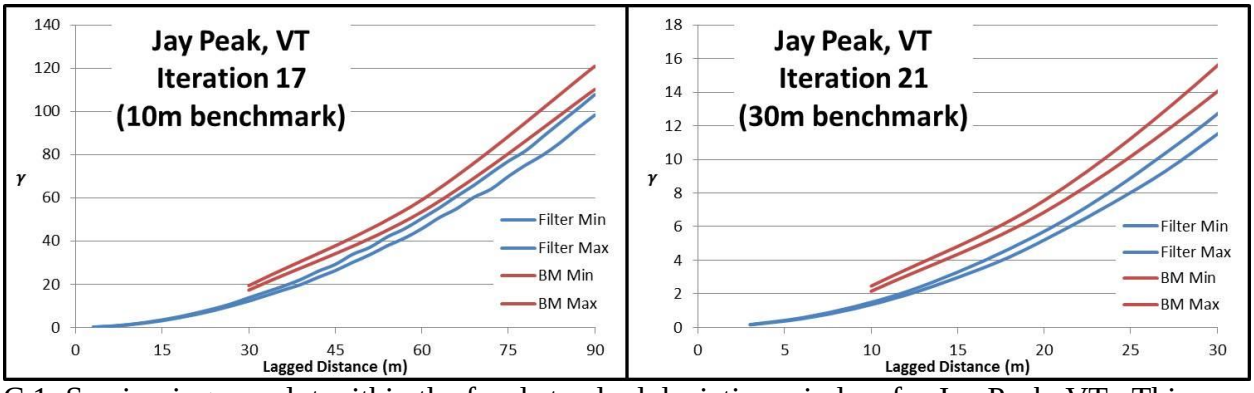

C.1: Semivariogram plot within the focal standard deviation window for Jay Peak, VT. This study site is classified as rugged, humid. Within the standard deviation window, the filtered DEM is under generalized compared to the 10-meter benchmark. The filtered DEM is also under generalized compared to the 30-meter benchmark.

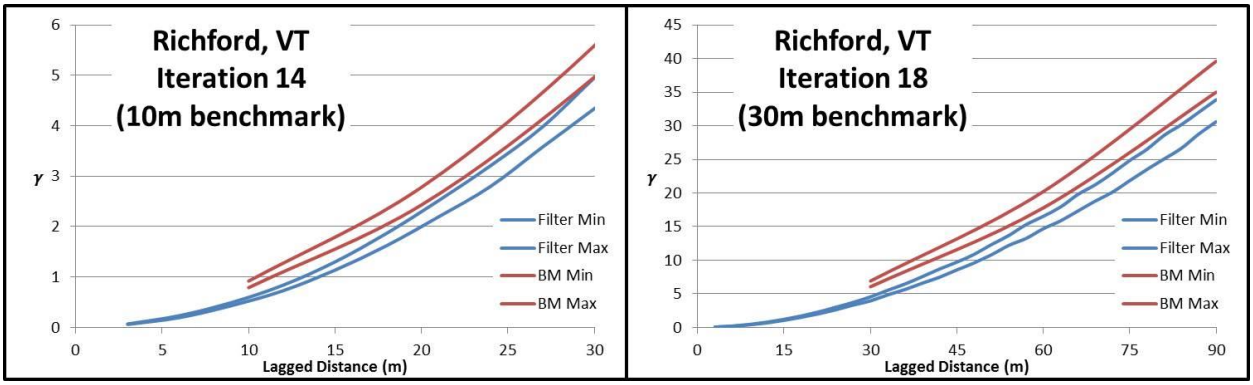

C.2: Semivariogram plot within the focal standard deviation window for Richford, VT. This study site is classified as rugged, humid. Within the standard deviation window, the semivariance envelope of the filtered DEM just touches the envelope of the 10-meter benchmark. This intersection could be indicative of why the standard deviation analysis has matched this filtering iteration to the 10-meter benchmark. However, the filtered DEM is under generalized when compared to the 30-meter benchmark.

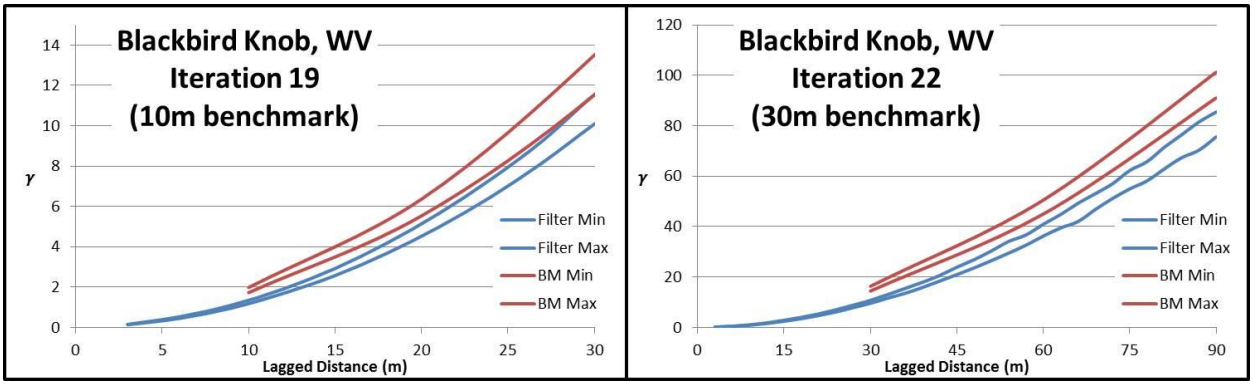

C.3: Semivariogram plot within the focal standard deviation window for Blackbird Knob, WV. This study site is classified as rugged, humid. Within the standard deviation window, the semivariance envelope of the filtered DEM just touches the envelope of the 10-meter benchmark. This intersection could be indicative of why the standard deviation analysis has matched this filtering iteration to the 10-meter benchmark. However, the filtered DEM is under generalized when compared to the 30-meter benchmark.

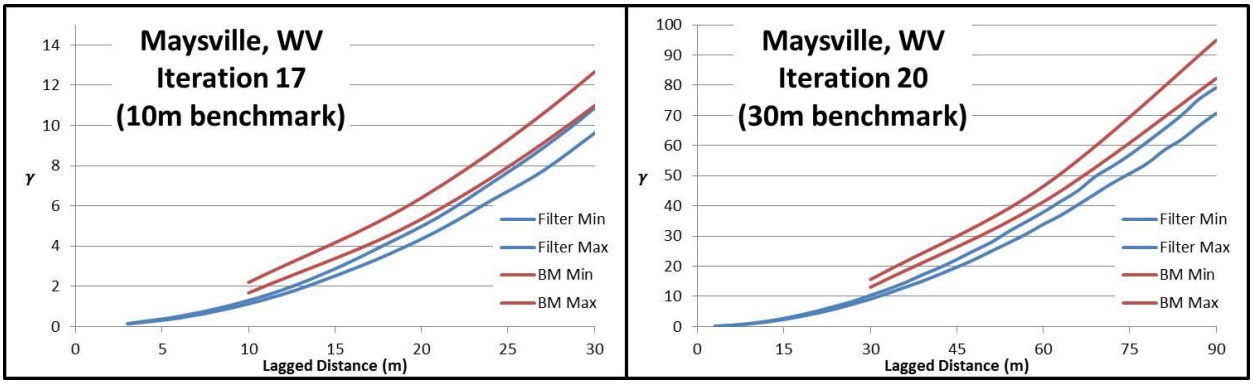

C.4: Semivariogram plot within the focal standard deviation window for Maysville, WV. This study site is classified as rugged, humid. Within the standard deviation window, the

semivariance envelope of the filtered DEM just touches the envelope of the 10-meter benchmark. This intersection could be indicative of why the standard deviation analysis has matched this filtering iteration to the 10-meter benchmark. However, the filtered DEM is under generalized when compared to the 30-meter benchmark.

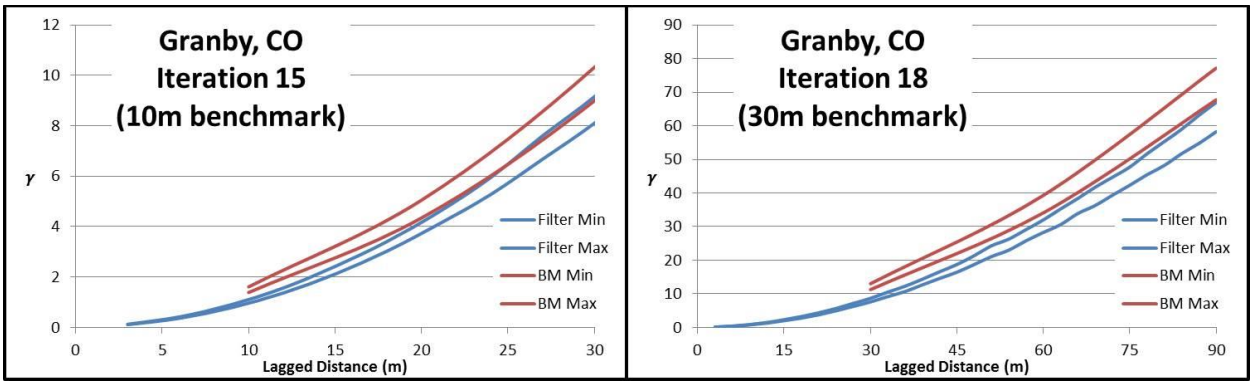

C.5: Semivariogram plot within the focal standard deviation window for Granby, CO. This study site is classified as rugged, dry. Within the standard deviation window, the semivariance envelope of the filtered DEM slightly overlaps the envelope of the 10-meter benchmark through the majority of the lag distances. This intersection is likely indicative that the filtered DEM is a plausible realization of the 10-meter benchmark. The semivariance envelope of the filtered DEM just touches the envelope of the 30-meter benchmark, which indicates that this filtering iteration is a less likely realization of the 30-meter benchmark.

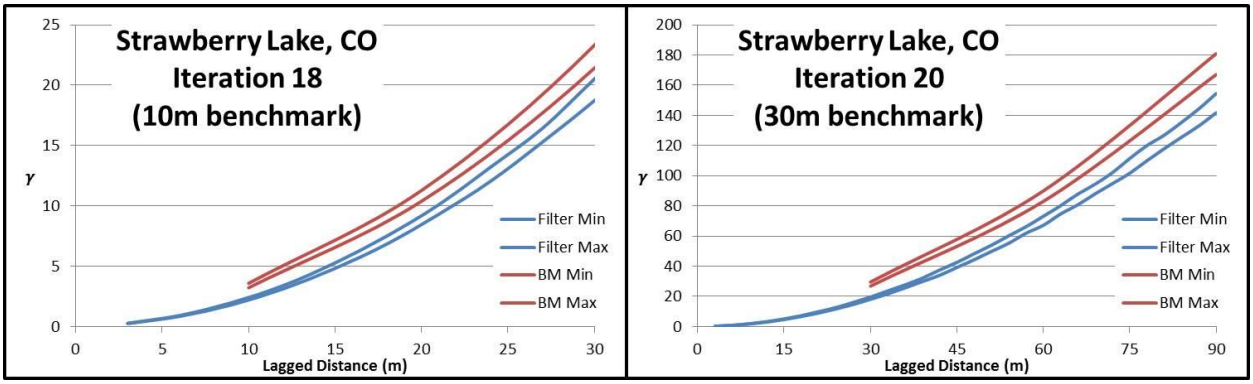

C.6: Semivariogram plot within the focal standard deviation window for Strawberry Lake, CO. This study site is classified as rugged, dry. The semivariogram envelope of the filtered DEM never overlaps the envelope of the coarser resolution benchmarks. This suggests that while the attribute resolutions may match, the filtered DEM is not a possible realization of the benchmarks.

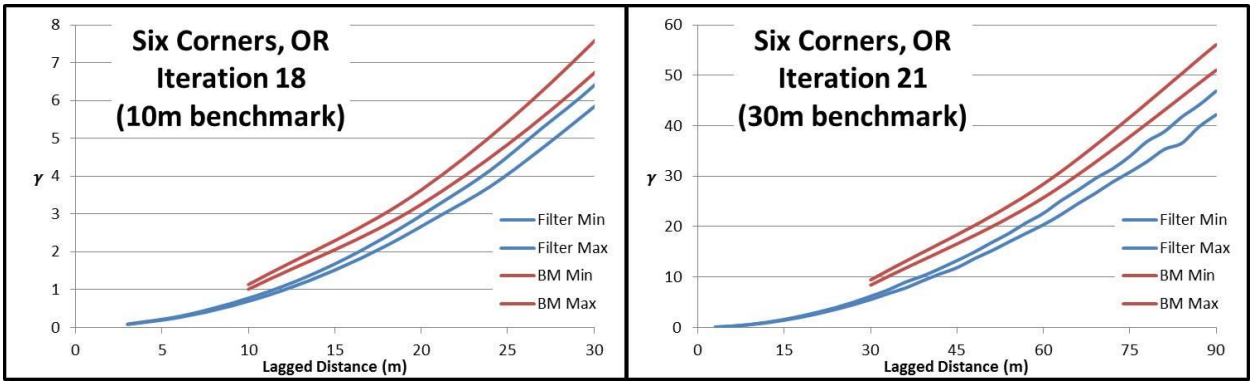

C.7: Semivariogram plot within the focal standard deviation window for Six Corners, OR. This study site is classified as rugged, dry. The semivariogram envelope of the filtered DEM never overlaps the envelope of the coarser resolution benchmarks. This suggests that while the attribute resolutions may match, the filtered DEM is not a possible realization of the benchmarks.

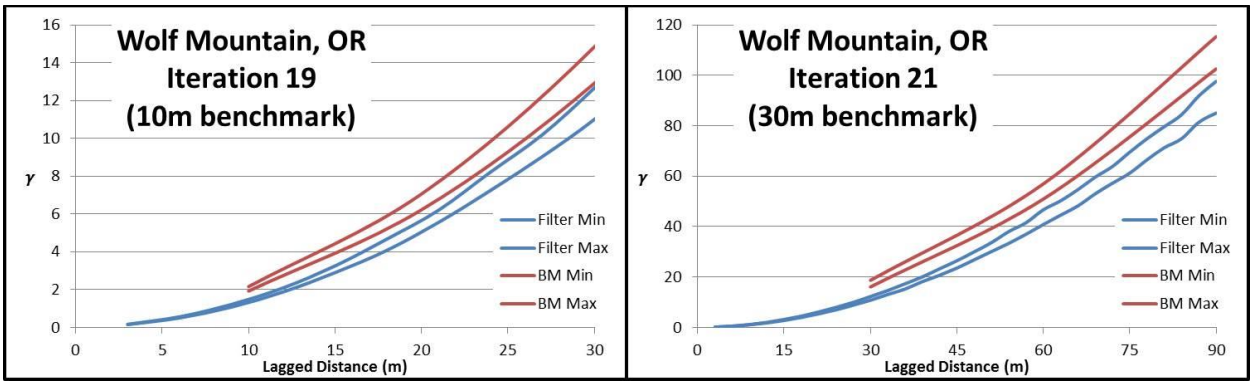

C.8: Semivariogram plot within the focal standard deviation window for Wolf Mountain, OR. This study site is classified as rugged, dry. The semivariogram envelope of the filtered DEM never overlaps the envelope of the coarser resolution benchmarks. This suggests that while the attribute resolutions may match, the filtered DEM is not a possible realization of the benchmarks.

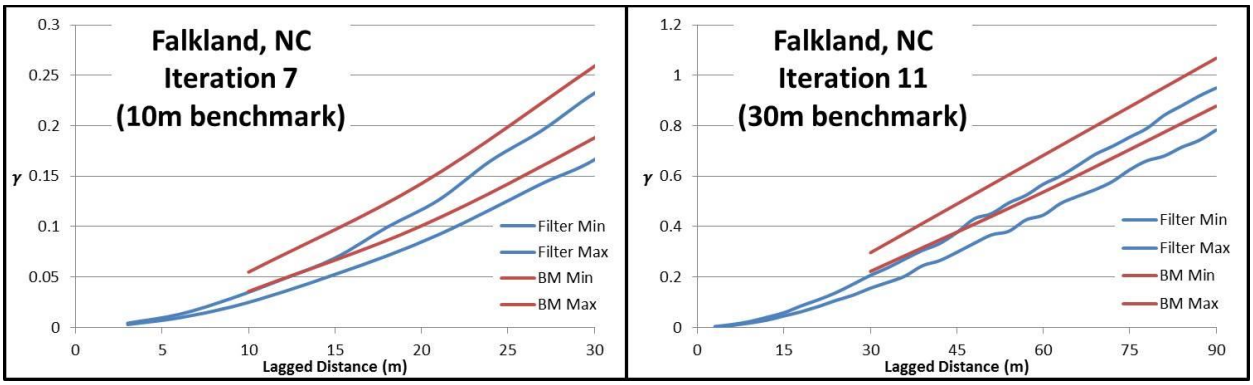

C.9: Semivariogram plot within the focal standard deviation window for Falkland, NC. This study site is classified as flat, humid. There is a fairly large degree of overlap between the filtered DEM semivariance envelope and that of the 10-meter benchmark. The amount of overlap decreases when compared to the 30-meter semivariance envelope. Nonetheless, this is indicative that the filtered DEMs match the benchmark resolutions well.

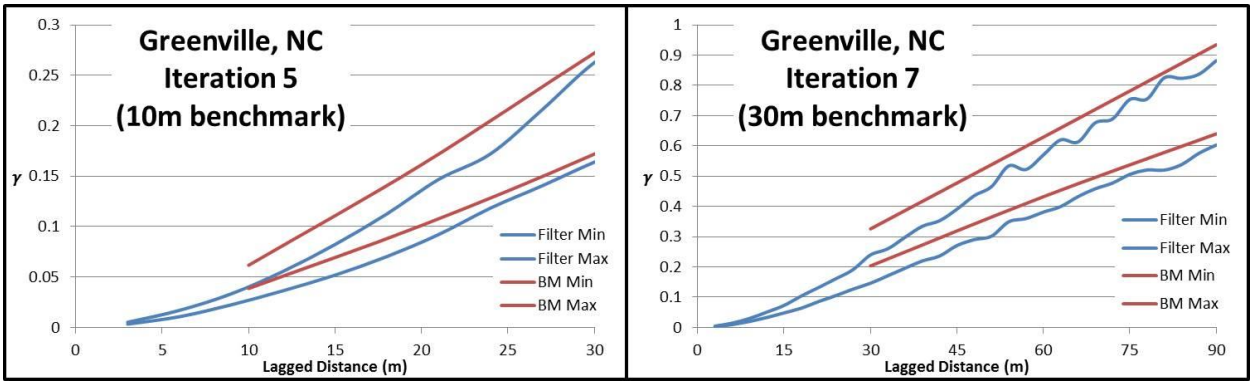

C.10: Semivariogram plot within the focal standard deviation window for Greenville, NC. This study site is classified as flat, humid. The semivariogram envelope of the filtered DEM greatly overlaps the envelope of the 10-meter benchmark. The same trend is observed for the 30-meter benchmark. This suggests that there is a high degree of correspondence between the filtered DEMs and the benchmarks.

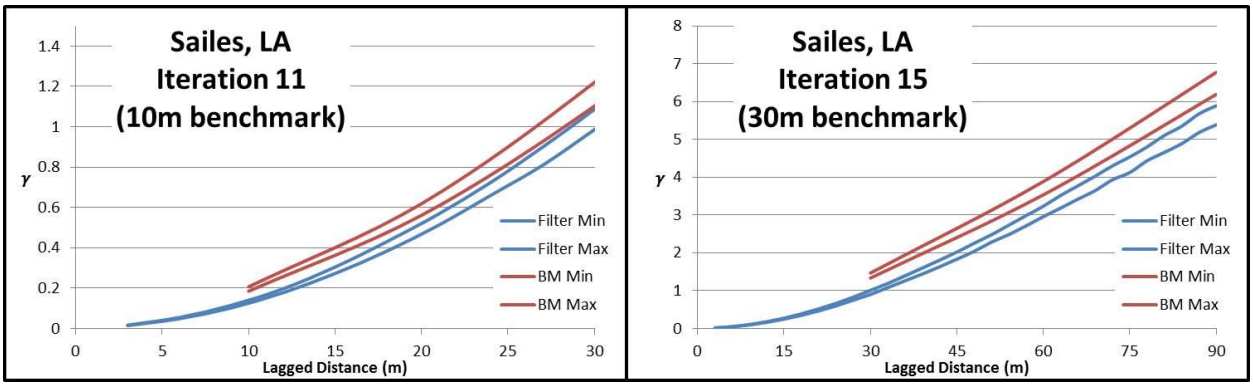

C.11: Semivariogram plot within the focal standard deviation window for Sailes, LA. This study site is classified as flat, humid. Within the standard deviation window, the semivariance envelope of the filtered DEM just touches the envelope of the 10-meter benchmark. This intersection could be indicative of why the standard deviation analysis has matched this filtering iteration to the 10-meter benchmark. However, the filtered DEM is under generalized when compared to the 30-meter benchmark.

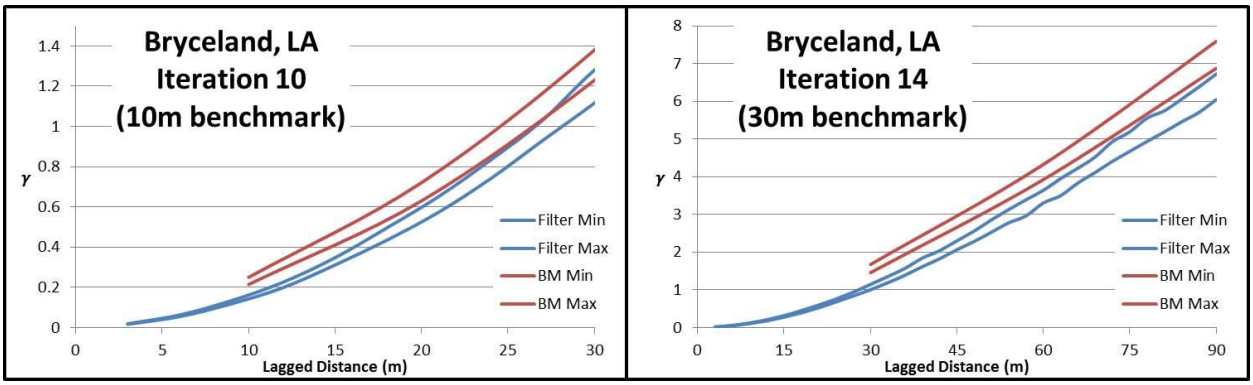

C.12: Semivariogram plot within the focal standard deviation window for Bryceland, LA. This study site is classified as flat, humid. Within the standard deviation window, the semivariance envelope of the filtered DEM just touches the envelope of the 10-meter benchmark. This

intersection could be indicative of why the standard deviation analysis has matched this filtering iteration to the 10-meter benchmark. However, the filtered DEM is under generalized when compared to the 30-meter benchmark.

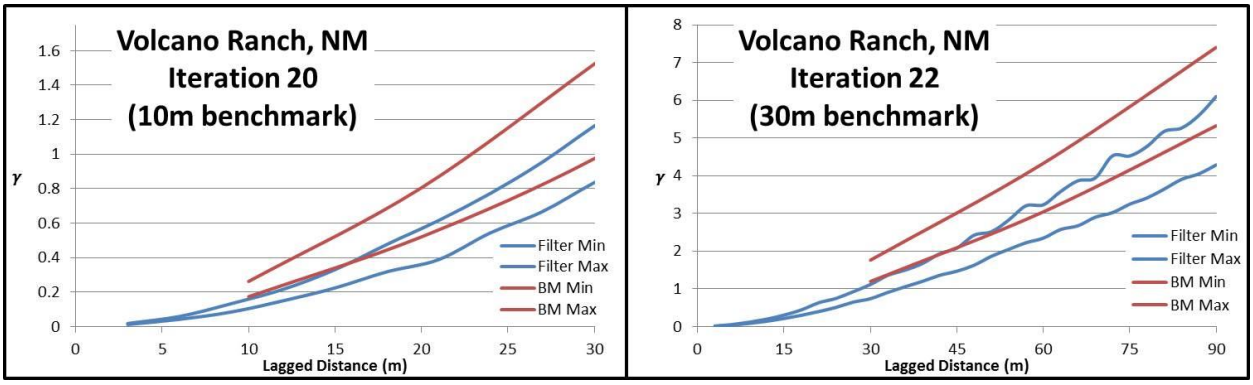

C.13: Semivariogram plot within the focal standard deviation window for Volcano Ranch, NM. This study area is classified as flat, dry. Within the standard deviation window, the semivariance envelope of the filtered DEM slightly overlaps the envelope of the 10-meter benchmark through the majority of the lag distances. This intersection is likely indicative that the filtered DEM is a plausible realization of the 10-meter benchmark. A similar trend can be observed when comparing the filtered DEM semivariance envelope to that of the 30-meter envelope. While both of the filtered DEM iterations may match their coarser resolution benchmark counterpart, they both appear to be over generalized.

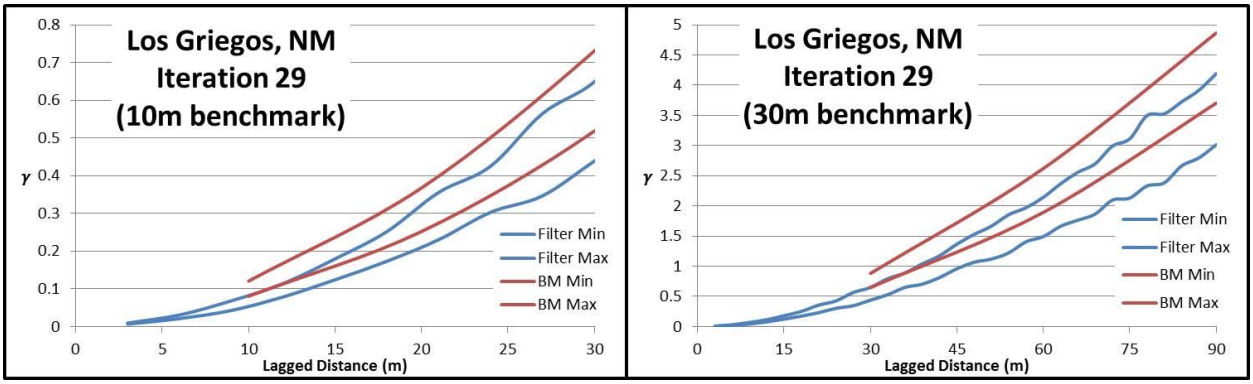

C.14: Semivariogram plot within the focal standard deviation window for Los Griegos, NM. This study site is classified as flat, dry. There is a fairly large degree of overlap between the filtered DEM semivariance envelope and that of the 10-meter benchmark. The amount of overlap decreases when compared to the 30-meter semivariance envelope. Nonetheless, this is indicative that the filtered DEMs match the benchmark resolutions well.

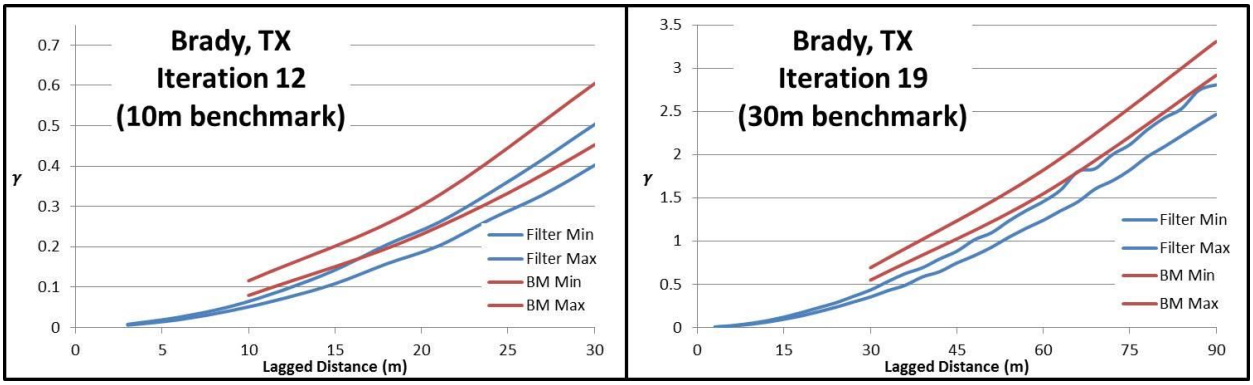

C.15: Semivariogram plot within the focal standard deviation window for Brady South, TX. This study site is classified as flat, dry. This study site is classified as flat, dry. Within the standard deviation window, the semivariance envelope of the filtered DEM slightly overlaps the envelope of the 10-meter benchmark through the majority of the lag distances. This intersection is likely indicative that the filtered DEM is a plausible realization of the 10-meter benchmark. However, the filtered DEM is under generalized when compared to the 30-meter benchmark.

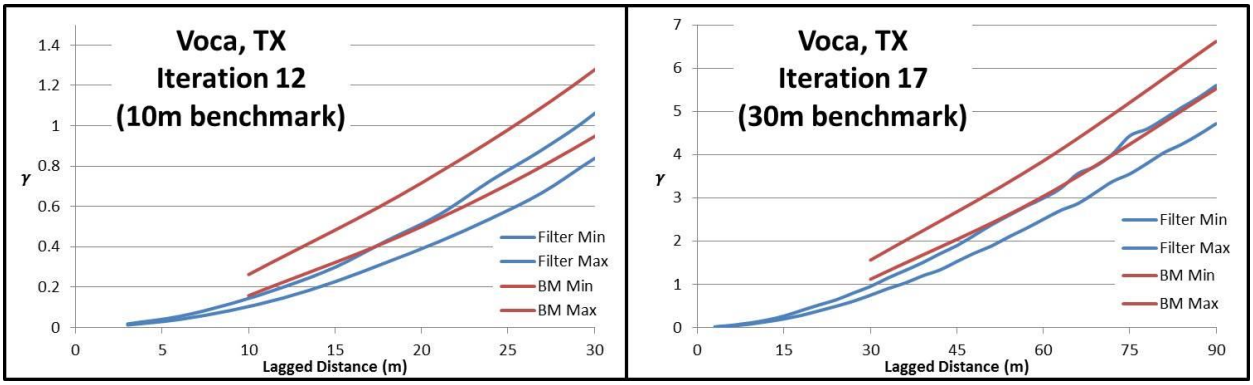

C.16: Semivariogram plot within the focal standard deviation window for Voca, TX. This study site is classified as flat, dry. Within the standard deviation window, the semivariance envelope of the filtered DEM slightly overlaps the envelope of the 10-meter benchmark through the majority of the lag distances. This intersection is likely indicative that the filtered DEM is a plausible realization of the 10-meter benchmark. A similar trend can be observed when comparing the filtered DEM semivariance envelope to that of the 30-meter envelope. While both of the filtered DEM iterations may match their coarser resolution benchmark counterpart, they both appear to be over generalized.

Appendix D: Semivariograms for all Study Sites

Empirical semivariograms are created for the generalized DEM and for the benchmark DEM. These semivariograms demonstrate more precisely how well the resolutions of the two DEMs match locally. Where the semivariance of the generalized DEM is greater than the semivariance of the benchmark DEM, it is considered under-generalized. Conversely, when the semivariance of the generalized DEM is less than that of the benchmark, it is considered overgeneralized. The standard deviation analysis will be a two-part process. The first will examine how the filtering process has affected the DEM within the focal standard deviation window (local effects). The second will examine how the filtering process has affected the DEM across the entire dataset (global effects).

The semivariograms were calculated at a lag distance of 50 meters. Five hundred (500) experimental semivariograms were calculated within the focal standard deviation window. Ten thousand (10,000) point pairs were used to calculate the semivariance at each lag distance. Within the 500 semivariograms, the semivariance values at each lag distances were normally distributed. The minimum and maximum semivariance values were extracted from each of the 500 semivariograms at each lag distance to create a semivariance envelope, or possible realizations of the true semivariance.

In the following graphics, the red lines represent the semivariance envelope of the benchmark (10- or 30-meter DEM). The blue lines represent the semivariance envelope of the filtered DEM after the listed filtering iteration. The left panel shows the semivariance envelope interaction between the filtered DEM and the 10-meter benchmark and has a maximum lag distance of 30 meters. The right panel shows the semivariance envelope interaction between the filtered DEM and the 30-meter benchmark and ha a maximum lag distance of 90 meters.

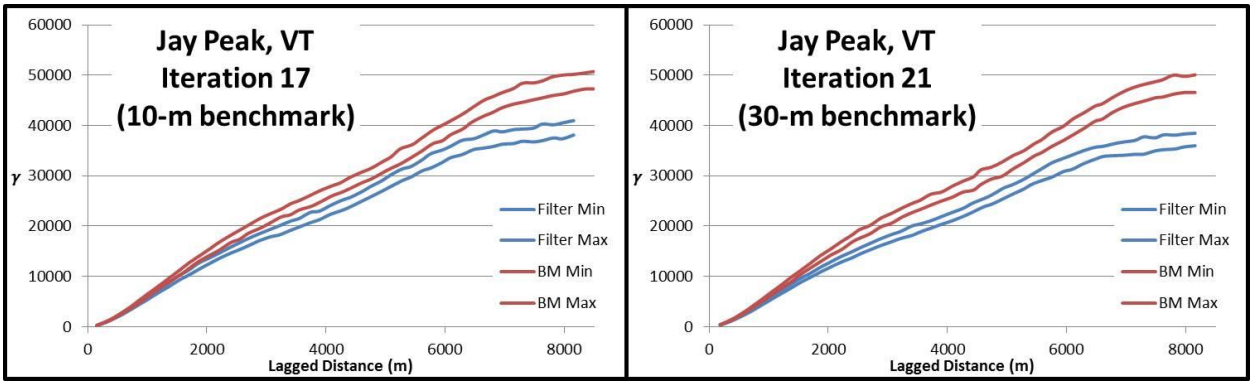

D.1: Semivariogram plots for Jay Peak, VT. This study site is classified as rugged, humid. The overlap between filter iteration 17 and the 10-meter benchmark is 0.00% while the overlap between filter iteration 21 and the 30-meter benchmark is 0.00%. This suggests that the attribute resolution has been overgeneralized at both local and global scales. This is one of three rugged study sites that experience no semivariance overlap. This is likely due to the filtering process altering minor valleys such that they no longer match what exists in the coarser resolution benchmark DEMs. Additionally, this is one of five study sites that show a sill in the semivariogram and is one of the two rugged study sites to do so.

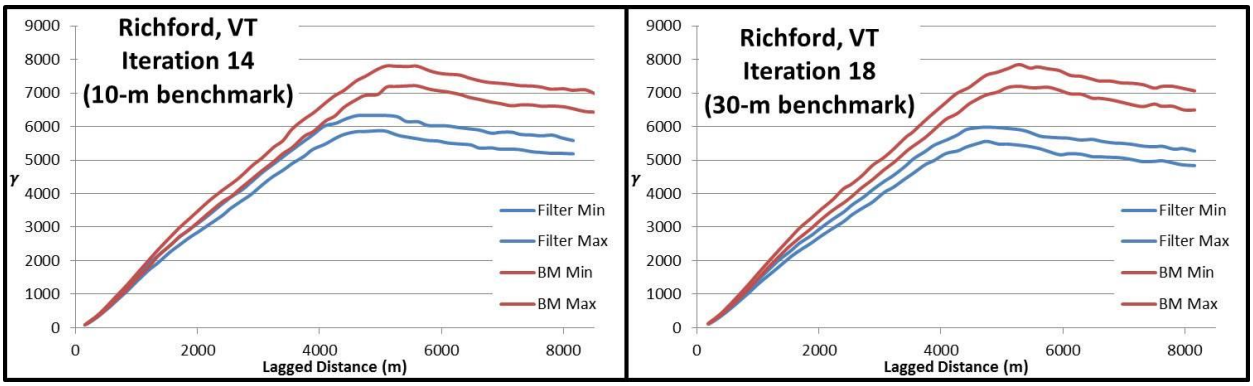

D.2: Semivariogram plots for Richford, VT. This study site is classified as rugged, humid. The overlap between filter iteration 14 and the 10-meter benchmark is 47.24% while the overlap between filter iteration 18 and the 30-meter benchmark is 0.00%. Richford, VT, demonstrates the highest rate in overlap with the 10-meter benchmark than any other rugged site. This is likely due to the transitional landscape within the area. Additionally, this is one of five study sites that show a sill in the semivariogram and is one of the two rugged study sites to do so.

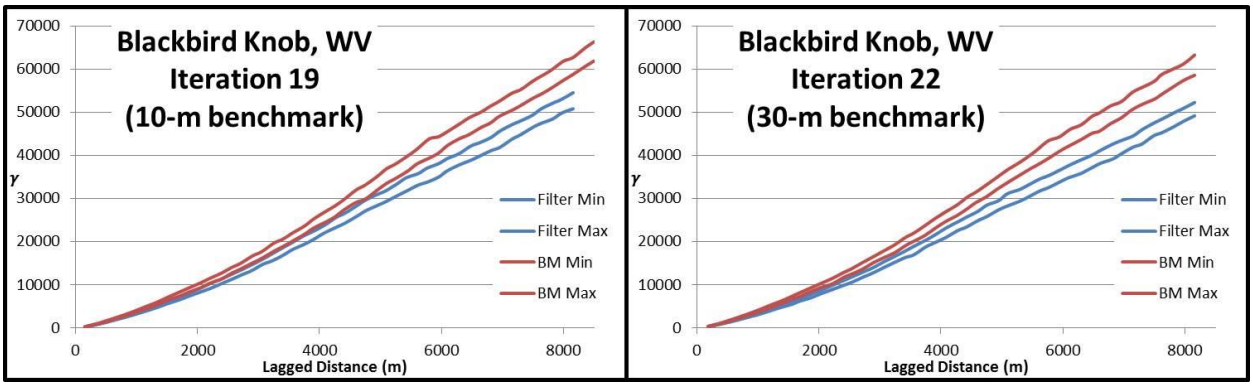

D.3: Semivariogram plots for Blackbird Knob, WV. This study site is classified as rugged, humid. The overlap between filter iteration 19 and the 10-meter benchmark is 10.14% while the overlap between filter iteration 22 and the 30-meter benchmark is 0.00%. This is the lowest overlap rate among the 10-meter benchmark study sites that have any overlap. The parts of the semivariance envelope that overlap occur at lag distances less than 2000 meters. This suggests that the filtering is altering the attribute resolution at a localized scale in a manner that best matches the 10-meter benchmark. However, at large lag distances, the attribute resolution is becoming overgeneralized.

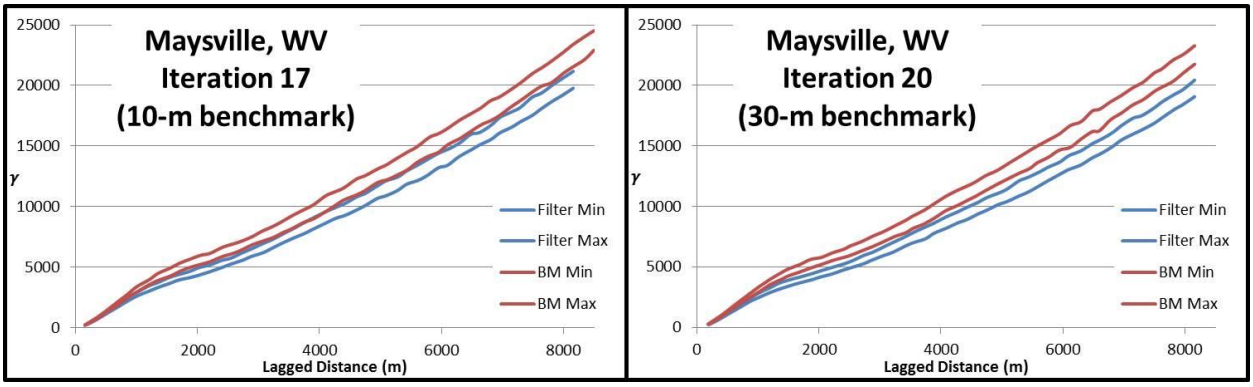

D.4: Semivariogram plots for Maysville, WV. This study site is classified as rugged, humid. The overlap between filter iteration 17 and the 10-meter benchmark is 19.68% while the overlap between filter iteration 20 and the 30-meter benchmark is 0.00%. The semivariogram experiences a dramatic change in semivariance slope at about 1500 meters. While the two semivariance envelopes don't overlap much, they remain very close to the semivariance values shown by the benchmark envelopes.

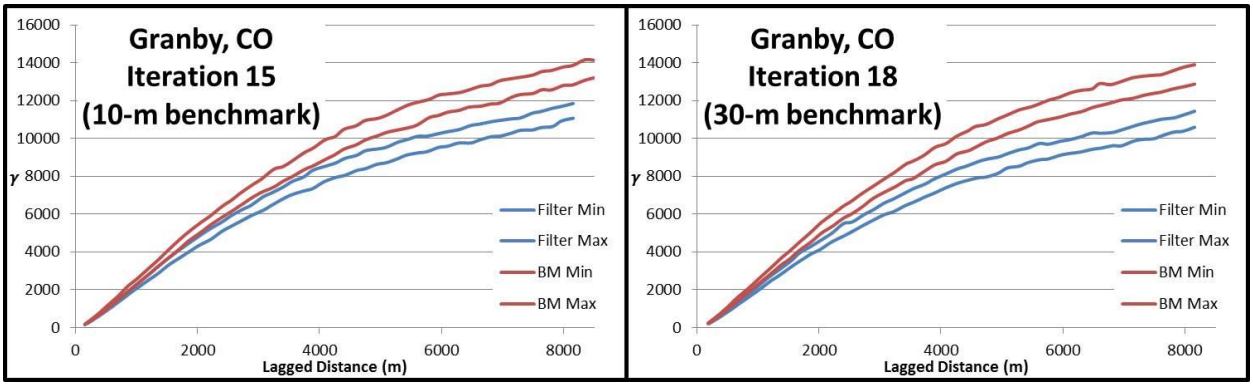

D.5: Semivariogram plots for Granby, CO. This study site is classified as rugged, dry. The overlap between filter iteration 15 and the 10-meter benchmark is 34.88% while the overlap between filter iteration 18 and the 30-meter benchmark is 0.00%.

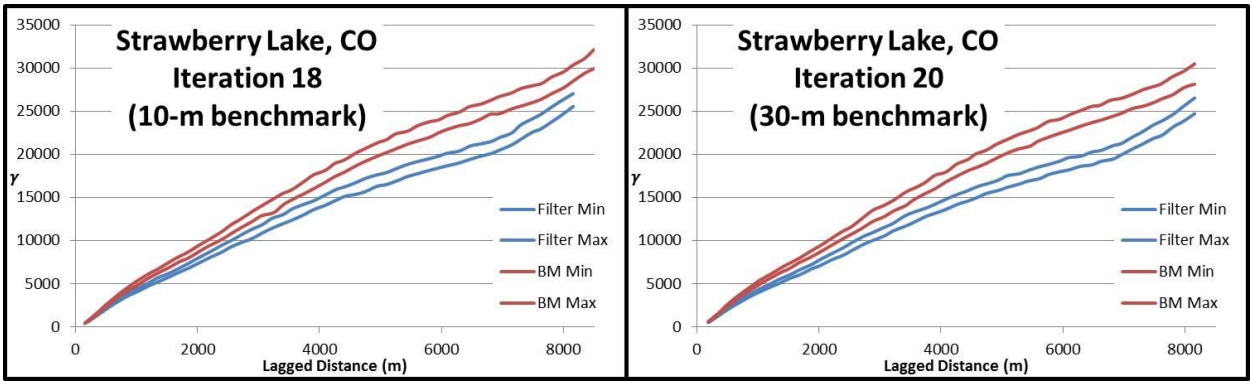

D.6: Semivariogram plots for Strawberry Lake, CO. This study site is classified as rugged, dry. The overlap between filter iteration 18 and the 10-meter benchmark is 0.00% while the overlap between filter iteration 20 and the 30-meter benchmark is 0.00%. This suggests that the attribute resolution has been overgeneralized at both local and global scales. This is one of three rugged study sites that experience no semivariance overlap. This is likely due to the filtering process altering minor valleys such that they no longer match what exists in the coarser resolution benchmark DEMs. Strawberry Lake is the only study site in which the filtered semivariance envelope changes slope relative to what is seen in the benchmark. At about 6000 to 7000 meters, the filtered semivariance envelope dips away from the benchmark before changing slope again to wind up nearly intersecting the benchmark envelope at the 8000 meter lag.

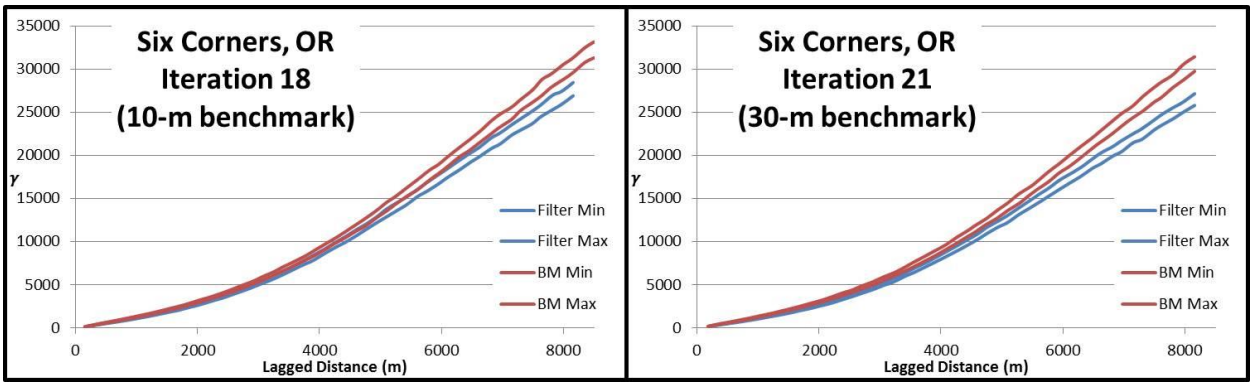

D.7: Semivariogram plots for Six Corners, OR. This study site is classified as rugged, dry. The overlap between filter iteration 18 and the 10-meter benchmark is 0.00% while the overlap between filter iteration 21 and the 30-meter benchmark is 0.00%. This suggests that the attribute resolution has been overgeneralized at both local and global scales. This is one of three rugged study sites that experience no semivariance overlap. This is likely due to the filtering process altering minor valleys such that they no longer match what exists in the coarser resolution benchmark DEMs. Despite that the semivariance envelopes don't experience any overlap, the filtered envelope hovers extremely close to that of the benchmarks.

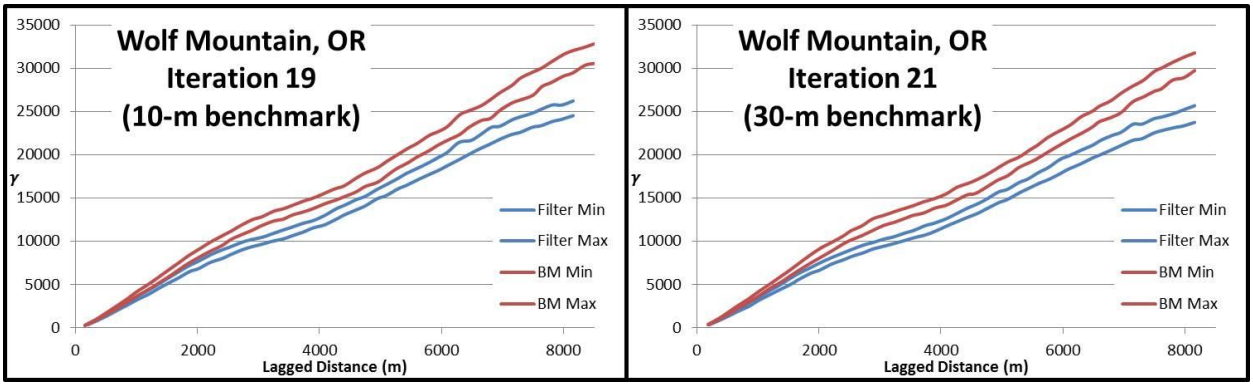

D.8: Semivariogram plots for Wolf Mountain, OR. This study site is classified as rugged, dry. The overlap between filter iteration 19 and the 10-meter benchmark is 10.65% while the overlap between filter iteration 21 and the 30-meter benchmark is 0.00%.

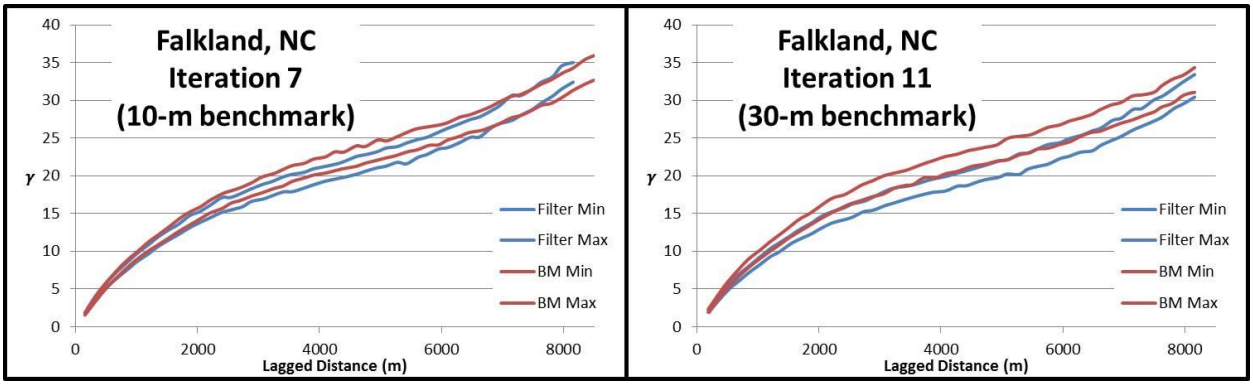

D.9: Semivariogram plots for Falkland, NC. This study site is classified as flat, humid. The overlap between filter iteration 7 and the 10-meter benchmark is 74.08% while the overlap between filter iteration 11 and the 30-meter benchmark is 20.84%. Falkland shows the second

highest overlap in semivariogram envelopes. It also is the only study site that shows signs of potentially being under generalized at a large lag distance. This result suggests that the filtering process is altering the attribute resolution equally at local and global scales.

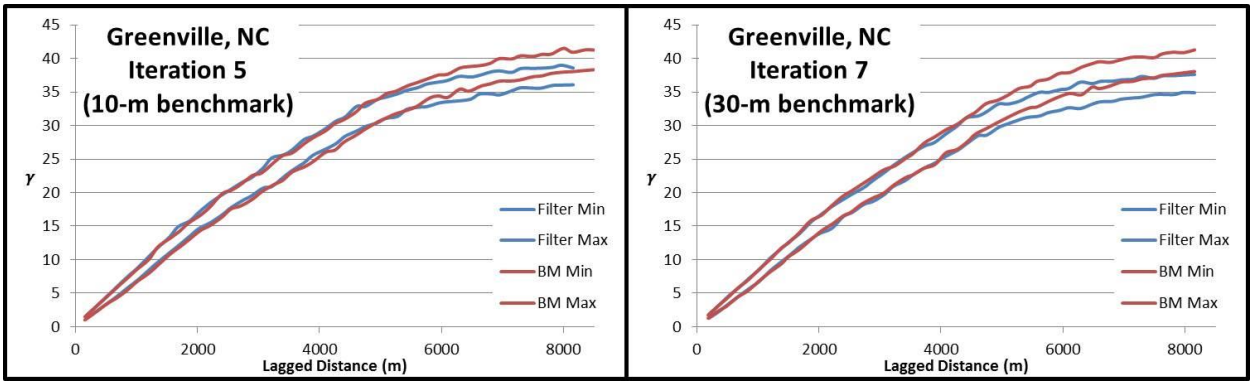

D.10: Semivariogram plots for Greenville, NC. This study site is classified as flat, humid. The overlap between filter iteration 5 and the 10-meter benchmark is 86.74% while the overlap between filter iteration 7 and the 30-meter benchmark is 66.99%. Greenville shows the highest rate of overlap between the filtered DEM and both benchmark DEMs. However, the areas of least overlap are seen at large lag distances. This study site is one of five study sites that show a sill in the semivariogram.

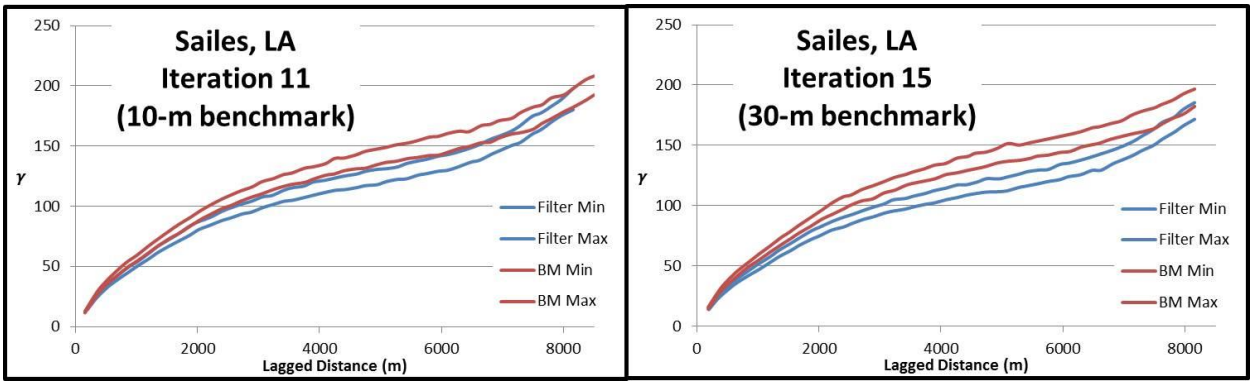

D.11: Semivariogram plots for Sailes, LA. This study site is classified as flat, humid. The overlap between filter iteration 11 and the 10-meter benchmark is 34.05% while the overlap between filter iteration 15 and the 30-meter benchmark is 0.00%. This study site has the lowest amount of semivariance envelope overlap of all flat sites. This may be caused by the highly dendritic landscape in the area. While the relief is low, it seems to behave more similar to rugged study sites.

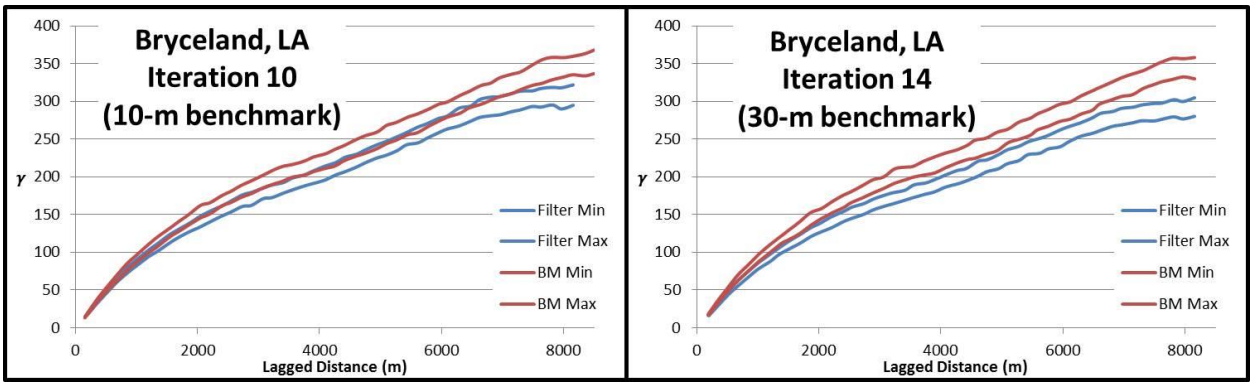

D.12: Semivariogram plots for Bryceland, LA. This study site is classified as flat, humid. The overlap between filter iteration 10 and the 10-meter benchmark is 52.05% while the overlap between filter iteration 14 and the 30-meter benchmark is 0.00%. This study site shows a relatively high degree of overlap between the filtered DEM and the 10-meter benchmark. However, this isn't focused in one area (small lag distances versus large lag distances). Instead the semivariogram envelopes overlap slightly though all lag distances.

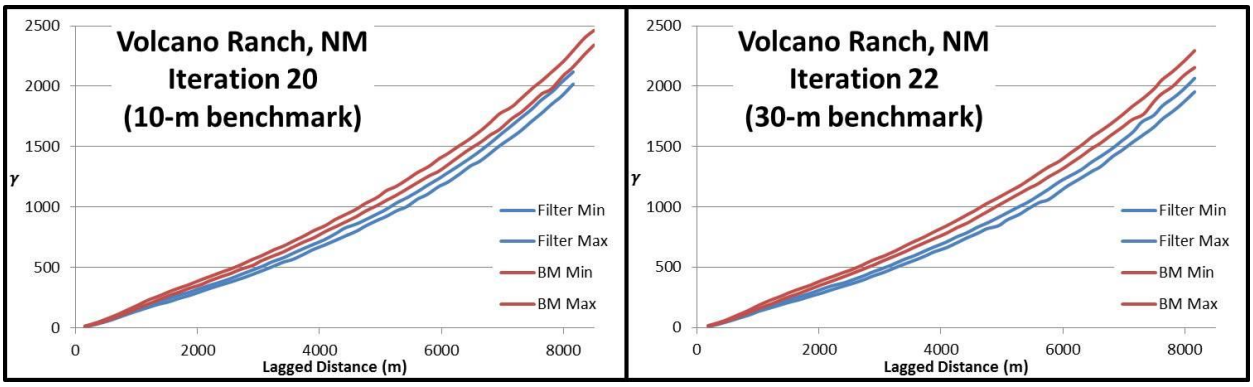

D.13: Semivariogram plots for Volcano Ranch, NM. This study site is classified as flat, dry. The overlap between filter iteration 20 and the 10-meter benchmark is 35.43% while the overlap between filter iteration 22 and the 30-meter benchmark is 18.01%.

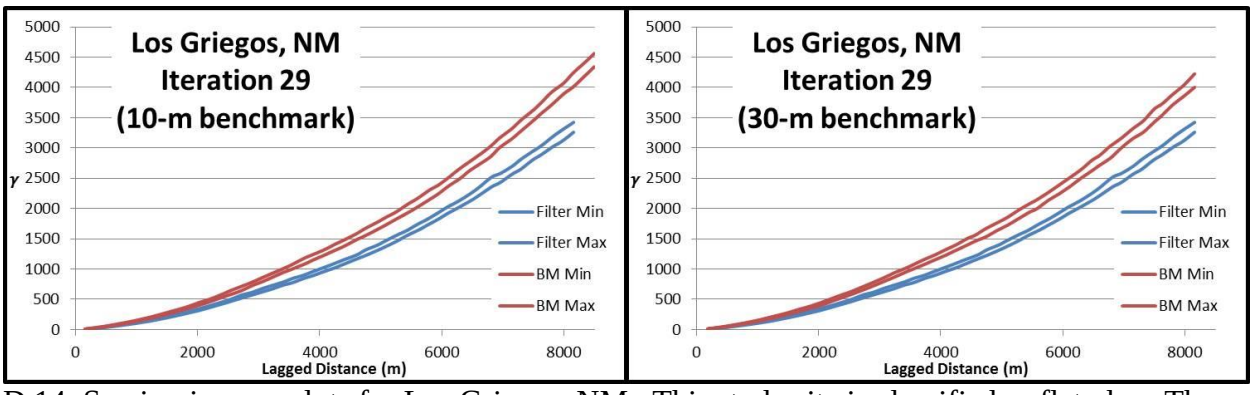

D.14: Semivariogram plots for Los Griegos, NM. This study site is classified as flat, dry. The overlap between filter iteration 29 and the 10-meter benchmark is 45.75% while the overlap between filter iteration 29 and the 30-meter benchmark is 25.54%. Despite many filtering iterations, this study site shows the second highest rate of overlap between the filtered DEM and

the 30-meter benchmark. However, this overlap occurs at small lag distances. The semivariogram envelopes are quite different at large lag distances.

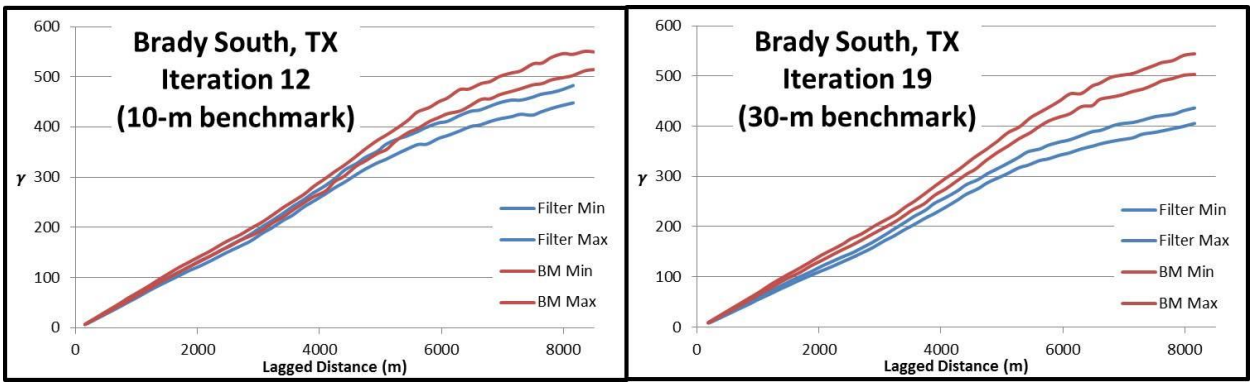

D.15: Semivariogram plots for Brady South, TX. This study site is classified as flat, dry. The overlap between filter iteration 12 and the 10-meter benchmark is 64.67% while the overlap between filter iteration 19 and the 30-meter benchmark is 0.00%. Despite the high percent overlap between filtered DEM and the 10-meter benchmark, there is no overlap between the filtered DEM and the 30-meter benchmark. This suggests that the effects of filtering and rate of resolution change occurred quickly after the filtered DEM reached the 10-meter benchmark. This study site is one of five study sites that show a sill in the semivariogram.

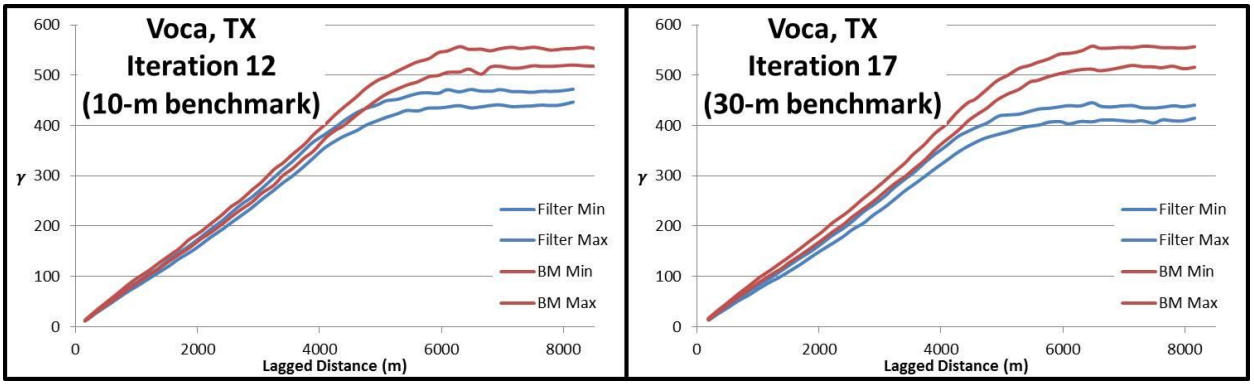

D.16: Semivariogram plots for Voca, TX. This study site is classified as flat, dry. The overlap between filter iteration 12 and the 10-meter benchmark is 55.98% while the overlap between filter iteration 17 and the 30-meter benchmark is 2.59%. This study site is one of five study sites that show a sill in the semivariogram.

Appendix E: CLC Result Maps Showing Matching, Omission, and Commission Stream for all Study Sites

The ability to identify a dataset's resolution allows a cartographer to display the data at an appropriate range of mapping scales. However, being able to generalize data to a given resolution may still not be enough for proper cartographic representation. The generalized data must integrate with other layers in the same way it was able to in an un-generalized state. A third metric will be used for evaluating possible problems that might arise with vertical data integration of the smoothed data. The Coefficient of Line Correspondence (CLC) will be calculated to describe the conflation between the hydrography of a known resolution to that derived from the generalized DEM.

The CLC analysis is conducted by extracting stream features from the DEM with similar characteristics (total length and number of confluence-to-confluence features) to the NHD benchmark. Once streams are extracted from the filtered DEM, buffers are applied to the elevation derived stream and NHD benchmark. An overlay is performed to measure the degree of match or conflation between the two stream datasets. Finally, the CLC metric is computed based on the length of stream matches, commissions, and omissions. Commissions are features that exist in the benchmark dataset, but not in the elevation derived stream. Omissions are features that exist in the elevation derived streams, but not in the NHD benchmark.

In the following graphics, the stream matches (gray lines), omissions (blue lines), and commissions (red line) are shown. Visualizing the distribution of these features can help describe why a relatively high or low CLC value was calculated.

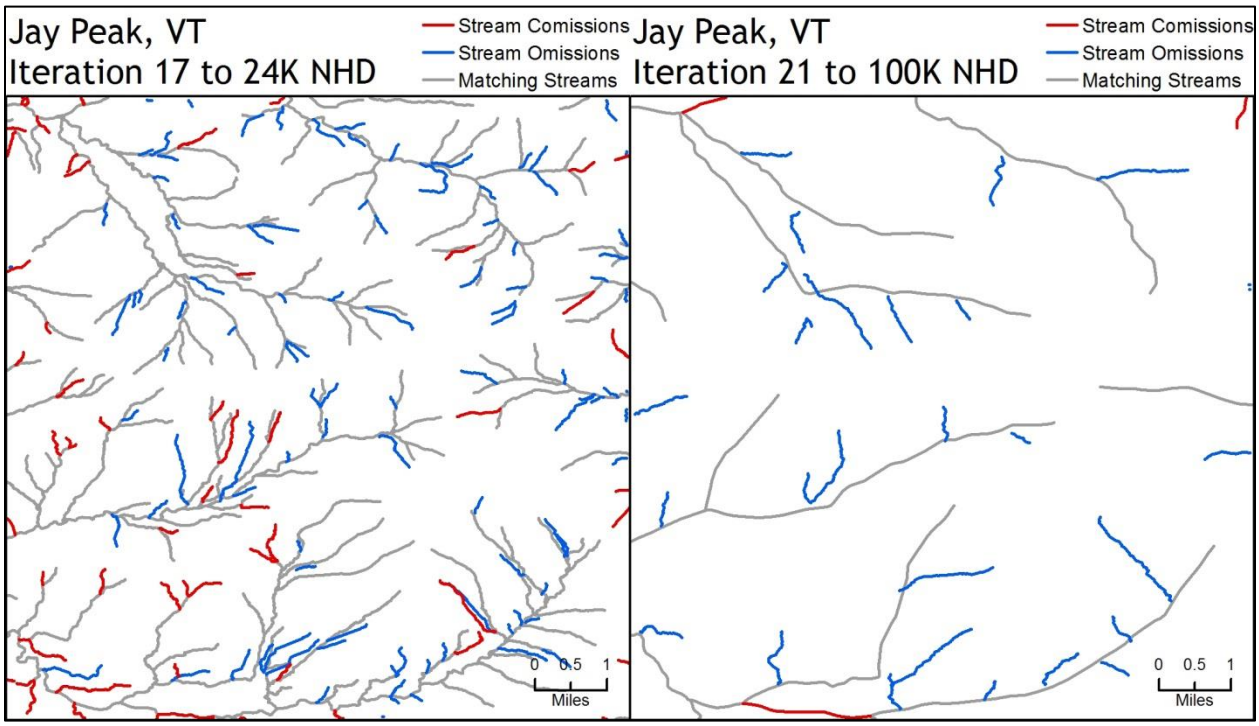

E.1: Semivariogram plots for Jay Peak, VT. This study site is classified as rugged, humid. The CLC for iteration 17 is 0.67 (comparison to high resolution NHD benchmark). The CLC for iteration 21 is 0.51 (comparison to medium resolution NHD benchmark). Iteration 21 does not

perform as well as expected. The stream extraction process is extracting more headwater streams than it should.

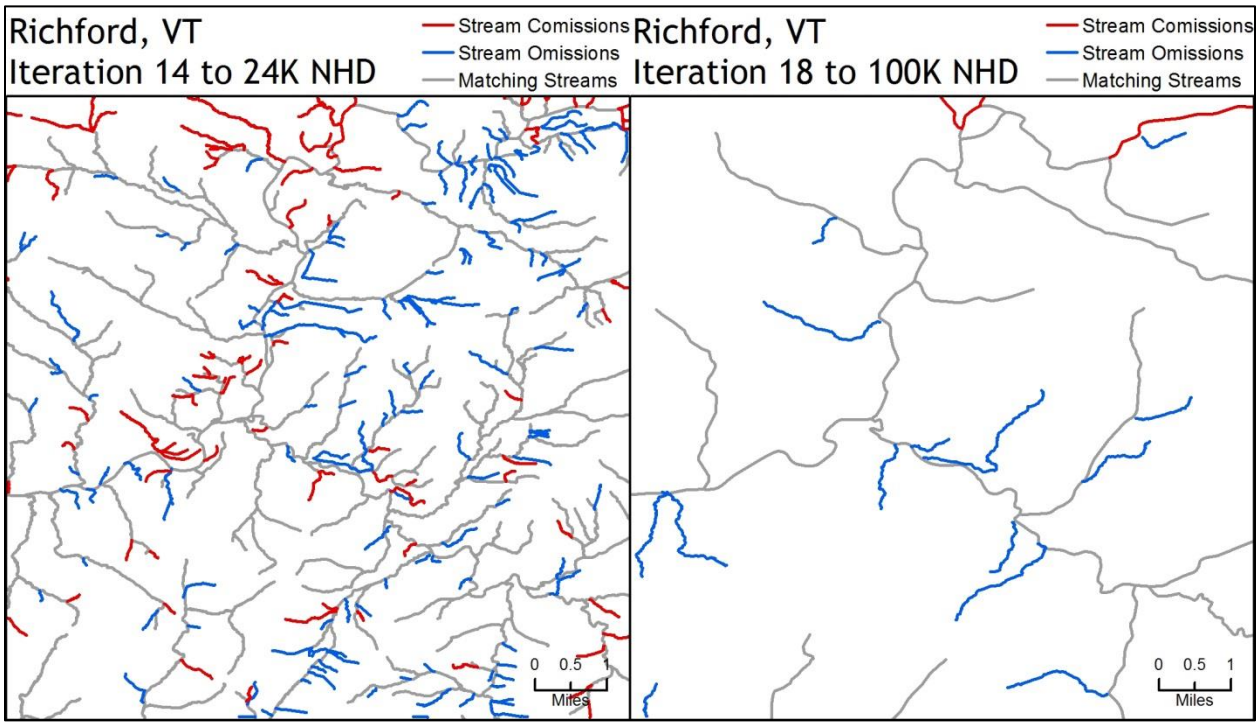

E.2: Semivariogram plots for Richford, VT. This study site is classified as rugged, humid. The CLC for iteration 14 is 0.69 (comparison to high resolution NHD benchmark). The CLC for iteration 18 is 0.64 (comparison to medium resolution NHD benchmark).

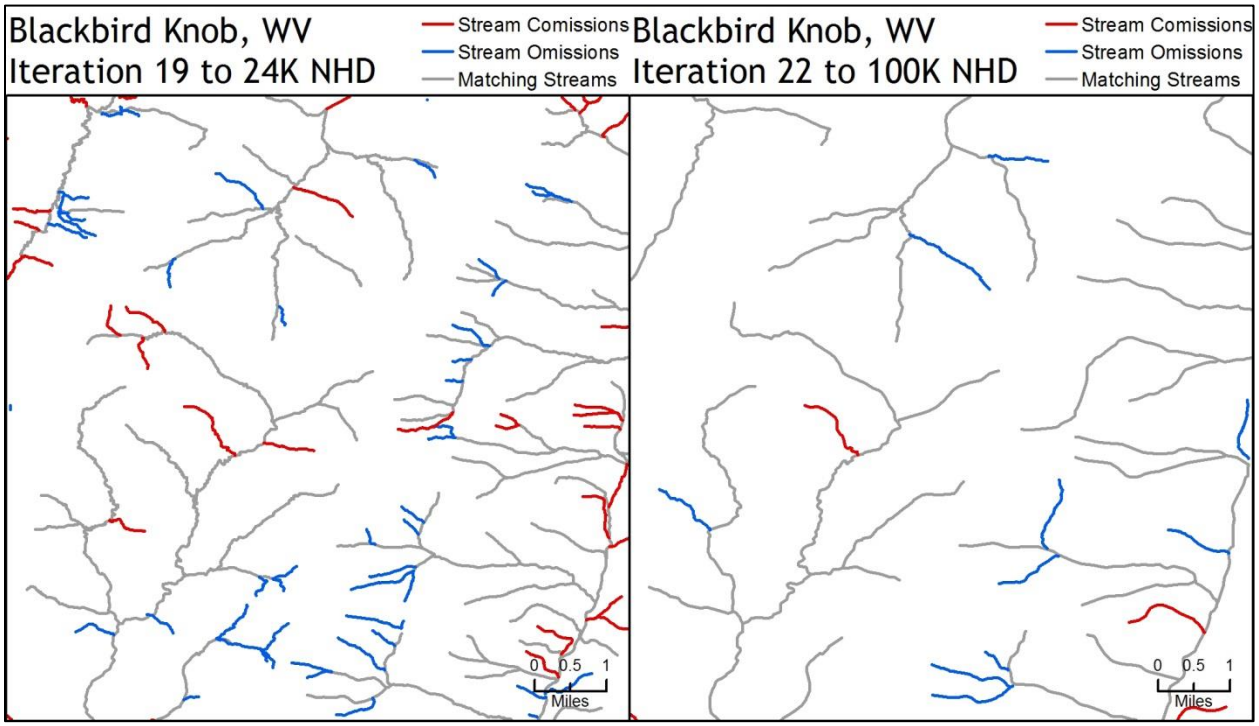

E.3: Semivariogram plots for Blackbird Knob, WV. This study site is classified as rugged, humid. The CLC for iteration 19 is 0.66 (comparison to high resolution NHD benchmark). The CLC for iteration 22 is 0.67 (comparison to medium resolution NHD benchmark). The CLC values are very similar which indicates the generalization process is being applied consistently as the attribute resolution changes.

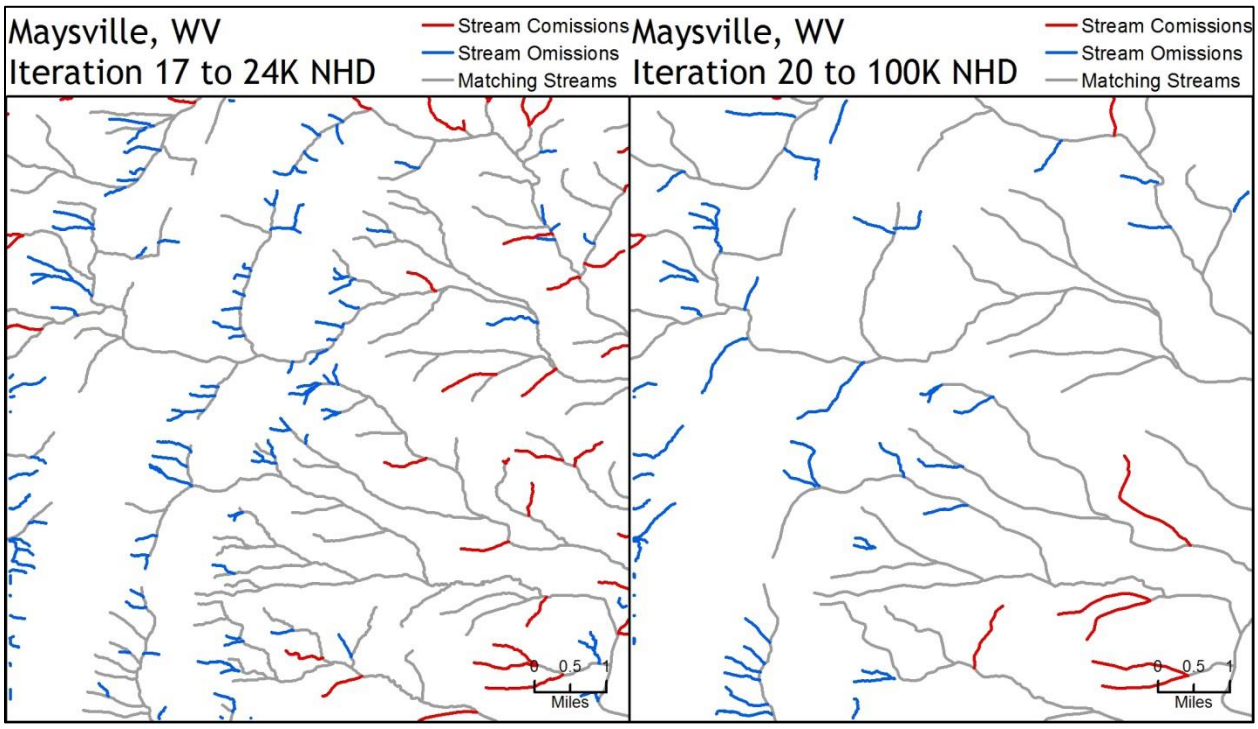

E.4: Semivariogram plots for Maysville, WV. This study site is classified as rugged, humid. The CLC for iteration 17 is 0.68 (comparison to high resolution NHD benchmark). The CLC for iteration 20 is 0.64 (comparison to medium resolution NHD benchmark). The omissions (blue lines) demonstrate that the stream extraction process is continuing to extract too many small headwater channels.

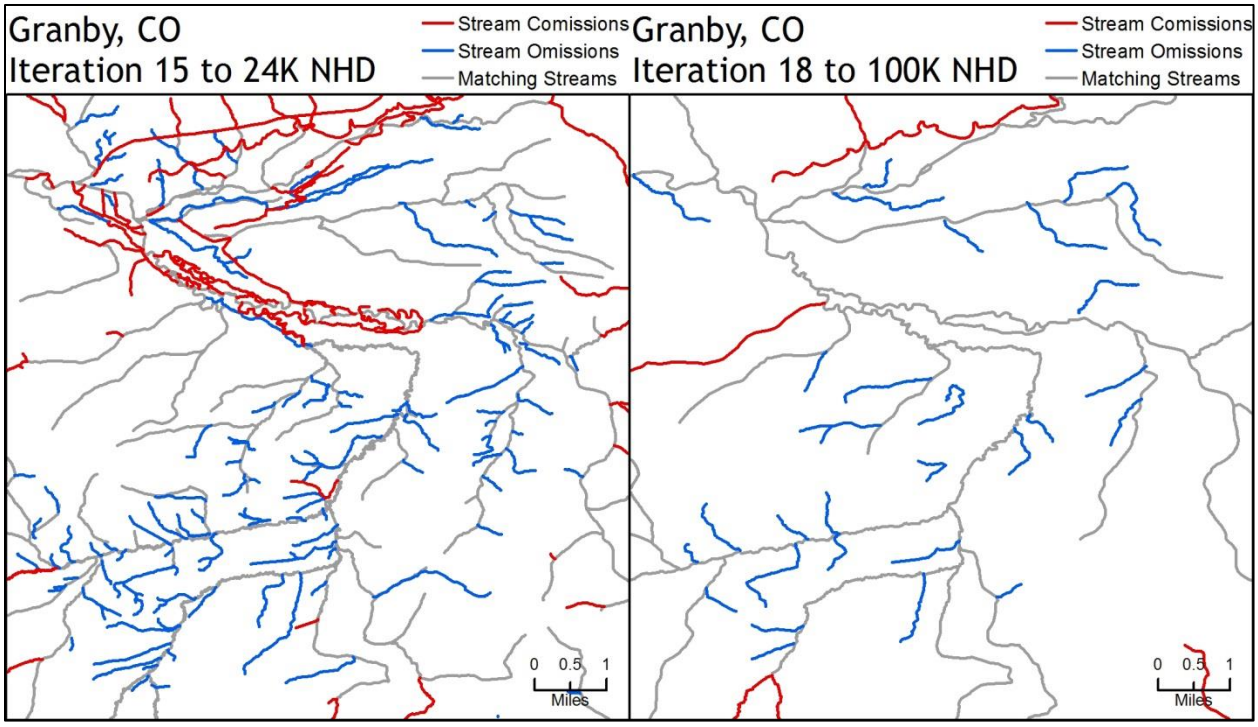

E.5: Semivariogram plots for Granby, CO. This study site is classified as rugged, dry. The CLC for iteration 15 is 0.54 (comparison to high resolution NHD benchmark). The CLC for iteration 18 is 0.56 (comparison to medium resolution NHD benchmark). This study site has a braided stream present. It is highlighted by the commissions (red lines) in iteration 15. The stream extraction process has difficulty extracting complex features such as braided channels. The CLC for iteration 18 is slightly higher. This is likely do to the braided channels not being present in the medium resolution NHD.

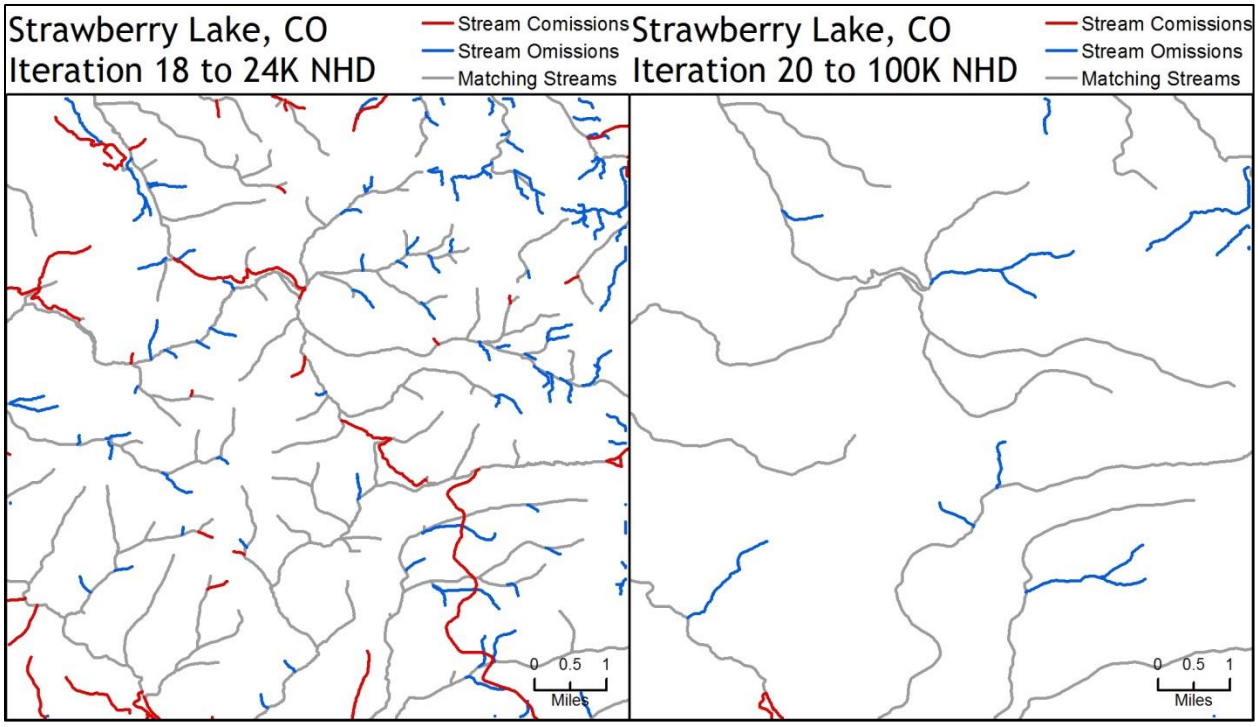

E.6: Semivariogram plots for Strawberry Lake, CO. This study site is classified as rugged, dry. The CLC for iteration 18 is 0.65 (comparison to high resolution NHD benchmark). The CLC for iteration 20 is 0.72 (comparison to medium resolution NHD benchmark). Iteration 18 has a lower CLC value than iteration 20. By examining the CLC map, especially the commissions, of the high resolution NHD, there are several artificial connectors or pipelines that are present in the vector benchmark but not resolved in either the 10m or the 30m NED. Since these aren't easily modeled, they were not identified in the stream extraction process.

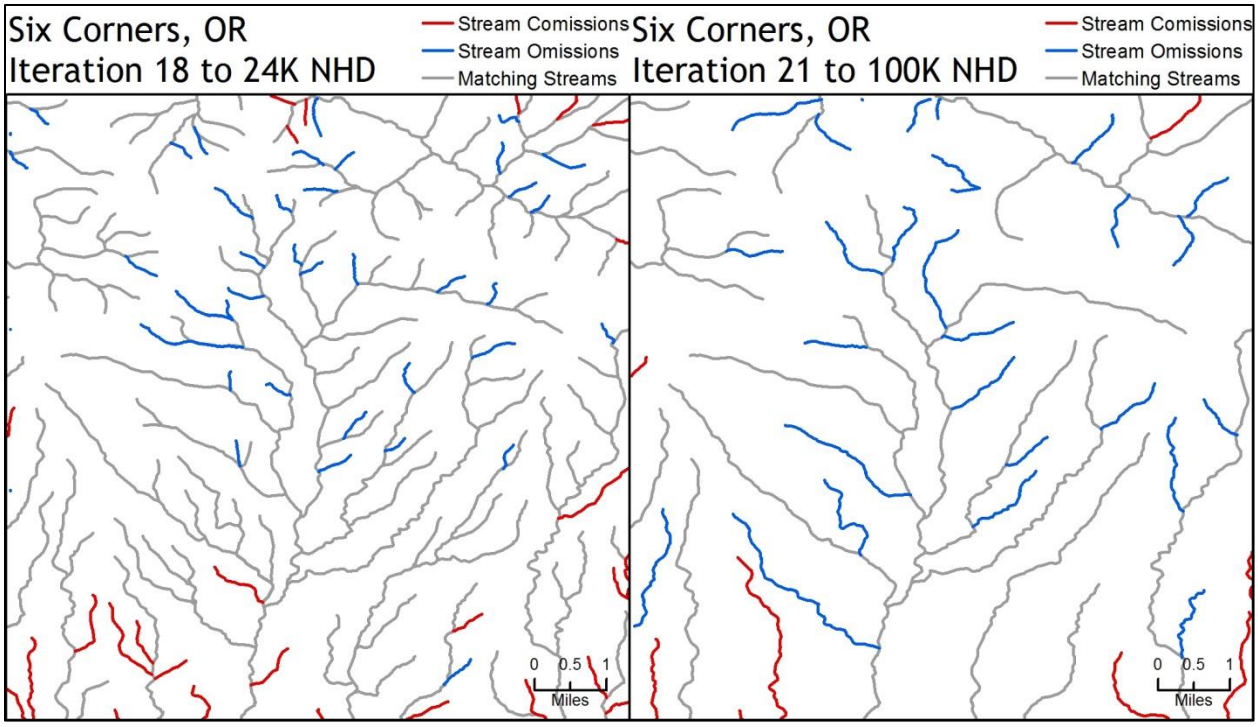

E.7: Semivariogram plots for Six Corners, OR. This study site is classified as rugged, dry. The CLC for iteration 18 is 0.82 (comparison to high resolution NHD benchmark). The CLC for iteration 21 is 0.62 (comparison to medium resolution NHD benchmark).

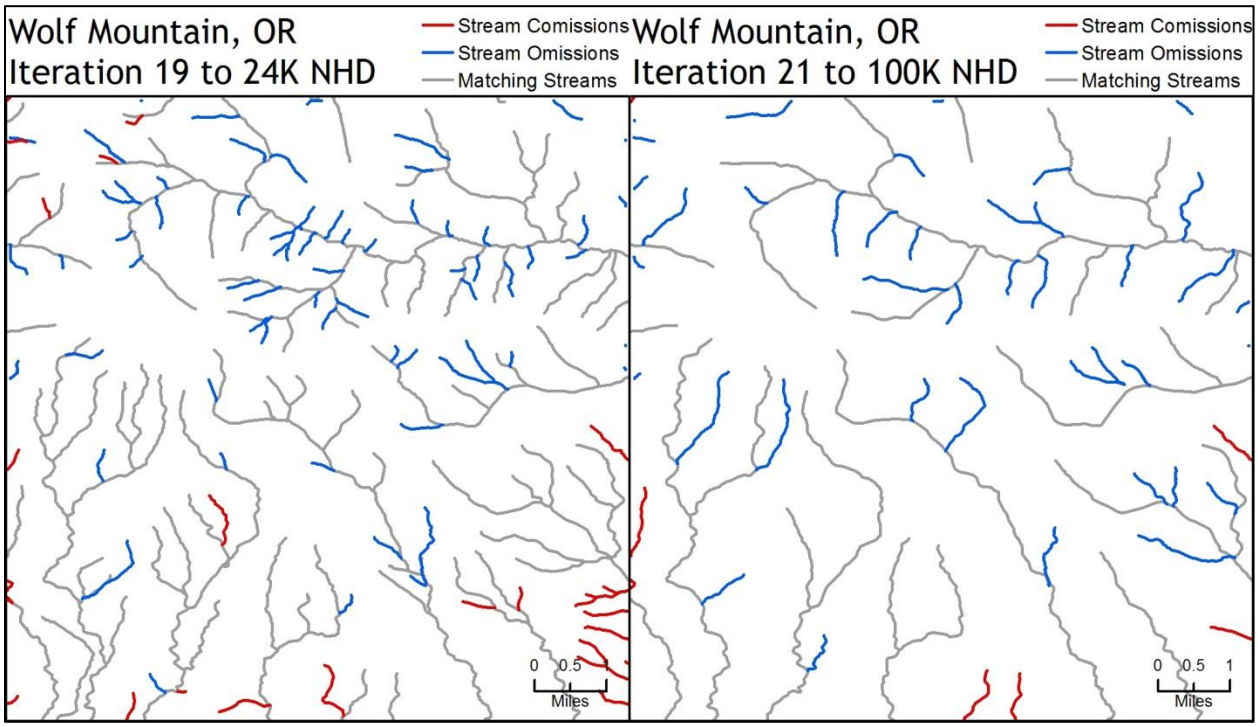

E.8: Semivariogram plots for Wolf Mountain, OR. This study site is classified as rugged, dry. The CLC for iteration 19 is 0.75 (comparison to high resolution NHD benchmark). The CLC for iteration 21 is 0.63 (comparison to medium resolution NHD benchmark).

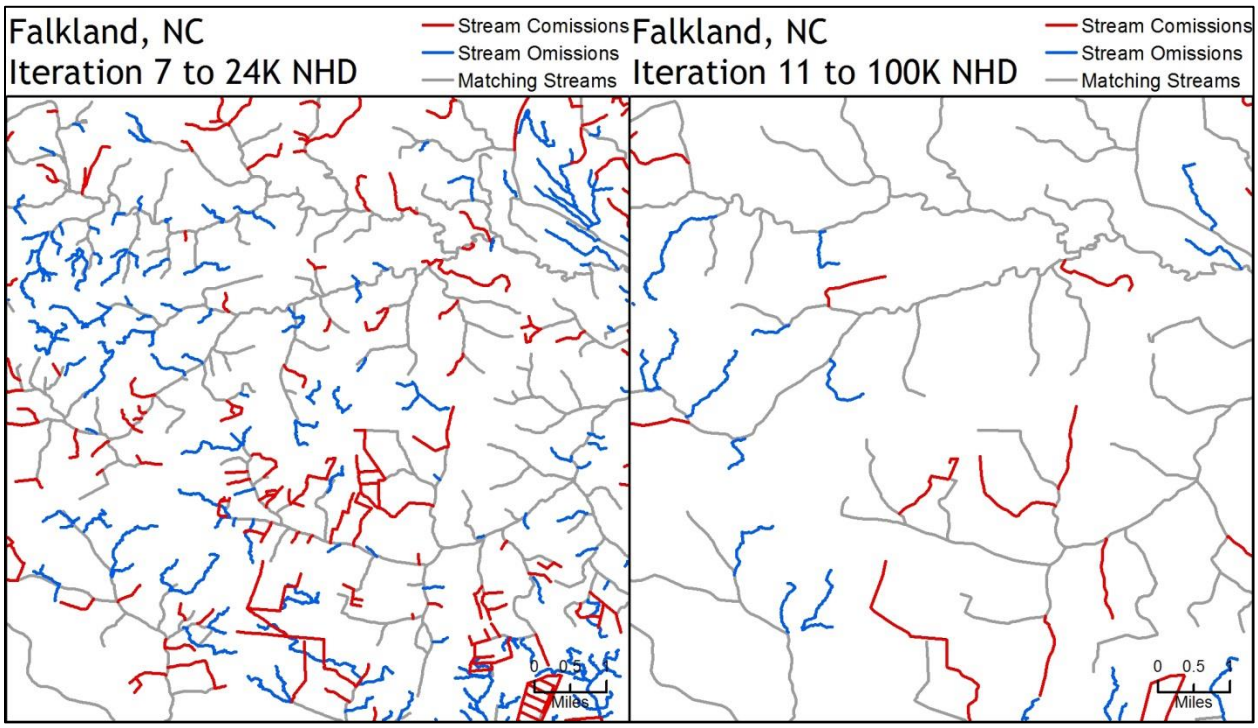

E.9: Semivariogram plots for Falkland, NC. This study site is classified as flat, humid. The CLC for iteration 7 is 0.51 (comparison to high resolution NHD benchmark). The CLC for iteration 11 is 0.61 (comparison to medium resolution NHD benchmark). The CLC value for iteration 7 is rather low. While there appears to be some urbanized channels in the southeast of the map, this doesn't seem to be the main cause for the low CLC value. There is a mixture of omissions and commissions, suggesting that the stream extraction process isn't collecting the correct flowlines. This is likely due to the low relief of Flankland.

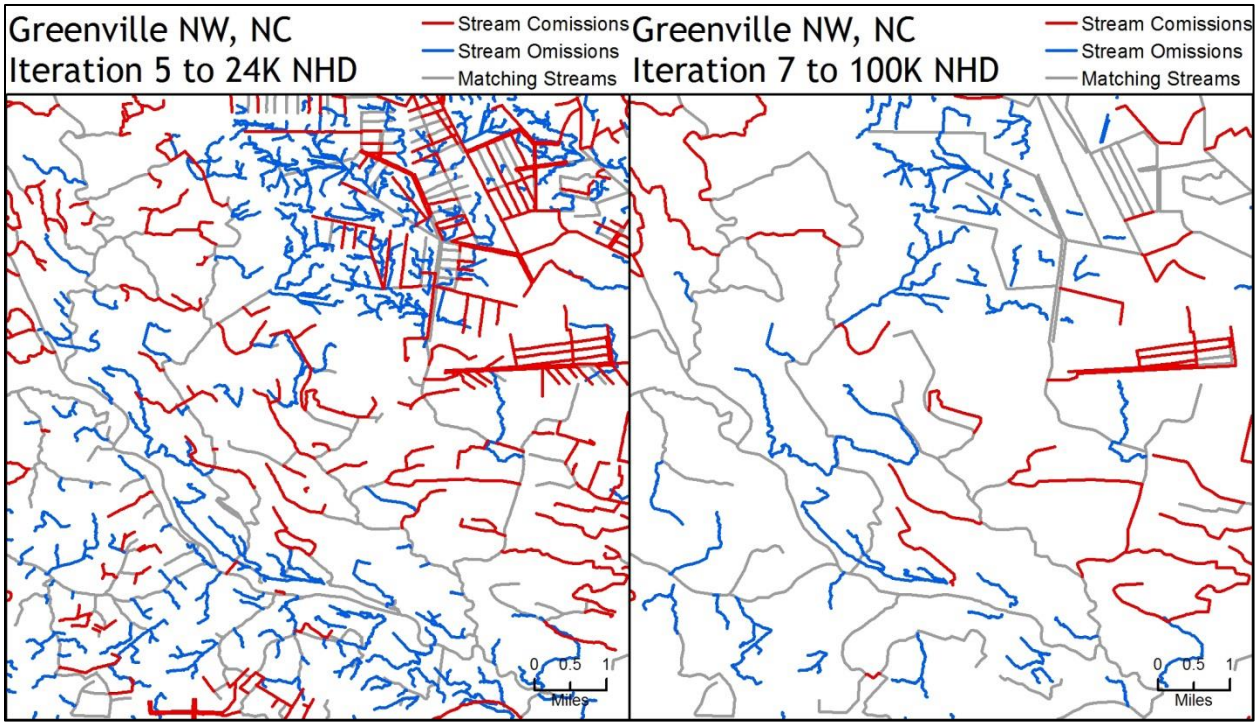

E.10: Semivariogram plots for Greenville, NC. This study site is classified as flat, humid. The CLC for iteration 5 is 0.31 (comparison to high resolution NHD benchmark). The CLC for iteration 7 is 0.50 (comparison to medium resolution NHD benchmark). The CLC for iteration 5 is very low. This is likely due to the presence of the urban area in the northern part of the study site. Since urbanized channels of flow aren't easily picked up by the stream extraction process, it causes a relatively low. Many of the channels have been removed in the medium resolution NHD and as a result, has a much higher CLC value.

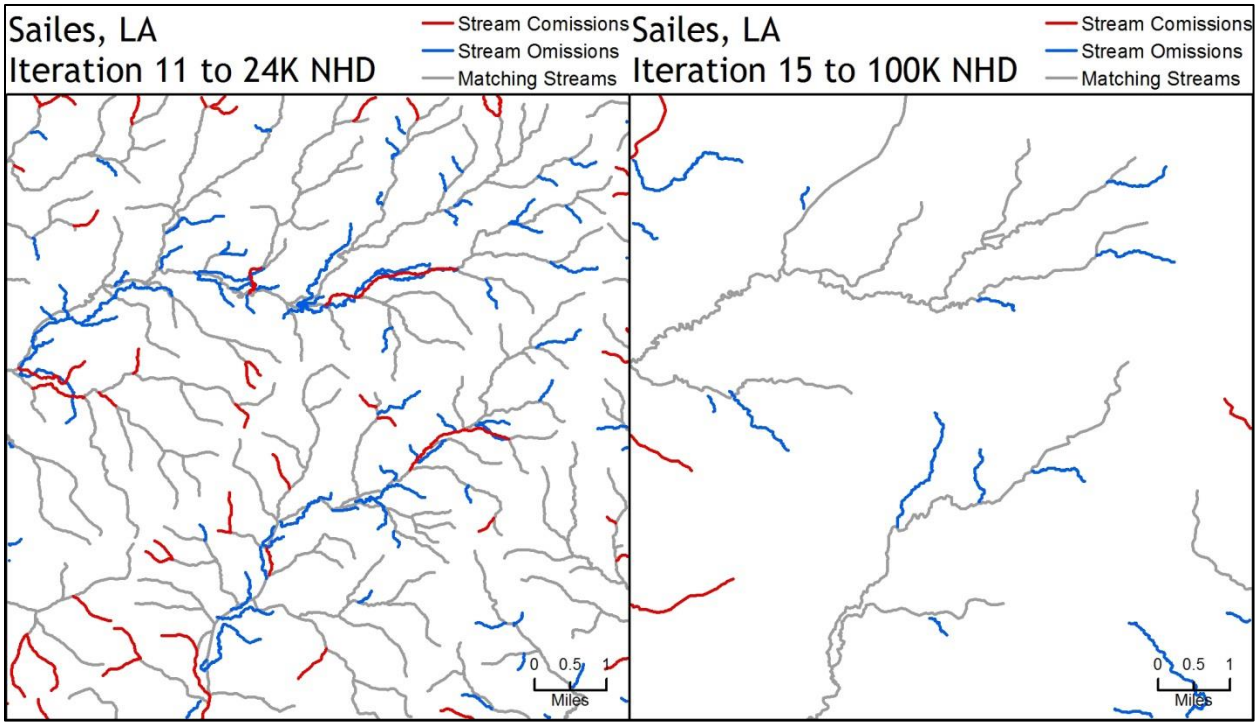

E.11: Semivariogram plots for Sailes, LA. This study site is classified as flat, humid. The CLC for iteration 11 is 0.73 (comparison to high resolution NHD benchmark). The CLC for iteration 15 is 0.53 (comparison to medium resolution NHD benchmark).

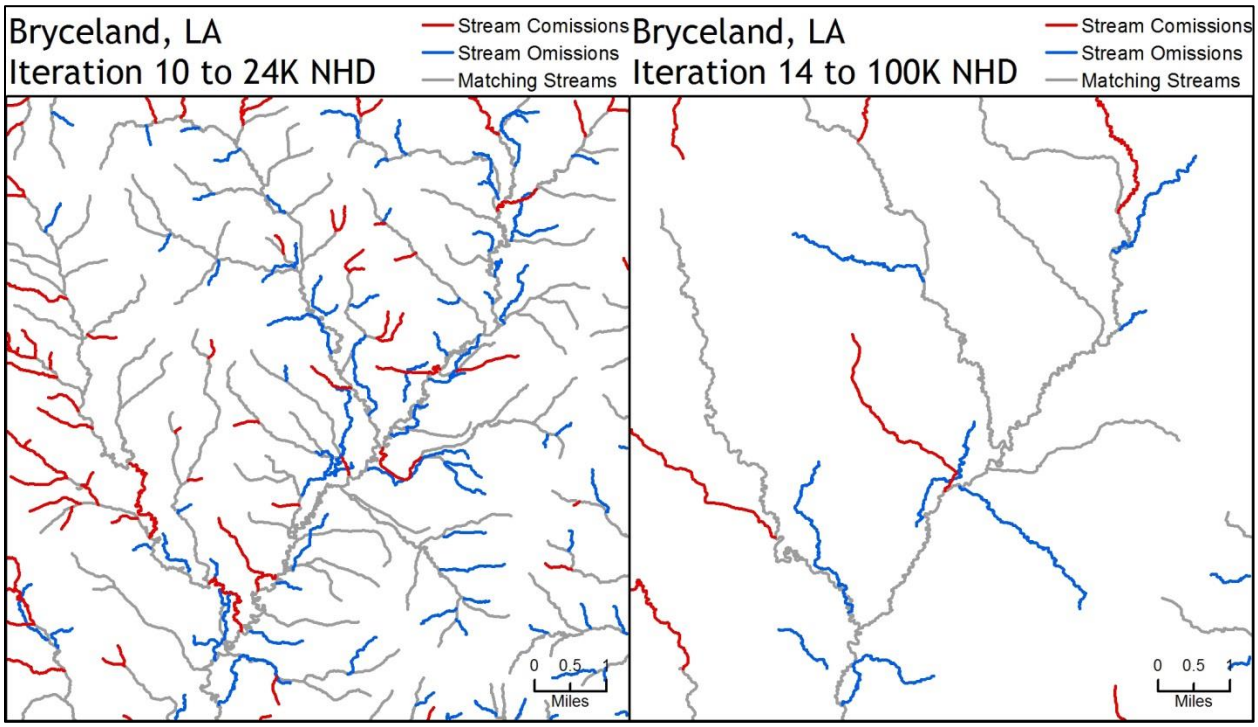

E.12: Semivariogram plots for Bryceland, LA. This study site is classified as flat, humid. The CLC for iteration 10 is 0.67 (comparison to high resolution NHD benchmark). The CLC for iteration 14 is 0.56 (comparison to medium resolution NHD benchmark).

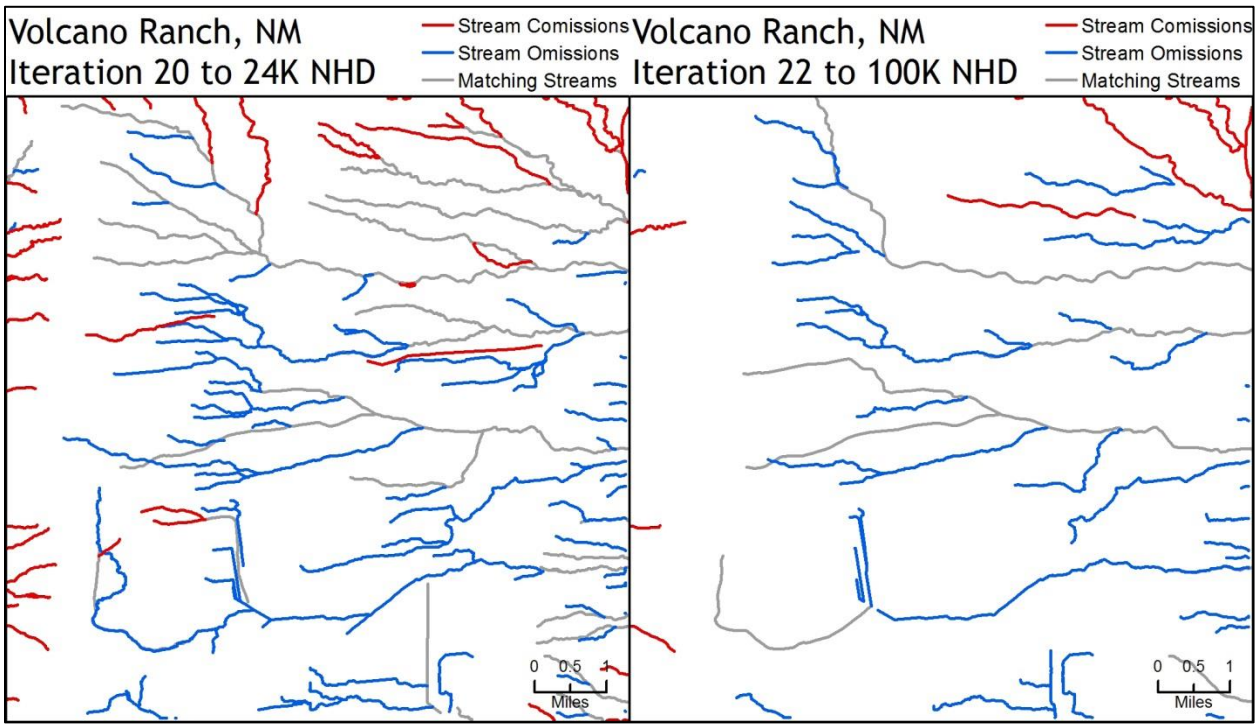

E.13: Semivariogram plots for Volcano Ranch, NM. This study site is classified as flat, dry. The CLC for iteration 20 is 0.38 (comparison to high resolution NHD benchmark). The CLC for iteration 22 is 0.24 (comparison to medium resolution NHD benchmark). Volcano Ranch has a very low CLC. There could be two reasons for this. The first is that the study site straddles two watersheds, making the stream extraction process attempt to identify very small headwater streams that continue out of the study site. The second is the flatness of the study site. The filtering process may have eroded the stream channels to the point where the stream extraction process was inappropriately identifying streams.

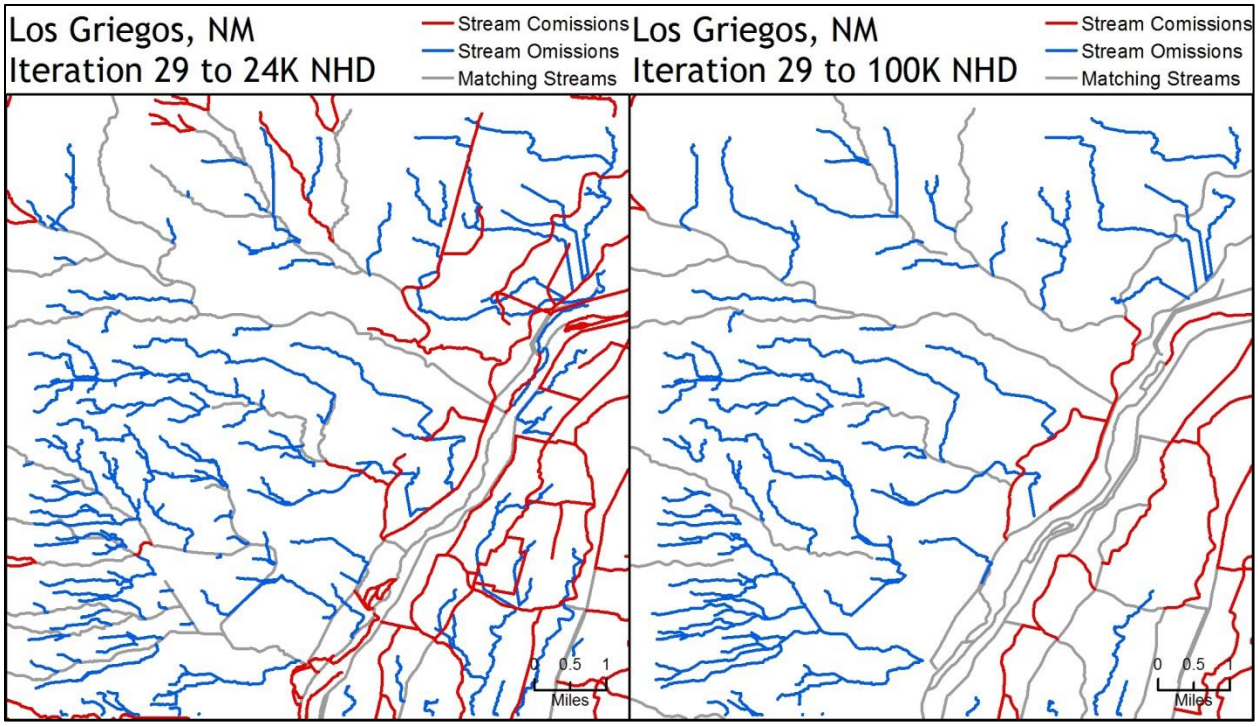

E.14: Semivariogram plots for Los Griegos, NM. This study site is classified as flat, dry. The CLC for iteration 29 is 0.26 (comparison to high resolution NHD benchmark). The CLC for iteration 29 is 0.32 (comparison to medium resolution NHD benchmark). Los Griegos, NM has a braided stream that runs through the southeastern corner. Because the stream extraction process has difficulty extracting complex features such as braided channels, additional headwater streams were extracted instead. This can be observed when performing the CLC for both NHD resolution benchmarks since many braided channels exist in both datasets.

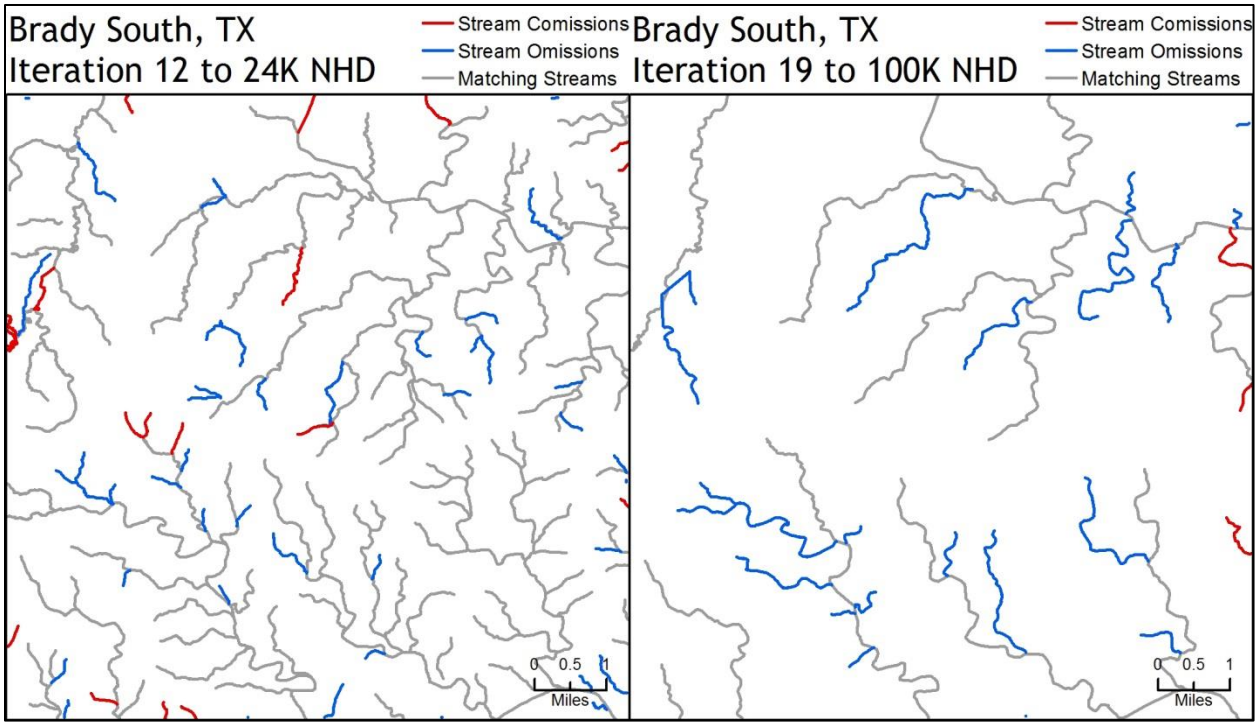

E.15: Semivariogram plots for Brady South, TX. This study site is classified as flat, dry. The CLC for iteration 12 is 0.79 (comparison to high resolution NHD benchmark). The CLC for iteration 19 is 0.55 (comparison to medium resolution NHD benchmark).

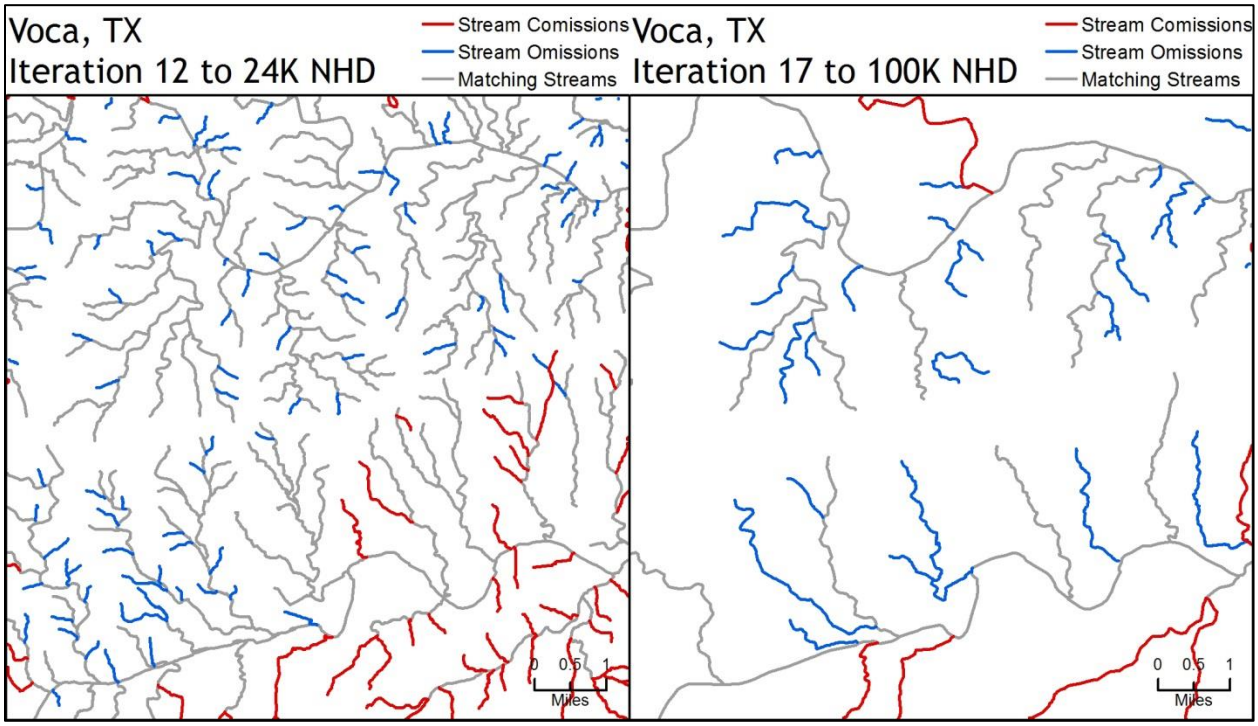

E.16: Semivariogram plots for Voca, TX. This study site is classified as flat, dry. The CLC for iteration 12 is 0.76 (comparison to high resolution NHD benchmark). The CLC for iteration 17 is 0.51 (comparison to medium resolution NHD benchmark). The artifact of data compilation of

NHD benchmark data can be observed when examining iteration 12 and the high resolution NHD benchmark. There is a well-defined border between streams identified as commissions and omissions. This suggests an error on the part of the NHD benchmark where an editor densified one area of the data.